# ESCUELA POLITÉCNICA NACIONAL

## FACULTAD DE INGENIERÍA QUÍMICA Y AGROINDUSTRIA

## MAESTRÍA DE INVESTIGACIÓN EN METALURGIA

# REVISIÓN DE LA INFLUENCIA DE LA MODIFICACIÓN DE LA HIDROFOBICIDAD DE LAS SILICALITAS DE TITANIO SOBRE SU ACTIVIDAD CATALÍTICA (INFLUENCE OF THE HYDROPHOBIC MODIFICATION OF TITANOSILICATES ON THEIR CATALYTIC ACTIVITY: A REVIEW)

**TESIS PREVIA A LA OBTENCIÓN DEL GRADO DE MAGISTER EN METALURGIA**

**ANA BELÉN LOZADA MINIGUANO**
ana.lozada@epn.edu.ec

**DIRECTORA: ING. LUCÍA ELIANA MANANGÓN PERUGACHI MSc.**
lucia.manangon@epn.edu.ec

**Quito, septiembre 2021**

# DECLARACIÓN

"Yo, Ana Belén Lozada Miniguano, declaro bajo juramento que el trabajo aquí descrito es de mi autoría; que no ha sido previamente presentado para ningún grado o calificación profesional; y, que he consultado las referencias bibliográficas que se incluyen en este documento.

Sin perjuicio de los derechos reconocidos en el primer párrafo del artículo 114 del Código Orgánico de la Economía de los Conocimientos, Creatividad e Innovación –COESC-, cedo los derechos patrimoniales de este trabajo, a la Escuela Politécnica Nacional."

Ing. Ana Belén Lozada Miniguano
C.I. 0503610602

## CERTIFICACIÓN

Certifico que el presente trabajo fue desarrollado por Ana Belén Lozada Miniguano, bajo mi supervisión.

Eliana L. Manangón P.

Ing. Lucía Eliana Manangón Perugachi MSc.
**DIRECTORA DE TESIS**

## AUSPICIO

La presente investigación contó con el auspicio financiero del proyecto PII-DEMEX-2020-03, que se ejecutó en el Departamento de Metalurgia Extractiva de la Facultad de Ingeniería Química y Agroindustria.

# AGRADECIMIENTOS

A Dios, por ser quien me fortalece y levanta en momentos de debilidad, por su constante muestra de amor y protección, por forjar mi camino y mi carácter, y por enseñarme que, a pesar de las dificultades, todas las cosas obran para bien.

A mi amada madre Gema, por su esfuerzo inmedible y su amor invaluable, por ser ese descanso para mi alma, por cada palabra de calma, de ánimo, y de fortaleza, y por ser mi ejemplo todos los días. Gracias por ser y estar siempre.

A mi querida hermana Jaqueline, por su cariño, apoyo y consejos, por su compañía siempre, y por inculcarme orden, disciplina y constancia.

A la memoria de mi padre Víctor, por el cuidado y protección en sus días, y por enseñarme que todas las cosas importantes se logran con firmeza, decisión y perseverancia. Te extraño siempre.

A memoria de mi abuelito Ricardo, por ser el ser más dulce, amoroso, y bondadoso que he conocido. Dios fue tan bueno al permitirme crecer a tu lado.

A mi Abuelita María, por las risas y el buen ánimo que imparte.

A mi tíos y primos, de forma especial a Hipatia, Holger, Roberto, Diana, Sayana, Doménica, y Juliet, gracias por su apoyo y cariño incondicional a lo largo de mi vida.

A mi directora de tesis, Ing. Eliana Manangón, por la dirección y el apoyo total en la realización de este trabajo. Un agradecimiento especial por la confianza, amistad, y estima, gracias por compartir sus conocimientos y permitirme aprender de Ud. Es una excelente persona y profesional.

Al personal docente y administrativo del Departamento de Metalurgia Extractiva de la Escuela Politécnica Nacional por su colaboración y disposición. Al Ing. Ernesto de la Torre, Ing. Diana Endara, Ing. Alicia Guevara, Ing. Eddy Pazmiño, Ing. Evelyn Criollo, Ing. Carlos Aragón, Ing. Kleber Collantes, Sra. Verito Díaz, y Wilmer Betun, gracias por contribuir cada uno en diferentes aspectos.

A la segunda cohorte de esta maestría, Patricia Jaramillo, Edmundo Cruz, y Luis Huilca, por el conocimiento y la experiencia compartidos.

A una persona muy importante, Solange Esquivel, por ser esa amiga incondicional, por estar siempre dispuesta a escuchar, por tu bondad y buen corazón. Gracias por qué de ti puedo recibir un consejo que siempre me hará bien.

A mi amiga Nathaly Rodríguez, por el cariño, apoyo, y buenos momentos que hemos podido compartir. Mi admiración a tu tesón y buen ánimo en todo lo que haces.

A personas que, con sus palabras de ánimo y sus deseos de superación, han hecho más llevadera esta etapa de estudio, Angie Huanga, por su carisma, cariño y por todos los momentos divertidos que hemos compartido. A Eduardo Rueda y Luis Zambrano, por su amistad y apoyo. A familia de la IBDLSA. Gracias siempre.

# DEDICATORIA

Dedico este trabajo con mucho amor y satisfacción a mi amada familia: a mi madre Gema Miniguano y a mi hermana Jaqueline Lozada, por ser mi apoyo y fortaleza en cada momento de mi vida. A mi padre Víctor Lozada (+) por sembrar en mí un compromiso de trabajo constante, dedicación, y superación. A mis abuelitos Ricardo (+) y María por ser ese reflejo de amor, ternura y cuidado.

En gratitud a su esfuerzo y amor, procuraré dar siempre lo mejor de mí.

*"Cuanto más grande es la dificultad, más gloria hay en superarla.*

*Epicuro".*

*Review Paper*

# Revisión de la influencia de la modificación de la hidrofobicidad de las silicalitas de titanio sobre su actividad catalítica (Influence of the hydrophobic modification of titanosilicates on their catalytic activity: A review)

**Ana Belén Lozada.**

**Escuela Politécnica Nacional, Maestría de Investigación en Metalurgia. E-mail estudiante: ana.lozada@epn.edu.ec**

**Resumen:** Las silicalitas de titanio son catalizadores que se han utilizado exitosamente en reacciones de oxidación selectiva por lo que se han desarrollado algunas alternativas para potenciar su actividad. Una de ellas es la modificación de la hidrofobicidad de la superficie de estos catalizadores. El carácter hidrofóbico de los catalizadores juega un papel importante en los procesos de adsorción/desorción de reactivos y productos y, en consecuencia, en el rendimiento catalítico. La hidrofobización de las silicalitas de titanio se ha estudiado en varias investigaciones, pero aún no se ha revisado el efecto sobre su actividad catalítica. Además, las metodologías para medir la hidrofobicidad difieren en cada investigación dificultando la comparación de esta propiedad. Por esta razón, en este trabajo se compararon silicalitas de titanio amorfas y cristalinas modificadas hidrofóbicamente. Se compararon y discutieron las metodologías usadas para la hidrofobización, las técnicas de caracterización de la hidrofobicidad y el efecto sobre su actividad catalítica. Se ha obtenido una mejora significativa en la medición de la hidrofobicidad como resultado de la combinación de dos o más técnicas analíticas. Sin embargo, no se puede atribuir la mejora en la actividad catalítica totalmente a la modificación de la hidrofobicidad debido a la complejidad de los sistemas de reacción y las interacciones entre la superficie del catalizador y el medio de reacción. Por lo cual, se requieren estudios más extensos para comprender mejor el efecto de la hidrofobización de la superficie de las silicalitas de titanio y otros catalizadores sólidos porosos.

**Abstract:** Titanosilicates are catalysts which have been successfully used in selective oxidation reactions whereby, some alternatives have been developed to enhance their activity. One of these is the modification of the hydrophobicity of the catalyst surface. The hydrophobicity of these materials plays an important role on the adsorption/desorption processes and consequently, on the catalytic performance. Several researchers have studied the hydrophobization of titanosilicates, but the effect on their catalytic activity has not been reviewed yet. In addition, the methodologies to measure the hydrophobicity differ in each work making difficult the comparison of this property. For this reason, in this work crystalline and amorphous titanosilicates that have been modified hydrophobically were addressed. A comparison and discussion of the methodologies for hydrophobic modification, the analytical techniques for characterization of hydrophobicity, and the effect of hydrophobization on their catalytic activity were performed. A significant improvement of hydrophobicity characterization has been reached as a result of the combination of two or more analytical techniques. However, the improved catalytic activity cannot be totally attributed to the hydrophobic modification due to the complexity of the reaction systems, interactions between catalyst surface and liquid medium. Thus, more extensive studies including kinetic, thermodynamic, spectroscopy, and computational analysis are required to gain more understanding of the effect of hydrophobizing the surface of titanosilicates and other porous solid catalysts.

**Keywords:** titanosilicates; hydrophobicity; hydrophobic modification; selective oxidation; silanol density

## Introduction

Titanosilicates are important materials with fast development since the synthesis of the first TS-1 [1–5]. They are used in selective oxidation of organic compounds displaying high catalytic activity. [1,2,6–11]. The growing application of these heterogeneous catalysts for both petrochemical and fine chemical industry has resulted in a substantial production of titanosilicates with improved catalytic performance which could replace the traditional ones [12]. In fact, more than 400 articles per year have been published in the last 5 years, according to a search in the Scopus database.

The active sites of titanosilicates are Ti atoms in tetrahedral coordination (also called framework-Ti) which are inserted in the silica framework. According to previous studies, a limit for isomorphous substitution of Ti atoms into the TS-1 framework was established at a maximum atomic ratio of 2.5% (Ti / (Si + Ti)) [13] to prevent the formation of octahedral Ti species (extraframework Ti), which is not active in selective oxidation reactions. For instance, when the Ti content in TS-1 was higher than 3%, octahedral Ti, which is the same Ti species present in the crystalline phase of $TiO_2$ (anatase), was detected by DRUV-Vis [14] and XPS [15]. In selective oxidation reactions, Ti active sites interact with the oxidant ($H_2O_2$ or organic peroxides) to produce Ti-peroxo intermediate species (Ti-OOH or Ti-OOR) which are the active catalytic oxidation centers [14,16,17]. It is known that tetrahedral Ti in titanosilicates displays Lewis acidity which activates the oxidant, forming the activated complex that reacts with substrates such as olefins in epoxidation reactions [18–22].

Some alternatives have been used to improve the catalytic performance of titanosilicates, such as improving the textural properties [2,12], controlling the nature of the active sites [1,23], and modifying the hydrophobic/phylic surface character. In the last years, the adjustment of hydrophobicity/philicity of materials such as metal-organic-frameworks (MOFs) [24–26], aluminosilicates [27], and titanosilicates [28] has received more attention due to its great influence over their catalytic properties.

In the field of titanosilicates, the effect of hydrophobization has been particularly studied in the epoxidation of olefins in liquid phase. For instance, some authors believed that the hydrophobicity of titanosilicates affected the competitive adsorption between non-polar substrates (olefin) and polar products (epoxide) [29,30]. Consequently, several researchers focused on studying the effect of hydrophobizing titanosilicates to improve the olefin adsorption. Later, studies showed that epoxidation follows an Eley-Rideal mechanism, in which, only the oxidant is adsorbed on the catalysts surface, but a hydrophobic surface allows the rapid removal of epoxide preventing the oxidation to diol [31]. In addition, a hydrophobic surface reduces water adsorption that would cause the epoxide ring opening and deactivation of the titanium active sites [32]. Water is added to the reaction together with the oxidant. For example, the commercially available $H_2O_2$ is normally a 30%(w/w) solution in water. Thus, the modification of the hydrophobicity of the surface of titanosilicates could regulate the interaction between the catalyst with both the reactants and products and prevent side reactions, resulting in high conversion and/or selectivity [33].

Several crystalline and amorphous titanosilicates have been hydrophobized by different methodologies. TS-1, which is already a hydrophobic titanosilicate was further hydrophobized by controlling the silanol surface density to improve its catalytic activity. The use of $(NH_4)_2CO_3$ as crystallizing agent allows to regulate the silanol density of TS-1, and it also reduces the presence of extraframework Ti. The defects of the material decreased by increasing the degree of crystallization. The improved hydrophobic character and Ti dispersion of TS-1 yielded a significant increment of the activity of the catalyst [34]. Also, hydrophobic TS-1 functionalized by post-grafting achieved higher epoxide selectivity than non-modified one [35].

The small pores of TS-1 allow the catalytic oxidation of relatively small molecules efficiently, but its use in oxidation of greater substrates is restricted due to diffusion limitations. Therefore, large-pore titanium zeolites were synthesized to tackle this limitation. Ti-Beta zeolite has better textural properties than TS-1 zeolite, but it is more hydrophilic [36]. Therefore, Ti-Beta was hydrophobized by the synthesis in fluoride medium instead of the classical $OH^-$ medium. Hydrophobization of Ti-Beta helped to decrease the silanol surface density [37–39]. For many years, it was believed that

hydrophobic Ti-Beta performed better in catalytic epoxidation than the hydrophilic analogous, but a recent study published by Bregante et al. [39] demonstrated that hydrophilic Ti-Beta exhibits turnover rates 100 times larger than the hydrophobic one. This discrepancy highlights the necessity to clarify the real effect of the hydrophobization of Ti-Beta. Other large-pore titanosilicates such as Ti-MCM-41 [40–44], Ti-MCM-48 [42], and Ti-SBA-15 [33], and amorphous Ti-$SiO_2$ [11,45–49] were functionalized by one-pot and post-grafting procedures and showed greater catalytic performance in the epoxidation of olefins.

It is notable that hydrophobic properties of catalysts surfaces display an important role into the adsorption/desorption processes and consequently, in the catalytic performance of titanosilicates. In fact, several researchers have studied the hydrophobization of these materials and the modification resulted in positive, negative, or non-significant effects on their catalytic activity. Even though the modification of hydrophobicity has been addressed in previous investigations, the variety of types of titanosilicates and the analytical techniques used to measure this property has not allow to reach a consensus in the catalytic effects of hydrophobization. From the best of our knowledge, there is not yet a review article analyzing this effect. For this reason, a comparison and discussion about the effects of hydrophobization of titanosilicates will be here addressed, considering the type of titanosilicate, the hydrophobization strategy, the surface characterization, and the catalytic system.

## Section 1: Overview of the topic

### *1.1 Types of titanosilicates and description of their characteristics focusing on their active site and textural properties.*

Titanosilicates, both crystalline and amorphous are important materials with fast development from this inception [1–5]. The importance of these materials lies in their remarkable catalytic activity in selective oxidation reactions. Ordered titanosilicates have been employed as catalysts in selective oxidation of organic compounds (i.e., alkanes, alkenes, alcohols, aromatics) in liquid-phase using hydrogen peroxide and organic peroxides as oxidants [1,2,6]. Amorphous titanosilicates are conventional catalysts for olefins epoxidation [7–11]. Titanosilicates have been constantly developed since of the first Ti-zeolite TS-1 was synthesized in 1983. As shown in Figure 1, the number of publications per year related to titanosilicates has increased through the years.

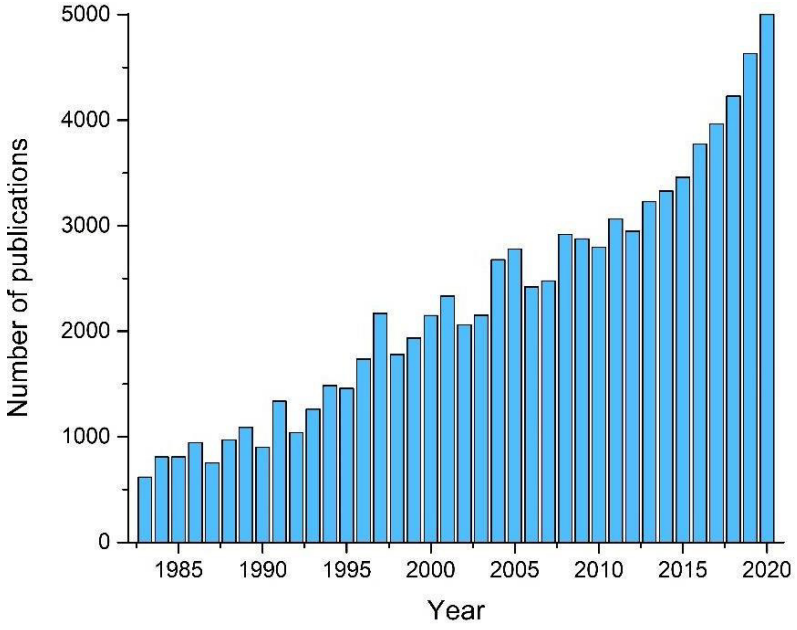


**Figure 1** Number of publications per year related to titanosilicates. Source: Scopus, June 2021.

In this work, titanosilicates are considered as materials that contain titanium atoms inserted in a silica matrix. We have classified them into two groups, the first group being formed by the titanosilicates based on zeolite frameworks (Ti-zeolite) that are crystalline materials and the second group including titanosilicates without zeolite framework (Ti-$SiO_2$) with amorphous structure.

### 1.1.1 Active sites of titanosilicates

Various types of titanosilicates with zeolitic as well as amorphous structure have been synthesized. All titanosilicates contain $Ti^{4+}$ transition metal. Zeolites have shown a significant impact on catalysis technology. A variety of zeolites containing atoms other than $Al^{+3}$ (heteroatoms i.e., $Ti^{4+}$, $Sn^{4+}$, $Ga^{4+}$) have been created and employed in acid-catalyzed reactions with higher performance than the traditional $SiO_2$-$Al_2O_3$ catalysts [50].

Ti atoms were introduced into the silica matrix by isomorphous substitution of $Si^{4+}$ by $Ti^{4+}$[51]. The substitution of $Si^{4+}$ by heteroatoms in the crystalline lattice has been extensively studied since this replacement can produce important effects on the physical, chemical, and catalytic properties [52,53]. An important parameter to be considered is that Ti can be inserted into the zeolite structure in tetrahedral and/or octahedral coordination. In fact, minerals with Na, Ti and Si (zorite and vinogradovite) contain Ti atoms in octahedral coordination. In addition, the ionic ratio (cation radius/anion radius) of Ti-O bond corresponding to 0.515 exceeds the range of 0.225 to 0.414 to produce tetrahedral coordination. Thus, the isomorphous substitution of $Si^{4+}$ by $Ti^{4+}$ seemed improbable [54].

The substitution of $Si^{4+}$ by $Ti^{4+}$ in the TS-1 titanosilicate was verified by modification of the unit-cell parameters as a function of the substitution degree and the difference between Si-O and Ti-O bond distance. No substantial changes were detected in XRD spectra of TS-1 compared with silicalite-1 and the minor changes were attributed to the formation of titanium dioxide which corresponds to octahedral coordination (extraframework titanium, EFW-Ti (Figure 1b)). This means that the isomorphous substitution cannot be perfect. Subsequent studies reached great development about the synthesis and reproducibility of TS-1 in industrial laboratories. According to TS-1 characterization, it was possible to determine that $Si^{4+}$ was mainly substituted by $Ti^{4+}$ in tetrahedral coordination (framework titanium, FW-Ti (Figure 1a)) [50]. In the case of TS-1 the substitution limit based on the lattice constants is around 2.5% (Ti/(Ti+Si)). Above this value, EFW-Ti appears [55]. There is not a theoretical value for all types of zeolites since it depends on the structure type and the presence of internal defects (Si-OH groups), whichever the synthesis methodology [23].

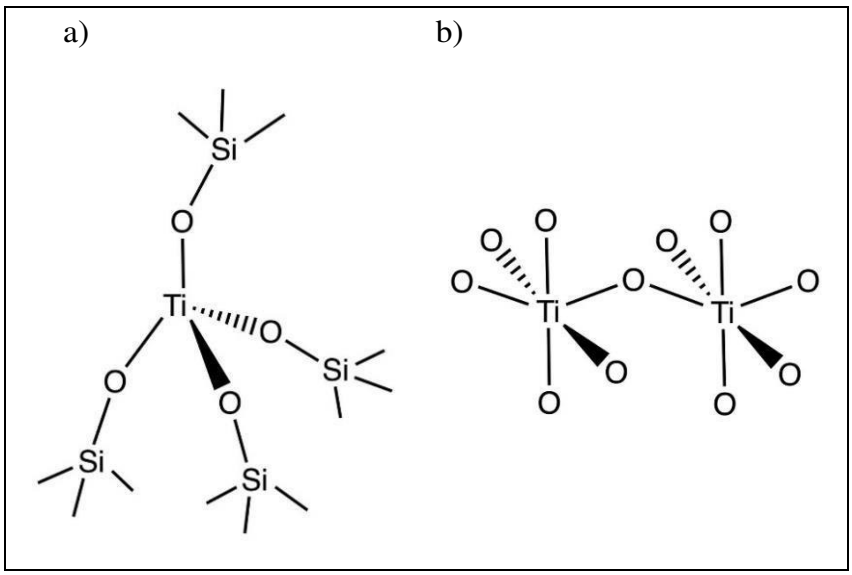


**Figure 2** Titanium species in titanosilicates: a) Framework titanium (FW-Ti) and b) Extraframework titanium (EFW-Ti).

Different analytical techniques were developed for better characterization of Ti sites in titanosilicates such as Fourier transform infrared spectroscopy (FTIR), Raman vibrational spectroscopies, Electron Paramagnetic Resonance (EPR), X-Ray Absorption Fine Structure (EXAFS), X-Ray Absorption Near Edge Structure (XANES), and Diffuse Reflectance DRUV-Vis. Specifically, tetrahedral titanium can be detected by Infrared/Raman band at 960 $cm^{-1}$ and UV peak at 210 nm (absorption in 330 nm exhibits the presence of octahedral Ti). The presence of tetrahedral Ti has even been associated to a change of color to yellow upon the addition of $H_2O_2$ to a TS-1. An interesting compilation of these analytic procedures was presented by Vayssillov in 2008 [1].

The presence of EFW-Ti affects the catalytic activity of titanosilicates in selective oxidation reactions since EFW-Ti is not active for these reactions, increases the $H_2O_2$ decomposition, and blocks the access of reactants to internal Ti active sites [1]. Tetrahedral Ti active sites react with the oxidant to produce surface titanium peroxo complexes which oxidize organic substrates including olefins [56].

### 1.1.2 Acidity

Acidity in zeolites was originated from the substitution of $Si^{4+}$ by different heteroatoms. In principle, zeolites are composed by $SiO_4$ units, in which the positive charge of $Si^{4+}$ is balanced with the negative charge of oxygens, thus $SiO_4$ is electrically neutral. In the case of aluminosilicates, a disequilibrium of charges is produced due to the substitution of $Si^{4+}$ by $Al^{3+}$, and organic or inorganic cations or protons (i.e. $H^+$) are introduced to achieve electrical neutrality [50,57].

It was found that the introduction of $Al^{3+}$ in the zeolitic framework can produce both Brønsted acid sites (BAS) and Lewis acid sites (LAS). BAS are produced by the bridging between the tetrahedrally coordinated $Al^{3+}$ with neighboring hydroxyls (Si-OH-Al on the surface of the zeolite framework), and LAS are assigned to extraframework Al [58]. Bridging hydroxyl groups Si-OH-Al as well as silanol groups (Si-OH) on the surface of the zeolite form BAS, and both catalyze oxidation reactions. The formation of Si-OH-Al is related to the Si/Al ratio, thus a decrement in the Si/Al ratio (higher Al content) results in the increment of Si-OH-Al [59–62].

BAS are also related to the hydrophobicity/hydrophilicity of zeolites. Previous studies demonstrated that Si-O-Si bonds are hydrophobic [63], and hydroxyl groups (Si-OH and Si-OH-Al) are hydrophilic [64]. Free-defect siliceous surfaces formed by Si-O-Si bridges present resistance to adsorbing water [63], while hydroxyl groups adsorb water molecules and water clusters [64]. The hydrophilic character increases while the surface density of silanol groups increases [65]. In fact, according to Cundy et al., the hydrophobicity index (HI) decreased with the increase of BAS [66]. The presence of hydroxyl groups on the catalysts surface is determined from the absorption in the 3200-3800 $cm^{-1}$ region of the infrared spectra on dehydrated samples [23]. Brønsted acidity is evaluated by measuring the wavenumber shift after adsorption of probe molecules (CO, tert-butylnitrile, acetonitrile and pyridine) [67–69].

Titanol groups (Ti-OH) could also contribute to the Brønsted acidity of titanosilicates. Some studies detected both silanol and titanol groups in TS-1 [70] and other titanosilicates such as Ti-SBA-15 [33] and Ti-TUD-1 [71]. In contrast, other studies found that the insertion of $Ti^{4+}$ atoms in the framework did not generate Brønsted acid detectable sites. For example, the characteristic band at 3676 $cm^{-1}$ was not detected in dehydrated TS-1. In fact, this band appeared after contact with $H_2O_2$. In the structure of TS-1, neighboring Si vacancy defects produce internal hydrogen-bonded silanols (Si-OH) which can act as weak Brønsted acid sites [72].

On the other hand, $Ti^{4+}$ atoms in titanosilicates act as Lewis acid sites (LAS). It has been extensively studied that LAS catalyze efficiently oxidation reactions [23]. LAS were detected by infrared spectroscopy using acetonitrile as probe molecule in adsorption experiments [73]. Other Ti active species with different Lewis acidic strengths can also affect the oxidation mechanism (i.e., distorted tetrahedral species, tripodal $Ti(OSi_3OH)$ and octahedral Ti), but there is a consensus that the species with the highest Lewis acidity are the most capable of oxidizing organic substrates such as olefins [23,31].

### 1.1.3 Titanosilicates based on zeolite frameworks (Ti-zeolite)

Ti-zeolites have a crystalline structure composed of $SiO_4$ tetrahedral units in which one or more Si atoms can be replaced by Ti atoms without introducing negative charges [74]. Ti-zeolites have been used as catalysts of selective oxidation reactions (e.g., epoxidation of olefins, hydroxylation of phenol, ammoximation of ketone, oxidative desulfurization and oxidation of pyridine derivatives) [75].

The differences in shape, size and channel topology of zeolites enable their use in a wide range of industrial applications. In addition, Ti-zeolites are important not only for the technical performance but also, they are environmentally friendly since the optimization of these catalysts has turn certain processes more efficient and less waste is generated, following the principles of green chemistry [2].

There is extensive information available about Ti-zeolites; for instance, Ratnasamy and co-workers in 2004 published the stat-of-the-art about the active sites and intermediate Ti species in crystalline titanosilicates [23]. Later in 2014, Moliner and Corma reviewed the advances in the preparation of ordered titanosilicates focusing on the texture [74]. An important contribution about the latest progress in the synthesis of titanosilicates was stated by Xu and Wu in 2017; in which topology, morphology and chemical environment were analyzed [12]. Recently in 2018, Přech described the catalytic performance of titanosilicates in selective oxidation reactions [2].

Přech presented a precise classification of Ti-zeolites according to their textural properties, shape, pore size, Ti active sites content and Ti active sites location. In Přech's publication, Ti-zeolites were divided in 4 groups: i) conventional Ti-zeolites (Table 1) with same order of magnitude of the 3 crystal dimensions without cavities and other defects, ii) hierarchical Ti-zeolites that exhibit typical micropore structure (zeolitic structure) and more or less ordered system of mesopores (20-430 Å in diameter), iii) lamellar Ti-zeolites containing mesoporous between lamellae, and iv) mesoporous titanosilicates with amorphous structure, but ordered system of mesopores (20 Å) [2].

**Table 1** Pore size of conventional Ti-zeolites. Adapted from Přech [2].

| Group | Sub-group | Ring pores | Diameter (Å) |
|---|---|---|---|
| Conventional Ti-zeolites | Medium-pore | 10 | 4.5-5.5 |
| | Large-pore | 12 | 5.5-7.0 |
| | Extra-large-pore | 14 | >7.0 |

Since the synthesis of TS-1, more than 30 Ti-zeolites (Table 2) have been developed. However, only few of them, including Ti-Beta, Ti-MWW, Ti-MOR have been used on industrial scale [12,75]. TS-1 has been efficiently used as catalyst of oxidation of small molecules using aqueous $H_2O_2$ as oxidant. However, TS-1 and other medium-pore Ti-zeolites such as Ti-YNU-2 [76] presented limitations in the diffusion of reactants and products due to its intrinsic microporosity. Large substrates such as linear olefins or phenol cannot access to the internal active sites causing the reaction to occur only on the outer surface [77,78]. In order to solve this limitation, new Ti-zeolites have been synthesized including large-pore Ti-zeolites as: Ti-MCM-41 [79], Ti-MCM-48 [80], Ti-Beta [81] and Ti-MOR [82], and extra-large Ti-UTL [83].

Another alternative to improve the porosity and exposure of the active sites is the introduction of mesoporous systems in the intrinsic microporosity to obtain hierarchical zeolites [13,75,78] or lamellar zeolites such as Ti-MFI [84], Ti-MWW [85] and Ti-FER [86,87]. The synthesis of nanocrystals of Ti-zeolites has also appeared as an interesting strategy to increase the specific surface area of these materials [88]. The improvement of the textural properties allows the diffusion of bulky substrates. However, these materials display more hydrophilicity, which affects their catalytic performance, compared to TS-1 [89–91]. For this reason, modifying the hydrophobicity of the catalyst surface could enhance the catalytic performance as it has been proposed by some researchers [41,92,93].

254 **Table 2** Microporous and mesoporous Ti-Zeolites. Adapted from Xu and Wu [12].

| Year | Material | Framework type code |
|---|---|---|
| | **Microporous materials** | |
| 1983 | TS-1 | MFI |
| 1989 | ETS-1 | |
| 1990 | ETS-4 | |
| | TS-2 | MEL |
| 1992 | Ti-Al-Beta | BEA |
| | Ti-ZMS-48 | MRE |
| 1994 | Ti-SAPO-5 | AFI |
| 1995 | Ti-ZSM-12 | MTW |
| | Ti-UTD-1 | DON |
| | Ti-UTD-8 | |
| 1996 | Ti-Beta | BEA |
| | Ti-MOR | MOR |
| 1998 | Ti-FER | FER |
| 1999 | Ti-ITQ-2 | MWW |
| 2000 | Ti-MWW | MWW |
| | Ti-ITQ-6 | FER |
| | Ti-ITQ-7 | ISV |
| 2004 | Ti-YNU-1 | MWW |
| 2007 | Ti-MCM-36 | MWW |
| 2008 | IEZ-Ti-MWW | MWW |
| | Ti-MCM-56 | MWW |
| | Ti-MCM-68 | MSE |
| 2011 | Ti-COE-4 | |
| | L-TS-1 | MFI |
| 2014 | Ti-ECNU-8 | FER |
| | Ti-YUN-2 | MSE |
| 2016 | Ti-UTL | UTL |
| | Ti-IPC-2 | OKO |
| | Ti-IPC-4 | PCR |
| | **Mesoporous materials** | |
| 1994 | Ti-MCM-41 | |
| | Ti-HMS | |
| 1995 | Ti-MSU | |
| 1996 | Ti-MCM-48 | |
| 1999 | Ti-SBA-15 | |
| 2001 | Ti-MMS | |
| 2002 | MTS-9 | |
| 2004 | Ti-MMM-1 | |
| | Ti-MMM-2 | |

255255

256 In general, many titanosilicates have been created but only few of them are used in industrial
257 processes such as TS-1, Ti-Beta, Ti-MCM-41, Ti-MCM-48, Ti-SBA-15, Ti-MWW and Ti-MOR. The last
258 two are not presented in this section but the description of these titanosilicates is presented in
259 ANNEX I.

The aim of this work is to discuss about the titanosilicates that have been hydrophobically modified, according to the literature. Our discussion will be focused on the influence of such modification on their catalytic activity.

1.1.3.1 TS-1

The TS-1 titanosilicate was synthesized by Tamarasso et al. [51] in 1983. TS-1 is an aluminum free Ti-zeolite categorized as a common medium pore (10-ring pore channels) zeolite with MFI framework type and Ti atoms introduced in its structure [55]. TS-1 has been employed as one of the most efficient catalyst in several oxidation processes [94–99]. Reviews about the synthesis and properties of TS-1 were published by Notari in 1993 [100] and 1996 [50]. TS-1 has been synthesized by several routes varying the Si and Ti sources as well as the template and mineralizing agent, in function of their industrial use. These different methodologies were collected in the work of Perego et al. [101]. However, one of the most common method of synthesis of TS-1 is the hydrothermal method using tetraethyl orthosilicate (TEOS) as precursor of Si, and different precursors of titanium such as tetrapropyl orthotitanate (TPOT) or tetrabutyl orthotitanate (TBOT)), with tetrapropyl ammonium hydroxide (TPAOH) as structure-directing agents (SDA). The preparation of TS-1 often requires the use of microporous SDAs due to the low synthesis yield [34,51,102]. The maximum atomic percentages of tetrahedral Ti active sites in the MFI zeolite framework is 2.5% (Ti/Ti+Si) [13]. The methodologies for preparation of TS-1 are focused in obtaining more tetrahedral Ti(IV) active sites as possible and diminishing the formation of EFW-Ti [14].

1.1.3.2 Ti-Beta

Ti-Beta is a large-pore (12-ring pore channels) Ti-zeolite with BEA framework type and Ti atoms incorporated in the zeolite structure. Originally, Ti-Beta was described as a titano-aluminosilicate by Camblor et al. [103]. Aluminum containing Ti-Beta was prepared by conventional hydrothermal synthesis to introduce Ti directly into the zeolite structure using tetraethylammonium hydroxide (TEAOH) as SDA. The Ti/Al ratio was around 50 for all samples [103].

The presence of Al in the Beta framework produces acid centers which can act as acid/redox active sites. The selectivity and activity of oxidation reactions was affected by the acidity of the Al-containing Ti-Beta catalysts. For instance, the selectivity to epoxide decreases in epoxidation of olefins with the increase of Al [1]. For this reason, Al-free Ti-Beta was synthesized by Camblor et al. using dealuminated Beta-zeolite as crystallization seeds [104]. These seeds were obtained from Beta zeolites prepared according to Camblor et al. [105], and then, they were dealuminated by acid treatment using $HNO_3$ (60%) at 80°C during 24 h with liquid/solid ratio of 60. The Si/Al ratio was higher than 1 000 [106]. The dealuminated Beta-zeolite seeds were added to a mixture of Si and Ti precursors, tetraethylammonium hydroxide (TEAOH), $H_2O$, and $H_2O_2$. The Si/Al ratio increased over 10 000 [104]. Another study proposed the synthesis of Al-free Ti-Beta by unseeded method in fluoride ($F^-$) medium [37]. A recent method to obtain Al-free Ti-Beta involved the post-grafting of Ti onto dealuminated Beta. For this purpose, commercial Beta zeolites with specific Si/Al ratio were dealuminated by acid treatment with $HNO_3$ and then, Ti atoms were inserted by adding $TiCl_4$ to a suspension of dealuminated Beta zeolite in dichloromethane ($CH_2Cl_2$) [39].

Ti-Beta is an efficient catalyst for epoxidation of cyclic and long linear alkenes and also cyclic and branched alkanes [107]. For example, Ti-Beta exhibits better catalytic performance in the epoxidation of cyclohexene in comparison to TS-1 [108]. However, due to the limitation of the number of tetrahedral Ti active sites, some alternatives have been developed to improve the Ti content of these catalysts [38,109–113].

1.1.3.3 Ti-MCM-41

The MCM zeolite with a one-dimensional channel system is a widely studied mesoporous material due to its interesting structural and textural features. It consists of a hexagonal array of unidirectional tubular pores. Ti-MCM-41 high surface area (frequently above 1000 $m^2g^{-1}$) and pore

size (2-10 nm) allow the use of this zeolite as catalyst of a wide range of chemical processes [114,115]. The Ti-MCM-41 with regular pores of 35 Å is an extra-large Ti-zeolite obtained by direct synthesis using tetramethylammonium hydroxide (TMAOH) [79,116]. Important variables such as the $OH/SiO_2$ ratio and the content of alkali metal cation must be considered to prepare catalysts with Ti active sites in tetrahedral coordination. In absence of alkali cations, an optimum $OH/SiO_2$ ratio of 0.26 allowed the formation of Ti-MCM-41 with high content of FW-Ti and undetectable EFW-Ti [79]. The pore size of Ti-MCM-41 with high crystallization may be controlled by regulating the temperature of synthesis [117] whereas the Ti-MCM-41 channel diameter can be adjusted by using different surfactant templates [118].

Other modifications of the synthesis of Ti-MCM-41 have been applied to increase the number of Ti active sites. For example, electrostatic assembly of Ti-MCM-41 achieved higher catalytic activity in the liquid-phase oxidation of styrene, methyl methacrylate and 2,6-di-tert-butyphenol [119], post-grafting of titanium atoms to form Ti-MCM-41 based materials [120], synthesis of Ti-MCM-41 by hydrothermal method using supercritical fluid as an extraction medium to remove of SDA [121], and post-synthesis salt solution treatment with alkaline and ammonium salts which increases the tetrahedral Ti and improves the catalytic activity and selectivity in the epoxidation of cyclohexene [122], among others.

The mesoporous Ti-MCM-41 are important in the reactions of bulky substrates. For example, Ti-MCM-41 showed higher catalytic activity for cyclooctene and cyclododecene epoxidation than TS-1, Ti-Beta and Ti-MWW [123]. Ti-MCM-41 has been used in the phenol and 2,3,6-trimethylphenol hydroxylation and styrene epoxidation [124], propylene epoxidation [125–127] and cyclohexene epoxidation [128]. Also, Ti-MCM-41 and MCM-41 has been used as support of catalysts for oxidation reactions [129,130].

#### 1.1.3.4 Ti-MCM-48

The MCM 41 and MCM 48, and other structures are members of a family of mesoporous molecular sieves denoted M41S with high importance into the catalysis and materials fields. The MCM-48 zeolite framework has a cubic array and a 3-dimmensional channel system [80,131]. MCM-48 displays catalytic advantages over a MCM-41 due to the 3-dimmensional pore system and its better resistance to obstruction by strange materials [80].

A study about the stabilization of the M41S was developed by Tatsumi *et al.*, in 1998. It is known that the MCM-41 and MCM-48 molecular structures collapsed by mechanical compression due to the hydrolysis of Si-O-Si bonds in presence of water adsorbed into the sieve. The trimethylsilylation was carried out to modify the hydrophobicity of these materials and improved their stability in water [132]. The Ti-MCM-48 was synthesized by a one-stage hydrolysis method and two-stage method using a solution of tetraethylorthosilicate (TEOS) and TBOT as precursors and *n*-hezadexyltrimethylammonium hydroxide and cetyltrimethylammonium chloride [80]. Also, Ti-MCM-48 was prepared using the cetyltrimethylammonium bromide as surfactant [133]. The Ti-MCM-48 has been employed as catalyst in the epoxidation of 2-buten-1-ol [134], methallyl chloride with $H_2O_2$ [135], allylic compounds with $H_2O_2$ [136], crotyl alcohol [137], photocatalytic degradation of rhodamine B [138] and in the removal of Cd(II) by adsorption [139]. CdS has been incorporated in the Ti-MCM-48 material for photocatalytic decomposition of water [140] and solar hydrogen generation [141]. Metals such as Fe [142] and Pd [143] and oxides such as CuO [144] and Cu-porphyrin [145] have been impregnated in Ti-MCM-48 structure for different applications. Also, Ti-MCM-48 has been used as support of Au for the vapor-phase propylene epoxidation [125].

#### 1.1.3.5 Ti-SBA-15

The SBA-15 structure has pores with diameters between 50 and 300 Å, a surface area of 600-1000 $m^2g^{-1}$ and pore volumes of 0.6-1.3 $cm^3g^{-1}$. The SBA-15 zeolite was synthesized using triblock copolymers as a template under acid conditions. The resulting SBA-15 contained high silanol groups on the surface which then offer reactive sites for post-functionalization. Ti was introduced into the

SBA framework by both hydrothermal and post-grafting methods. These methods produced catalysts with high catalytic activity and high surface area capable of oxidize molecules with large size [146,147].

Ti-SBA-15 is an ultra-large mesoporous Ti-zeolite similar to Ti-MCM-41, except Ti-SBA-15 has a one-dimensional system with hexagonal array, but the main channels are connected by micropores [148]. Fluoride medium has been applied in the synthesis of Ti-SBA to accelerate the hydrolysis rate of Si precursors. The catalytic activity and selectivity of this Ti-SBA was higher in the styrene epoxidation [149].

The Ti-SBA has been used as catalyst of several reactions such as oxidation of methyl-propyl-thioether using $H_2O_2$ as oxidant [150], alkene epoxidation [148], hydrodesulfurization [151] and hydrogenation of tetralin [152]. Among other applications, Ti-SBA-15 has been applied as support for different metals such as NiMoW and CoMoW [153], and CoMo [154] for hydrodesulfurization reactions, ionic liquids with Brønsted-Lewis acidity also were deposited on Ti-SBA-15 by impregnation method and then were used as catalyst for esterification of acetic acid [155].

### 1.1.4 Titanosilicates without zeolite frameworks (Ti-$SiO_2$)

The discovery of TS-1 represents a breakthrough in the oxidation of organic compounds with solid catalysts under mild conditions. However, due to the mass-transfer limitations in microporous TS-1, several large and ultra-large Ti-zeolites have been synthesized. There is an increasing interest in the fabrication of titanosilicates with even larger pore sizes and higher number of Ti active sites that can be used with bulkier substrates. In this way, amorphous titanosilicates with no zeolitic framework (Ti-$SiO_2$), also called titania-silica ($TiO_2$-$SiO_2$) mixed oxides, have been prepared for oxidation reactions [3,156].

The first Ti-$SiO_2$ was synthesized by Shell researchers in 1971 [157] and they were used as catalyst of propylene epoxidation with alkylhydroperoxides as oxidants. The active sites of this type of catalysts are tetrahedral Ti isolated by O-Si fragments. The formation of Ti-O-Si bonds renders chemical stability to the Ti-$SiO_2$ catalysts and prevents leaching problems [158]. Also, the dispersion of titanium into the silica matrix generates Lewis acid sites. The catalyst acidity increases with the higher dispersion of titanium in the silica matrix [159].

Ti-$SiO_2$ catalysts can be prepared by sol-gel method. The first attempts to use sol-gel to synthesize Ti-$SiO_2$ for cyclohexene and cyclooctene epoxidation with $H_2O_2$ were reported by Neumann *et al.* in 1993. Ti-$SiO_2$ were efficient in the olefin's epoxidation after 20 hours [160]. The influence of the sol-gel preparation method and drying conditions on the structural and chemical properties of Ti-$SiO_2$ were studied by Hutter et al. in 1990s [3]. It has been demonstrated that by an appropriate preparation and drying conditions, an amorphous material with high surface area and outstanding titania dispersion (20 %wt $TiO_2$) in silica matrix can be achieved [3]. In a second part of their investigation, Hutter et al. reported about the catalytic properties of Ti-$SiO_2$ for epoxidation of olefins [161]. High catalytic activity and selectivity can be expected for Ti-$SiO_2$ with mesoporous structure regarding the epoxidation of linear or cyclic olefins and electron-deficient olefin such as α-isophorone which are difficult to epoxidize [158].

The remarkable catalytic activity of Ti-$SiO_2$ is related with their textural and structural properties (mesoporosity and high dispersion of Ti). Therefore, the Ti content has an influence on the structural and catalytic properties of Ti-$SiO_2$ catalysts and consequently in the accessibility of the reactants on the Ti active sites in tetrahedral coordination [3]. Initially, it was determined that an increase of the content of Ti from 2 to 20 wt% $TiO_2$ increased the Si-O-Ti heteroconnectivity, so a maximum of 20 wt% $TiO_2$ was appropriate for epoxidation catalysts. An increase to 30 wt% $TiO_2$ leads to agglomerates of $TiO_2$, bad dispersion of Ti and lower catalytic activity. Another relevant factor that regulates the textural properties is the aging of the wet sol-gel which strengthens the gel network and thereby preserves the porous network of the dried gel [162].

Ti-$SiO_2$ catalysts are commonly used for olefin isomerization [163–165], aromatics amination [163], alcohols dehydration [166], aromatics dealkylation [166] and selective oxidation [46,47,175–

178,167–174]. Since the first synthesis of Ti-$SiO_2$, several researchers focused on the study of this group of materials. A review, published by Davis and Liu in 1997, summarizes valuable information about the microstructural characteristics and catalytic activity of Ti-$SiO_2$ catalysts [179]. Other applications of Ti-$SiO_2$ in the catalytic field can be found in the literature [167,169,180–185].

A drawback of Ti-$SiO_2$ catalysts is their strong hydrophilic character caused by the silanol groups present on the surface. This property limits their use in aqueous media or in presence of hydrogen peroxide as oxidant. The deactivation of Ti active sites in tetrahedral coordination can be decreased by hydrophobization of the surface. Therefore, some researchers have studied the influence of hydrophobic modification of the catalyst surface on their catalytic activity [45,172,173,186,187].

### *1.2 Description of the hydrophobization methodologies and techniques for measuring the hydrophobicity of titanosilicates.*

#### 1.2.1 Hydrophobicity basics

The term hydrophobicity/philicity refers to the affinity that exists between a solid surface and water. A hydrophobic surface can be defined similarly as a hydrophobic substance. Nonpolar substances are hydrophobic and have low solubility in water at room temperature. The accumulation of the nonpolar molecules in aqueous media produces a high cohesive energy density of water that decreases the interface between the nonpolar substance and water, explaining the hydrophobic effect. Therefore, to transfer nonpolar molecules into a aqueous media, the enormously stable hydrogen bond among water molecules must be disrupted [32,188]. A summary of intermolecular interactions is presented in ANNEX II.

Although there are some analytical techniques that provide information about hydrophobicity of flat surfaces, there is not a specific technique for porous solid surfaces. The hydrophobic effect in solids is related to the absence of interfacial interactions with water or similar dipolar and protic molecules. And more exactly, a better definition can be achieved contemplating the possible forces between a solid surface and an adsorbate molecule. The interactions of water with a solid surface are commonly generated from specific surface sites such as functional groups that can act as Brønsted or Lewis acids or bases (Table 3) [32].

**Table 3** Functional groups that affect the hydrophilic character of solid porous surfaces [32].

| Functional group | | Occurrence |
|---|---|---|
| Hydroxyl | -OH | Oxides, hydroxides |
| Carboxyl | -COOH | Carbons |
| Carbonyl | -C=O | Carbons |
| Ether | -O- | Oxides, carbons |
| | Ionic species (i.e., $H^+$, $Na^+$, $Mg^{+2}$, $Cl^-$) | Ion exchanger |

The mutual molecular interactions that affect the wettability of a solid surface are reflected in a macroscopic parameter known as contact angle (CA) formed between the solid phase boundary and the liquid phase [189]. It is possible to quantify the hydrophobicity of the solid surface as a function of the CA. However, there are some limitations to measure the CA of rough solid surfaces or surfaces with defects such as functional groups (i.e., silanol groups) [32].

It should be noted that hydrophobicity/hydrophilicity is a relevant property that must be considered for the synthesis of porous solid catalysts. The catalytic performance of a solid catalyst is not only associated to the active sites but is also influenced by the catalyst wettability which affects the adsorption and desorption processes and mass transfer on the surface (Figure 3). Adjustment of the surface hydrophobicity could enhance the activity, selectivity and lifetime of catalysts [190]. Thus, it is necessary to inquire into the concepts of hydrophobicity to apply measuring techniques in the correct form.

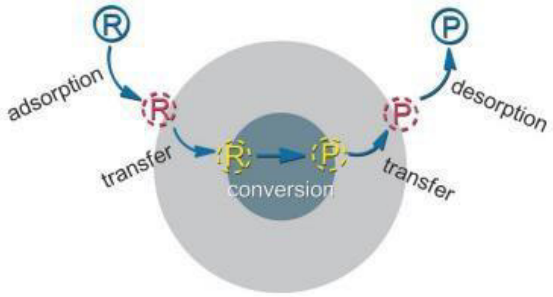


**Figure 3** Reaction process over a solid catalyst (R= reactants, P=products). Taken from [190]

### 1.2.2 Methodologies for hydrophobization of titanosilicates

The catalytic activity of titanosilicates depends not only on the dispersion of the tetrahedral Ti active sites, but also on the hydrophobic character of the material [191]. Two main strategies have been used to modify the hydrophobicity of titanosilicates. The first strategy is the modification of the hydrophobicity by the control of the silanol surface density. It is known that free-defect siliceous surfaces formed by Si-O-Si bonds are hydrophobic [63], whereas hydroxyl groups (Si-OH) and bridging hydroxyl groups (i.e., Si-OH-Ti, Si-OH-Al) are hydrophilic [64]. The hydrophilic character of these materials increases while the surface density of silanol groups increases, thus they adsorb more water [65].

The silanol surface density can be adjusted by improving the crystallization of the material, and by synthesizing the material in fluoride ($F^-$) medium instead of $OH^-$ medium. Highly crystallized TS-1 has less Si-OH terminal groups and is more hydrophobic [34]. Some heteroatom-substituted MFI zeolites (M-MFI), including Ti-zeolites, were synthesized in fluoride medium ($F^-$) using hydrofluoric acid (HF) with TPAOH as structure directing agent. Adsorption isotherms showed that M-MFI zeolites synthetized in $F^-$ medium adsorbed 100 times less water than the analogous materials synthesized in $OH^-$ medium. Also, the number of Si-OH groups decreased linearly with the increasing HF/TPAOH ratio [192]. Al-free Ti-Beta was another Ti-zeolite modified hydrophobically by synthesis in $F^-$ medium, and a lower content of Si-OH was detected compared to the conventional Ti-Beta [38].

The second strategy applied to modify the hydrophobicity of the titanosilicates is the functionalization with organic groups both on the catalyst external surface and on the internal porosity where the active sites are located [193]. The functionalization of the catalyst surface has been carried out by "post-grafting" of organic groups [93] and by “one-pot functionalization” [194,195]. For example, Ti-$SiO_2$ functionalized with poly(methylhydrosiloxane) (PMHS) by post-grafting was more hydrophobic than conventional Ti/$SiO_2$ [49]. In the same way, Ti-MCM-41 functionalized by the one-pot procedure with organosilanes exhibited lower silanol surface density and a strong hydrophobic character [40]. Hydrophobic environments, both on the external and internal surface could have important consequences on the reactivity of porous catalysts [65].

#### 1.2.2.1 Control of silanol density

The content of silanol defects on titanosilicates can be adjusted by the control of the crystallization process. This crystallization process of these materials is complex, and it is affected by some synthesis parameters such as the silica source, templates, and SDAs. Crystallization of titanosilicates is more difficult than crystallization of aluminosilicates because $Ti^{4+}$ displays a weaker structure-directing role compared to $Al^{3+}$. In addition, the Ti-O bond (1.80 Å) is longer than the Si-O bond (1.61 Å), which distorts the structure around Ti and results in a slow insertion of Ti into the zeolite framework and in the formation of undesired phases. These facts make more complex the isomorphous substitution of $Si^{4+}$ by $Ti^{4+}$ compared to that of $Al^{+3}$ by $Ti^{4+}$. The isomorphous substitution is influenced by the crystallization of titanosilicates. An effective crystallization-mediating agent was proved as an alternative to improve the crystallization of TS-1. The characterization of the TS-1

obtained by this method showed that the insertion of titanium into the framework was improved and the silanol defects decreased [34].

On the other hand, the presence of silica networks in microporous, mesoporous, and amorphous materials strengthen the coordination of heteroatoms united by oxygen which prevent hydrolysis and leaching. Hydrophobic structures in silica surface avoid the hydrolysis of Si-O-Si and Si-O-M bonds since they disturb the formation of long water phases near them, preventing the deactivation of active sites in aqueous media. Hydrophobic structures also avoid the deactivation of active sites produced by water adsorption. Silica and metal oxide networks (Si-O-M) are present in Brønsted and Lewis acid oxides [65].

In the case of aluminosilicates, the low silicious zeolites (Si/Al= 1-2) possess high amounts of $AlO_4$ units and Si-O-Al bridges, so they are more hydrophilic than high silicious zeolites (Si/Al= 10-∞) [196]. The Al-O bond is more polar (40% covalent and 60% ionic bond) than the Si-O bond (100% covalent bond) and thus, strong interactions with water are produced [197]. On the other hand, silanol groups and bridging hydroxyl groups form hydrophilic domains into the silica framework [64] and these polar hydroxyl groups adsorb water. Thus, the amount of water adsorbed is related to the Al content in zeolites. For instance, the water adsorption of ZSM-5 [198,199], Beta [64], MCM-41 [200], and Ti-Beta [38] gradually decreased with the increase of Si/Al ratio.

In this context, the combination of dealumination and post-insertion of heteroatoms can produce materials with higher hydrophobicity [39]. According to the IR characterization of dealuminated Ti-Beta, a higher content of Si-OH groups was detected with the decrease of Al content [104]. In contrast, when titanium heteroatoms were incorporated into dealuminated Beta zeolite, the density of isolated silanol groups decreased whereas silanol nests $(SiOH)_4$ decreased in Beta zeolites with less amount of Al compared with those with high Al content [39]. As shown in Figure 4, the dealumination process creates vacancy defects which result in the formation of silanol nests that consequently increases the hydrophilicity of these materials. The incorporation of Ti atoms in these vacancy defects decreases the concentration of silanol nests.

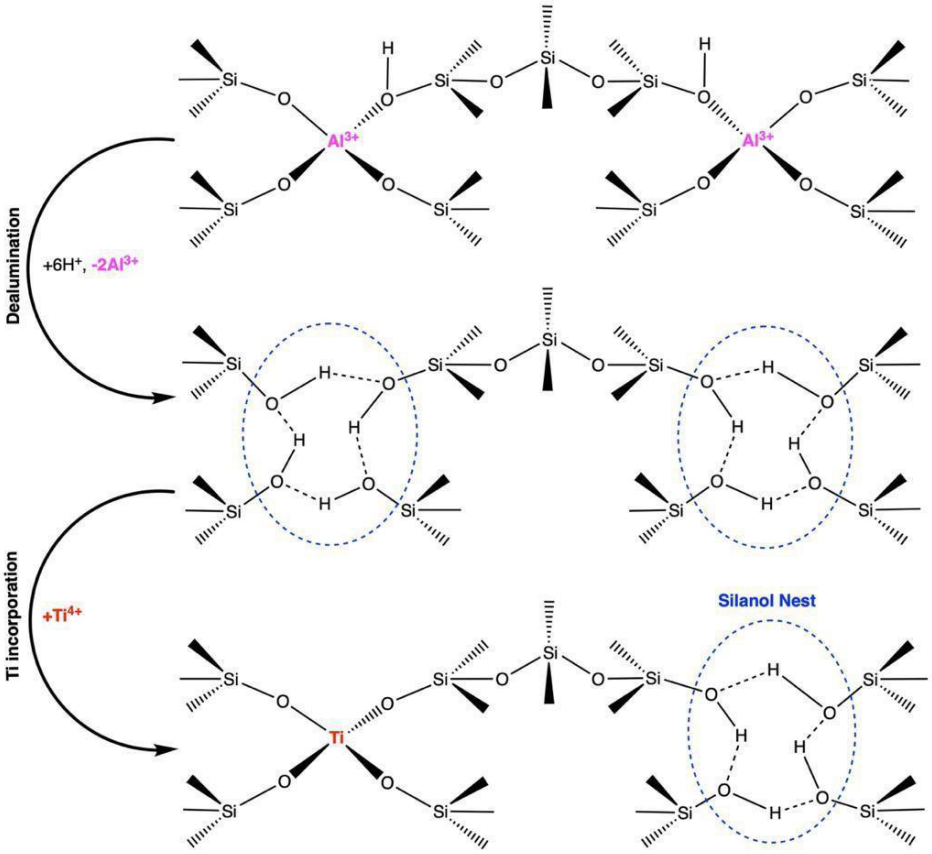


**Figure 4** Dealumination and post-incorporation of Ti to prepare Ti-Beta.

Al-free Ti-Beta can also be obtained by indirect ways, one of them is the dealumination of Ti-Beta. Another way is the synthesis of Ti-Beta using dealuminated seeds of Beta zeolite, and the last one is the post-synthetic modification of commercial Beta zeolite (see section 1.1.3.2).

A direct way to synthesize hydrophobic Al-free Ti-Beta is using fluoride ($F^-$) medium instead of aqueous ($OH^-$) medium. The $F^-$ medium prevents the formation of anionic framework vacancy defects since the cationic charges of SDAs employed in the synthesis are counterbalanced by $F^-$ forming strong ion-pairs [201,202]. As shown in Figure 5, when $OH^-$ anions are used in the synthesis, anionic framework vacancy defects are produced and after removal of SDA cations, silanol nests are formed in zeolite framework increasing the hydrophilicity of the material.

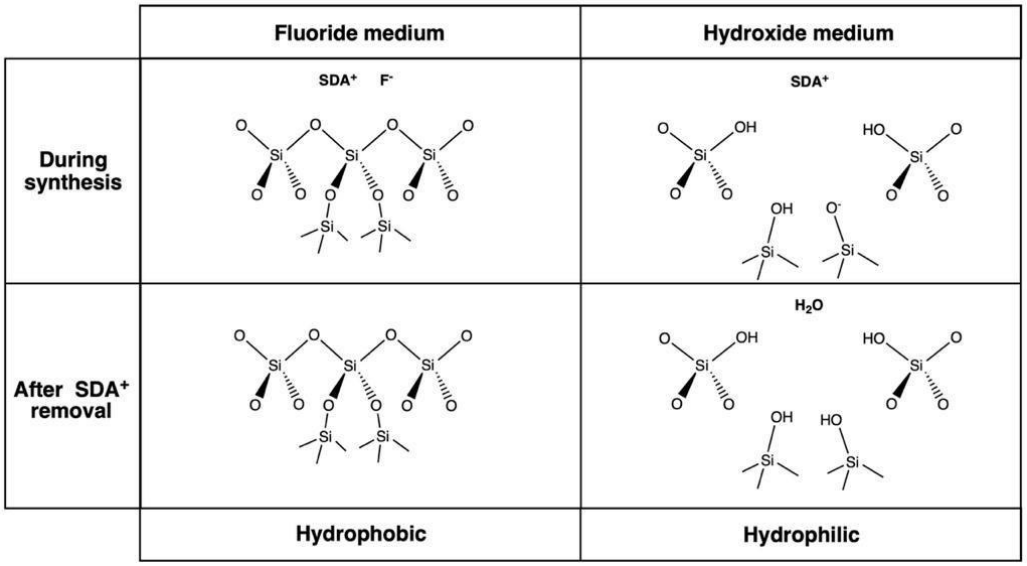


**Figure 5** Preparation of zeolites in fluoride medium and aqueous medium. Adapted from [202].

As already mentioned, the silanol surface density of titanosilicates could be modified through the presence of $F^-$ ions during synthesis. However, the presence of $F^-$ ions reduces the incorporation of Ti atoms into the final material. Therefore, determining the optimal concentration of $F^-$ ions able to decrease the silanol surface density while maintaining an effective incorporation of heteroatoms in the titanosilicates is essential. Indeed, the ratio between HF/SDA (TPAOH) was optimized by Bregante et al. for zeolitic materials with MFI structure (Silicalite-1) where heteroatoms Nb, Ta, and Ti were inserted. The relative silanol density was quantified using IR spectroscopy. The authors normalized the area of $\nu(Si-OH)$ relative to that of the $\nu(Si-O-Si)$, observing a linearly decrement as the HF/TPAOH ratio (x) increases. With x<1, the relative silanol density decreased by 4-8-fold, whereas for x=1.5, the relative silanol density decreased 30-100 times compared to materials synthesized in $OH^-$ medium. For x>1.5 the relative silanol density was undetectable. The formation of the strong ion-pairs between TPAOH cation ($TPA^+$) and $F^-$ is reversible and the concentrations of species are defined by the equilibrium. Finally, water adsorption experiments of TS-1 showed that TS-1 synthesized in $F^-$ medium stabilized ~5 water molecules at vapor pressure at 293 K and adsorbed 7−100 times less water than TS-1 synthesized in $OH^-$ medium. The number of water molecules stabilized by Ti was calculated from the difference between the $H_2O$ uptake of TS-1 and silicalite-1, which is then normalized by the number of Ti atoms [192].

1.2.2.2 Organic functionalization

Organic functionalization of titanosilicates through one-pot and post-grafting method were applied to obtain more hydrophobic catalysts. The silanol density in functionalized materials was lower than in the non-functionalized ones [28,40,41,45,48,49,203]. This low density was mainly

attributed to the substitution of Si-OH groups by organic moieties and it was confirmed by IR spectroscopy and $^{29}Si$ NMR analysis [40,41,45,49].

The effect of the organic functionalization on the catalytic activity was in some cases either positive for Ti-$SiO_2$ [48] and Ti/$SiO_2$ [49], or negative for Ti-Beta [6] or non-significant for TS-1 [6] and Ti/$SiO_2$ [204]. A possible explanation about the different catalytic effects was that the post-grafting can also modify the structure and textural properties of catalysts, and the nature of active sites [45].

The principal difference between post-grafting and one-pot methods lies on the Ti dispersion. According to XPS and DRUV-Vis analysis, titanosilicates functionalized by the one-pot method exhibited lower Ti dispersion. One-pot functionalization method is faster and it can be controlled by the chemistry of precursors [45]. Ti speciation was not affected by post-grafting in most of the cases. Regarding the textural properties, both functionalization procedures diminished the specific surface area and pore size. This difference in textural properties can affect the catalytic performance of functionalized catalysts [48].

Ti dispersion on one-pot synthesis was enhanced using aerosol-assisted sol–gel. With this method, not only the Ti dispersion but also the organic functionalization and textural properties were controlled [11]. The effective dispersion of Ti with this method was attributed to the fast drying of the atomized mixture of precursors, which produces the quenching of kinetic condensation and leads to the formation of stable solid phases with homogeneous compositions [205].

### 1.2.3 Determination of hydrophobicity of titanosilicates

Some analytical techniques applied for the characterization of the hydrophobic character of porous solids will be discussed in this section. Due to the absence of a precise definition of the term hydrophobicity and its origin, the analytical techniques applied to characterize this property in solids differ particularly regarding the experimental method and the physical/chemical properties considered for the evaluation of the porous solid surface. In fact, analytical techniques have ranked a given set of porous solids according to their hydrophobic character, but a quantitative assessment, considering the theory remains a challenge. Also, it is important to keep in mind that the conditions under which the experimental analysis is carried out not always correspond to the conditions in the application, especially in the case of catalysts. In addition, the applicability of the characterization techniques will depend on each type of porous solids [32].

#### 1.2.3.1 Contact Angle Measurement

As already mentioned in the section 1.2.1, the contact angle (CA) is a known technique that allows the characterization of surface wettability. The CA is related to the lowest state of the energy that characterizes a three-phase system (solid-liquid-gas). This experimental thermodynamic property corresponds to the observed angle at the contact line among these three phases. This angle is bounded by the tangent to the liquid–fluid interface and the tangent to the solid surface [206]. The CA is computed using the Young equation [207]. The Young's equation associates several terms as the solid surface energy $\gamma_{sv}$ , the solid-liquid surface tension $\gamma_{ls}$ , the liquid surface tension $\gamma_{lv}$ and the cosine of the contact angle θ. As a soon as a resting drop reaches the mechanical equilibrium on a plane solid surface, these three forces are balanced and can be described as expressed in Eq (1) [208].

$$\gamma_{sv} = \gamma_{ls} + \gamma_{lv} \cos\theta \quad (1)$$

For a drop with a certain radius of curvature, the CA equals the Young contact angle as long as this radius is larger than the nanometric scale. The Young contact angle is related to the equilibrium state reached by a drop on an ideal solid. However, a correction term needs to be applied for drops with smaller radii of curvature [206,209–211]. The ideal determination of the CA may encounter some difficulties, starting even before the measurements with the correct preparation of the solid surface and then during the measurements with the control of the equilibrium conditions. These challenges render the experimental determination not always feasible [206].

Contact angles are principally reported as static and dynamic. On the one hand, if the three-phase boundary is not moving and the droplet is sitting on the surface, measurements of static contact angles are obtained. On the other hand, if the three-phase boundary moves, measurements of dynamic contact angles are registered. These angles are defined as advancing (when the droplet front is advancing) and receding (when the droplet front is receding). The term hysteresis referred to contact angles is then established as the comparison between these two angles (advancing and receding). Experimental approaches like sessile drop and/or captive bubble [212–216] are preferred methods for the measurement of contact angles at ambient conditions on flat surfaces under different pressure and temperature conditions [217].

Several factors affect contact angles including deformation, roughness, contamination, and surface geometry. Thus, it is not uncommon to find more than one contact angle value reported for a certain system, taking into account all the variables that affect the experimental determination of the CA [206]. Furthermore, in most natural materials the effective contact angle observed at larger scales is influenced by the surface roughness detected at the nanometer scale. Regarding the porous media as the closest approach to understand the wettability of porous solids as titanosilicates, some challenges are identified. In general, contact angles in porous media can be not only variable throughout the pore space, but also scale-dependent and hysteretic owing to the presence of local surface roughness enhanced by variations in mineralogy and coating. However, it has been possible to determine geometrical contact angle values in the pore space. Some of the more common measurements include automated algorithms [218,219] or visual observation [220,221]. Other methods analyze the solid and fluid interfaces through the deficit curvature between them [222]. Recently, 3D images of fluids in the pore space generated by mCT (micro-computed X-ray tomography) were used for geometrical analysis of contact angles [223,224]. Nevertheless, the interpretation of these measurements are still difficult, regarding the broad range of variation found in the contact angle values obtained by this technique [225,226]. In fact, the scale of the pore size distribution of titanosilicates, which can vary from 5 Å to ~100 nm, is even smaller compared to the roughness scale range (~200 µm) reached through the most sophisticated techniques for determining the contact angle in porous media. Thus, the information that could be eventually obtained from the contact angle of titanosilicates does not adequately describe the whole hydrophilic-hydrophobic nature of the study material.

#### 1.2.3.2 Thermogravimetric Analysis (TGA)

Thermogravimetric Analysis (TGA) measures the mass variation of a sample while it is heated, cooled, or isothermally maintained under a defined atmosphere, inert or oxidizing. The analysis can be carried out at constant temperature or constant heating rate. A typical TGA curve shows the mass loss steps generally associated to the loss of volatile components, carbon black combustion, polymer decomposition, and final residues due to the temperature changes. This method permits the study of materials decomposition and their products, drawing conclusions about their individual components [227].

TGA is used to determine the water adsorption capacity that is the quotient between the mass loss due to the water desorption by the mass of dry sorbent [228]. In the hydrophobicity studies, TGA is a common analytical technique used for the determination of water affinity of solids or for the quantification of hydroxyl groups on the surface that is an indirect way to quantify the water affinity of solid surfaces [229]. However, the sample preparation and storage could have an impact over the measurement of physisorbed water and lead to imprecise conclusions about the hydrophobicity/philicity of a material. Additionally, comparison of the hydrophobicity of materials must be performed carefully since the measurement of physisorbed water is expressed per gram of sample, so materials with higher surface areas will display a higher amount of physisorbed water per gram of sample. The comparison is clearer when physisorbed water is normalized by the specific surface area.

One way to quantity the hydrophobicity of the surface of microporous solids is the "hydrophobicity index" (HI), which was firstly introduced by Anderson and Klinowski [230]. This model is based on water adsorption and is not useful for characterization of zeolitic sorbent. The mass losses at each temperature range are measured by TGA, and the HI is determined according to Equation (2).

$$HI = \frac{\text{Mass loss up to 150 °C}}{\text{Mass loss up to 400 °C}} \quad (2)$$

If HI=1, the material is considered hydrophobic, and when HI=0, is a hydrophilic material. Another definition of HI was given by Giaya et al. as shown in Equation (3):

$$HI = \frac{V_t - V_{>150\,°C}}{V_t} \quad (3)$$

where $V_t$ is the total pore volume of the sorbent and $V_{>150\,°C}$ is the volume of water desorbed at temperature above 150 °C. If HI=1, the material is presented as very hydrophobic, and when HI=0, the material is presented as very hydrophilic [231].

TGA measurements provide information about the water adsorbed physically, but not necessarily about the affinity. As Mueller et al. stated in 2003, the water mass loss at temperatures below 120 °C was attributed to the loss of water adsorbed physically, but this value is not related to the water affinity of the material surface. In fact, Mueller found that the presence of OH groups on the $SiO_2$ surface can be measured in the temperature range of 120-800°C, and the OH content was normalized to the specific surface area to be able to compare the OH/m$^2$ of each material [232].

It is actually a challenge to distinguish between adsorbed water and actual hydroxyl surface density, that is, distinguishing between dehydration and dihydroxylation [233]. For this, an alternative to measure the actual amount of water that a sample contains was proposed by Lin et al. In this study TG analysis were carried out starting from samples of Ti-MCM-41 Ti-zeolite saturated with $NH_4Cl$ solution to guarantee the maximum level of water adsorption. The total number of molecules of water adsorbed on the surface was determined from the mass loss between 25 and 150 °C [195]. In this procedure the authors controlled the ambient conditions of the sample before TGA experiments, which allowed to compare the samples independently of the synthesis and storage conditions.

1.2.3.3 Infrared Spectroscopy (IR)

Infrared Spectroscopy (IR) is a common technique applied to characterize solid catalysts. It can be used as a direct way to study the composition of solid surfaces or as an indirect way providing information about the interactions between the surface and adsorbate [229].

IR is a popular technique to measure the affinity of water on solids. With IR spectroscopy, the polar (e.g. OH) or non-polar groups of the solid surface can be directly quantified, providing an idea of the polarity of the surface [234]. Infrared spectra offer information about the types of sorbed water molecules that are identified through the measurement of the frequency of the corresponding IR peaks. The intensity of absorption band is used to measure the amount of water sorbed [228].

In comparison with TGA, IR spectroscopy provides more information about the distinction between physically adsorbed and chemically bound water. In fact, when IR spectra are analyzed the water deformation band and the hydroxyl stretching vibration do not overlap; nevertheless, water -OHs contribute to the intensity of the -OH stretching vibration, which entangles the separation between inner and surface hydroxyls [235]. One of the characteristic bands of the IR spectrum of silica is related to the presence of -OH groups at 3750 cm$^{-1}$, which is assigned to isolated -OH groups. A close-lying band (a tail) formed by the weakly H-bonded -OH groups, appears in the 3600-3750 cm$^{-1}$ region. The band of strongly H-bonded -OH groups and/or desorbed water appears in the 3400-3500 cm$^{-1}$ range. The water -OH groups band appears at 1630 cm$^{-1}$ (water deformation) and contributes to the bands in this region [236–238]. In order to quantify the hydrophobicity of metal-substituted zeolites, the silanol IR signals are usually normalized by the band of $\nu$(Si-O-Si) at 1990 and 1865 cm$^{-1}$ (assuming this band is constant in the compared materials) [39,239].

In the specific case of titanosilicates, the IR spectra in the OH region displays two intense bands at about 3740 and 4550 $cm^{-1}$ corresponding to terminal Si-OH and hydrogen-bonded silanol groups at defect sites, respectively [240–242]. For titanosilicates that have been functionalized by post-grafting, the silanol band intensity decreases since the silane binds to surface -OH groups producing Si-O bonds. The C-H vibrational frequency appears after functionalization with organosilane groups [243,244]. C-H stretching and bending vibration bands that reflect the incorporation of alkyl groups appears at 2850-2985 and around 1460 $cm^{-1}$ [243]. Thus, the lower intensity of the silane band can be used as an indicator of increase of hydrophobicity due to the functionalization success [242]. Additionally, the presence of Si-$CH_3$ at 1279 $cm^{-1}$ [45], Si-$CH_2$ at 1410 $cm^{-1}$ [245] as well as Si-C, Si-$CH_2$-$CH_3$ are also indicatives of functionalization. Furthermore, the IR analysis of titanosilicates shows the characteristic bands at 1082 and 802 $cm^{-1}$ attributed to the asymmetric and symmetric stretching vibration of Si-O-Si [244] and the Si-OH band that appears at 950 $cm^{-1}$ titanosilicates [162].

1.2.3.4 Adsorption Isotherms

Information about the affinity of the surface for a specific compound or in general properties related with the surface can be analyzed with the application of adsorption techniques. The adsorption from the gas phase on materials has been employed as a tool to evaluate the affinity for water [229].

Water affinity can be understood by recording the water adsorption isotherms. A hydrophobic material displays low affinity for water and low water adsorption capacity. In contrast, a hydrophilic material displays high affinity for water, but does not necessarily exhibit a high water adsorption capacity since the latter depends on the pore volume [228]. Therefore, to know if a material is more hydrophobic or hydrophilic, it is necessary to determine the amount of adsorbed water per unit area or mass in the range of low relative pressures [246]. In fact, the measurement of water adsorption capacity at higher relative pressures does not provide information about water affinity since the adsorbate–adsorbate interactions result in a multilayer adsorption and/or pore condensation. To solve this drawback, the water adsorption capacity must be analyzed at low loading (low amount of water adsorbed), without surpassing the monolayer adsorption, to minimize the influence of adsorbate–adsorbate interactions. Also, it is important to consider that using water as adsorbent, a defined monolayer is not easy to obtain and the presence of highly polar sites or acidic sites could increase the local water concentration due to hydrogen bonding. Consequently, it is better to compare materials of the same nature under similar conditions [32].

The hydrophobicity of sorbents has been classified according to the International Union of Pure and Applied Chemistry (IUPAC). This assignation is based on the type of the adsorption isotherm. As shown in Figure 6, there are some curves characteristic of hydrophilic and hydrophobic materials. For instance, the type I isotherm is assigned to a highly hydrophilic material, the type II isotherm corresponds to a hydrophilic material, the type III isotherm represents a hydrophobic/ low hydrophilic material with weak sorbent–water interactions, the type IV isotherm represents a hydrophilic material, the type V isotherm is associated to a hydrophobic/low hydrophilic material with weak sorbent–water interactions, the type VI isotherm corresponds to a hydrophilic material with multiple sorbent–water interactions and stepwise sorption, and the type VII isotherm is characteristic of a very hydrophobic material [228].

Figure 7 illustrates three water adsorption isotherms of zeolitic materials with different hydrophobicity degrees and with the same pore volume [247]. Curve (a) is a type I isotherm in which the sorption equilibrium in the material is reached after the adsorption of high amount of water at very low relative pressures ($P/P_0$), curve (b) is also a type I isotherm in which the sorption equilibrium is reached at higher $P/P_0$, the curve (c) corresponds to a type V isotherm where just a small amount of water is adsorbed at low $P/P_0$ until the sorption capacity is reached, this is a hydrophobic or weakly hydrophilic solid, and curve (d) represents a type VII isotherm where a very small amount of water is adsorbed in all range of relative pressures, this material is considered highly hydrophobic.

751 According to the adsorption isotherms of materials (a) and (b) at low loading, the material with
752 steeper slope is defined as more hydrophilic [228,247].
753

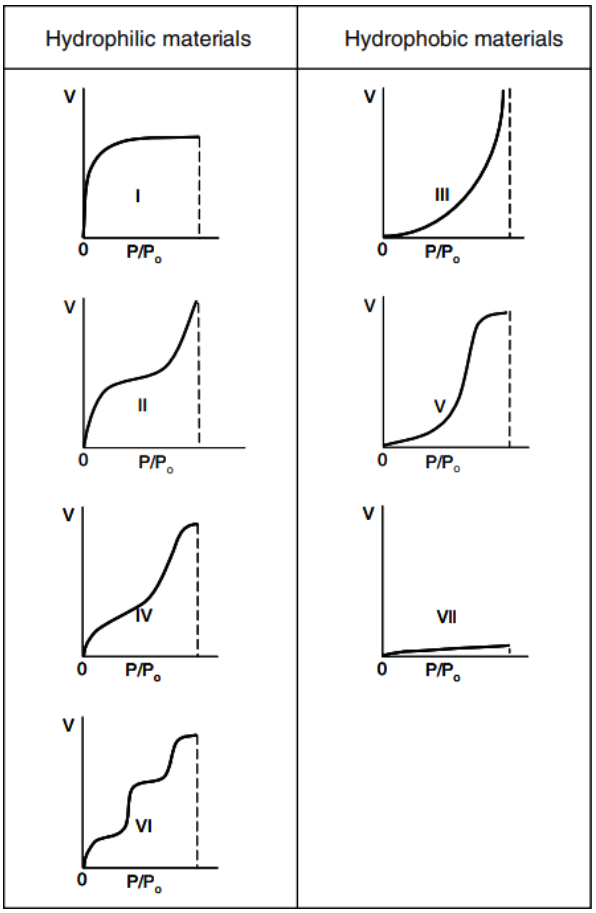


754
755 **Figure 6** Hydrophobicity of materials based of adsorption isotherms classified according to IUPAC.
756 Taken of Ref. [228].

757

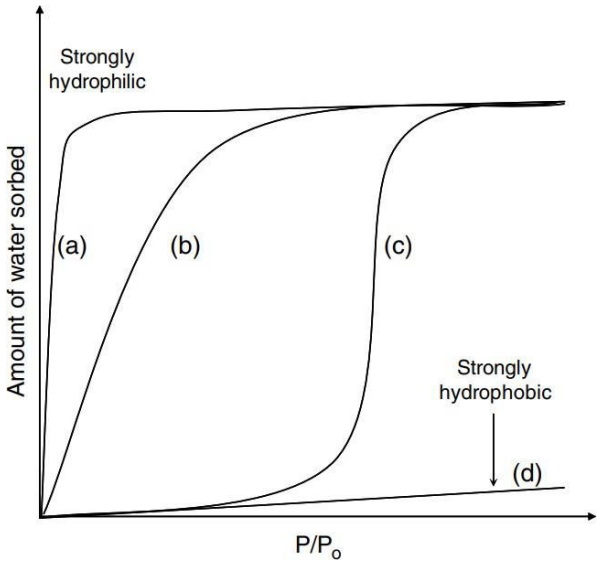


758
759 **Figure 7** Water adsorption isotherms for ideally hydrophobic and hydrophilic zeolitic materials
760 normalized to pore volume. Adapted from Ref. [228].

SiWeitkamp et al. used the HI of zeolites for multicomponent sorption based on a competitive sorption between hydrocarbon and water to quantify the hydrophobicity. The HI is calculated by the (4).

$$HI = \frac{X_{Hydrocarbon}}{X_{Water}} \quad (4)$$

where X is the content of molecules adsorbed. A higher HI means a higher adsorption of hydrocarbon compared to water, thus, it is a more hydrophobic material [248]. In addition, the water adsorption capacity can be obtained by the standard contact porometry and sorptometry which employ the mass change measures of the sorbents under constant water vapor pressure/humidity [249].

1.2.3.5 Calorimetric techniques

Calorimetry has been used to study solid surface of solids in liquid medium. Here, we will review one the most used calorimetric techniques to characterize solid surface affinity for water. This technique involves the measurement of the heat of immersion, also called heat of wetting or immersion enthalpy, which is the energy change at constant pressure and temperature when a solid is immersed in a liquid. The heat of immersion depends on both the chemical interactions of the liquid with the solid surface and the textural properties of the solid [32,228,250]. Therefore, characterization of microporous solids by calorimetry is not so simple due to the contributions of interactions of different nature [251]. This technique has been widely used to study the microporous material such as activated carbon and zeolites [252]. Silvestre-Alveró and co-authors used calorimetry of immersion to compare the hydrophobic character between Ti-MCM-41 and silylated Ti-MCM-41. They used different liquids as probe molecules, ranging from non-polar (i.e., hydrocarbons) and polar molecules (i.e., water, alcohols). According to their results, silylated Ti-MCM-41 demonstrated a hydrophobic character since the heat of immersion in water decreased for increasing silylation degrees. On the other hand, silylation displayed a lower effect on the heat of immersion measured in cyclohexane, indicating that the interactions between a hydrophobic surface with a non-polar liquid are smaller and probably also affected by the textural properties [250].

1.2.3.6 Solid State Nuclear Magnetic Resonance (Solid-State NMR)

The Nuclear Magnetic Resonance (NMR) spectroscopy consists in the application of a magnetic field strength. If a sample is placed in a magnetic field and it is radiated at the appropriate frequency, the nucleus of the sample can absorb energy. The radiation frequency necessary to generate absorption energy depends of the type of nucleus, the spatial location in the magnetic field, and the chemical environment [253,254].

Solid-state NMR can be used to evaluate the hydrophobic character of solids since the presence of hydrophilic sites (-OH) and organic moieties bonded to Si atoms can be determined. For example, the intensity of hydroxyl groups and molecular water signals can be measured from analyzing the $^{1}H$ NMR spectra at low temperature [228]. Additionally, some previous studies have used solid-state NMR to describe the degree of condensation of silicates by deconvoluting the $^{29}Si$ NMR spectrum using the contributions of $Q^4$ ($(Si(OSi)_4)$), $Q^3$ ($(Si(OSi)_3OH)$), and $Q^2$ ($(Si(OSi)_2(OH)_2)$) (See Figure 8) [39,47]. Besides the condensation degree, this analysis is strongly related to the hydrophobicity/philicity of the material since silanols (Si-OH) are hydrophilic sites, so the highest the fraction of $Q^3$ and $Q^2$ relative to $Q^4$ would indicate a hydrophilic character. If the hydrophobicity origin is the functionalization of the surface with organic fractions, solid-state NMR can be also used. For example, Muller et al, determined the fraction of Si bonded to methyl groups, in order to evaluate the effective methyl-functionalization of amorphous titanosilicates (Ti-$SiO_2$) [47]. There are two modes for the experimental approaches of solid-state NMR. The cross-polarization mode allows to excite the contributions of $T^2$ and $T^3$, so they are better appreciated even at low organic content. Nevertheless, this method cannot be used for quantification of each resonance. The direct excitation mode is applied for quantification, and once the spectra is recorded, contributions are quantified by

deconvolution of peaks using gaussian functions. Indeed, some previous studies have used cross-polarization to verify the surface functionalization [47].

Solid-state NMR cannot be used to study the Ti nucleus at very low Ti molar ratios [23]. Another nucleus that can be followed by solid-state NMR is $^{13}C$. In this case, the analysis provides information about organic functionalization or the degree of removal of the templating agents [255].

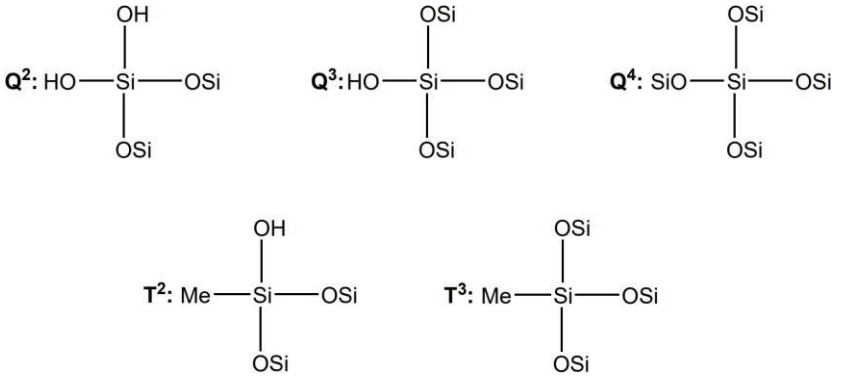


**Figure 8** Typical types of resonance contributions of a solid-state $^{29}Si$ NMR spectra. Adapted from [47].

A summary of the analytic techniques employed for evaluation of hydrophobicity of titanosilicates is presented in table 4.

**Table 4** Analytic techniques for the characterization of hydrophobicity.

| Characterization technique | Measurement | References |
|---|---|---|
| Thermogravimetric Analysis (TGA) | Mass losses of catalysts under controlled temperature | [11,33,34,42,45–48,195,203] |
| Infrared Spectroscopy (IR) | $OH^-$ adsorption band (isolated and hydrogen bonding), and Si-$CH_x$ vibration band in the IR spectrum | [11,33,192,203,256,34,38,39,41,45,47,48,172] |
| Adsorption Isotherms | Water adsorption capacity | [11,33,251,38–41,45,48,192,195] |
| Calorimetric Techniques | Heat of immersion (heat of wetting or immersion enthalpy) | [250] |
| Solid State Nuclear Magnetic Resonance (Solid-State NMR) | Hydrophilic sites (-OH) and organic moieties bonded to Si atoms of $^{29}Si$ NMR and $^{1}H$ NMR spectra | [11,34,195,256,38–41,45,47,172,192] |

## Section 2: Discussion of recent advances of the topic

### *2.1 Discernment of the results of the effect of the hydrophobic modification on the catalytic activity of titanosilicates*

Hydrophobization of titanosilicates has been proposed as a tool to improve their catalytic performance, hence several researchers embarked on this study to gain better understanding of this modification [2]. Some of them have found a positive effect of hydrophobization, but others have found a negative or negligible effect. This diversity in the points of view can be justified because there is a considerable number of variables influencing the catalytic performance of titanosilicates in oxidation reactions. The physical/chemical properties of each type of titanosilicate and the methodologies for hydrophobization affect their interactions with the reactants, products, intermediate species, and solvent. Furthermore, evaluating and comparing the hydrophobic

character of these materials are still a challenge due to the variety of analytical techniques applied to measure this property.

The catalytic effect of hydrophobizing titanosilicates could be studied for different model reactions (e.g., hydroxylation of phenol), each of them with different characteristics. The specific characteristics of each reaction make difficult the analysis of all these reactions as a single group; therefore, a comparison between effects of hydrophobization involved in all kinds of these reactions is outside the scope of this research. Nevertheless, in this work, the effects of hydrophobization over the catalytic activity in epoxidation reactions will be compared and discussed. The type of titanosilicate, the hydrophobization strategy, the surface characterization, and the catalytic system (reactants and solvent) will be considered. We have chosen the epoxidation of olefins since this reaction is represented in both fine and bulk chemical industry, and the epoxide is an important synthetic intermediate of organic transformations reactions [33,168,257]. Epoxides are used for the fabrication of epoxy resins, drugs, plasticizers, sweeteners and perfumery materials, among others [257]. Additionally, the epoxidation of olefins would be a good model to study the catalytic effects of adjusting the hydrophobic/hydrophilic character of catalyst surface since the olefin is hydrophobic while epoxide is hydrophilic, and thus, their interactions with catalysts are different. The epoxidation mechanism of olefins has been extensively studied, and it was found that epoxides can be produced by two competitive routes: the direct epoxidation, and the allylic oxidation (Figure 9). When the $H_2O_2$ is used as the oxidant, the direct epoxidation is mediated by the titanium-hydroperoxo complex (Ti-OOH). However, the presence of water in this reaction mixture promotes undesired epoxide ring opening which produces the corresponding diol. Diol can be also generated by the presence of acid sites on the catalysts surface. The allylic route is mediated by radicals (Ti-O· and HO·) which are formed by the homolysis of Ti-OOH. This route generates oxygenated products including epoxides, alcohols and ketones through consecutive reactions [258]. The mechanism of the direct epoxidation, which is our route of interest, has been studied and widely accepted to follow an Eley-Rideal mechanism. In this mechanism the oxidant (hydrogen peroxide or organic peroxide) adsorbs on the titanium active sites forming active intermediate species (Ti-OOR, where R=H or alkyl). These species react with the olefin producing the epoxide that is later desorbed from the surface of catalyst.

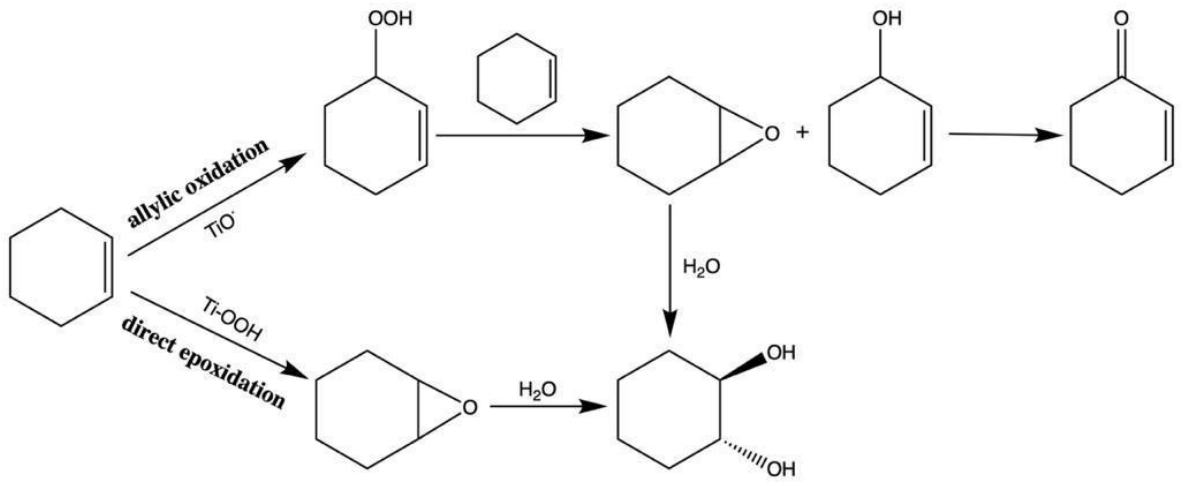


**Figure 9** Direct epoxidation and allylic route for cyclohexene oxidation. Adapted from [48,204].

In order to review the effect on the catalytic performance of hydrophobized titanosilicates, we will follow the order of the methodologies for hydrophobization since we believe the surface properties achieved by each methodology influence the catalytic activity. First, the control of the OH surface density will be analyzed, and later a discussion about the catalytic performance of functionalized titanosilicates will be addressed.

Modification of crystallinity in titanosilicates was used to regulate the amount of hydroxyl groups on the surface of TS-1. A YNU (Yokohama National University) method that consists in the use of $(NH_4)_2CO_3$ as crystallization-mediating agent was applied to increase the crystallinity of TS-1. The characterization of the catalyst by DRUV-Vis spectroscopy presented a band attributed to FW-Ti at 210 nm, and no band above 250 nm appeared which showed that most of Ti atoms were introduced into the framework (nominal Si/Ti=34.2). This was also confirmed by the band at 960 $cm^{-1}$ of the IR spectrum attributed to Ti-O-Si. The formation of FW-Ti (tetrahedral coordination) within TS-1 resulted in an increase of crystallinity and hydrophobicity due to the insertion of more Ti atoms which prevented the formation of defect sites (Si-OH). This was confirmed by IR and $^{1}H$ and $^{29}Si$ MAS NMR spectroscopies. The IR band at 3738 $cm^{-1}$ (corresponding to isolated Si-OH) and the $Q^4/Q^3$ ratio decreased with the incorporation of FW-Ti. A lower amount of defect sites makes the surface hydrophobic preventing the attack by adsorbed water molecules and, consequently, a collapse of the zeolite framework. An enhanced activity (TONs and conversion) of TS-1 in the epoxidation of 1-hexene and styrene using $H_2O_2$ as oxidant was attributed to a hydrophobic character [34].

Ti-Beta is one of the titanosilicates that has been hydrophobized by different methodologies [6,37,38], and one of them is the regulation of silanol surface density. It is known that the presence of $Al^{3+}$ heteroatoms introduces defects (Si-OH or Si-OH-Al) into the zeolite framework (when synthesized in $OH^-$ medium), conferring a hydrophilic character to Ti-Beta, but also more acidity (See section 1.2.2.1) [65]. Therefore, it was proposed that the synthesis of Ti- Beta by crystallization assisted by using dealuminated Beta seeds would produce more active Al-free Ti-Beta catalysts. These materials exhibited enhanced selectivity in the epoxidation of 1-hexene using $H_2O_2$ as oxidant. As expected, the selectivity to epoxide (~40% at 60% conversion of 1-hexene) increased when the Al content decreased. However, even with Al-free Ti-Beta (Si/Al>5000), epoxide ring opening was still detected. The authors attributed this ring opening to the silanols or the Ti species of different acidity. In fact, this phenomenon was confirmed by comparing the catalytic oxidation of the epoxide in Al-free Ti-Beta (ring opening observed) with the oxidation in Al-free Beta zeolite (without Ti), in which no ring opening was observed [104]. From this work, it was possible to conclude that the removal of Al improves the selectivity for epoxide, probably due to the removal of strong acid sites, but the relation with hydrophobicity cannot be discarded. Besides the control of the Al content, other alternatives to produce more hydrophobic titanosilicates, encompass for instance the synthesis in fluoride medium.

In this context, dealuminated Ti-Beta was further hydrophobized as mentioned in the reports published by Blasco *et al.*, in 1996 [37] and 1998 [38]. In these works, the silanol density was controlled by using fluoride ($F^-$) medium instead of aqueous ($OH^-$) medium during sol-gel synthesis. Al-free Ti-Beta produced in $F^-$ medium displayed improved crystallinity and very high thermal and hydrothermal stability. These improved characteristic in the Ti-Beta were verified according to the calcination process carried out at 1223 K where Ti-Beta ($F^-$) kept its crystallinity and no significant losses of Ti were observed. In contrast, crystalline structure of Ti-Beta ($OH^-$) was destroyed under the same conditions. In addition, Ti-Beta ($F^-$) remained stable under a hydrothermal treatment (exposure to 100% humidity, at 1023 K). The hydrophobization of Al free Ti-Beta showed a positive effect in the catalytic performance when it was used in the epoxidation of methyl oleate [37] and 1-hexene [38]. Ti-Beta ($F^-$) was more active and selective to the epoxide than Ti-Beta ($OH^-$), and the $H_2O_2$ efficiency increased too. The higher selectivity was the result of the improved desorption of the epoxide from the hydrophobic Ti-Beta ($F^-$) surface. The improved desorption of the epoxide prevents the epoxide ring to open which could occur if the epoxide remains long enough close to the active site [37,38]. The hydrophobic character of Ti-Beta ($F^-$) was confirmed by X-ray absorption where the Ti K edge spectra (XANES) showed a prepeak with similar intensities in the calcined and in the rehydrated samples while the prepeak for Ti-Beta ($OH^-$) significantly decreased its intensity and broadened upon rehydration. These results helped to conclude that there is a higher amount of Ti atoms that coordinate with adsorbed water molecules upon rehydration in the case of Ti-Beta ($OH^-$) compared to Ti-Beta($F^-$) [37].

Another study compared the catalytic activity and selectivity of Ti-Beta($F^-$) and Ti-Beta ($OH^-$) for the epoxidation of 1-hexene and oleic acid using $H_2O_2$ as oxidant and acetonitrile and methanol as solvents [38]. Characterization of the catalysts synthesized in ($F^-$) medium showed that only 50% of Ti was incorporated in the final material due to the formation of soluble complexes of Ti with $F^-$ at low pH that precluded the total incorporation of Ti atoms into the zeolite. The addition of $F^-$ decreased the pH. At high pH values ($OH^-$ medium), 100% of Ti was incorporated in the Ti-Beta ($OH^-$). FTIR, $^1H$ and $^{29}Si$ MAS NMR, and water adsorption techniques verified the hydrophobic character of Ti-Beta ($F^-$). The number of Si-OH connectivity defects was lower in Ti-Beta ($F^-$) than Ti-Beta ($OH^-$) (contribution at 960 $cm^{-1}$ was higher for Ti-Beta ($OH^-$)). $^{29}Si$ Bloch-decay (BD) MAS NMR indicated that the $Q^3$ contribution was not detected for Ti-Beta ($F^-$), whereas $^1H$ and $^{29}Si$ cross-polarization (CP) MAS NMR spectroscopy reflected the presence of negligible concentrations of Si-OH groups at the external surface of Ti-Beta ($F^-$). Contrarily, the concentration of Si-OH detected for Ti-Beta ($OH^-$) was higher. Water adsorption experiments suggested that the Ti site of Ti-Beta ($F^-$) adsorbed one molecule of water while Ti in the Ti-Beta ($OH^-$) could adsorb more than one water molecule. The catalytic activity of Ti-Beta ($F^-$) displayed no significant effect compared to that of Ti-Beta ($OH^-$) reaching similar values of conversion of 1-hexene of around 41% in the case of acetonitrile and 26% in the case of methanol. But the selectivity to epoxide in acetonitrile was higher (100%) for both Ti-Beta ($F^-$ and $OH^-$), while using methanol Ti-Beta ($F^-$) exhibited higher selectivity to epoxide than Ti-Beta ($OH^-$) (76.6% vs 54.9%). The low selectivity to epoxide using methanol (for Ti-Beta ($OH^-$)) was attributed to the opening of the oxirane ring which occurred even in the complete absence of Al, as mentioned in the ref [104], intermediate species related with Ti could contribute to the epoxide ring opening. Finally, the difference in the hydrophobicity of the catalysts surface was more evident for oxidation of alkenes with a polar fraction, as seen in the case of methyl oleate [37] and oleic acid [38] where the catalytic performance of Ti-Beta ($F^-$) was higher than Ti-Beta ($OH^-$) [38].

Fluoride medium not only helped to obtain a more hydrophobic material through the control of silanol density but also prevented the deactivation of the active sites. Even though the content of tetrahedral Ti in the material synthesized in $F^-$ medium is lower compared with materials synthesized in $OH^-$ medium, the catalytic activity was comparable in both cases. However, the addition of $F^-$ ions into the synthesis must be carefully controlled since an excessive amount of them could affect the insertion of Ti in the framework. An excessive addition of $F^-$ ions leads to the formation of $Ti(OH)_xF_y$ complexes, causing a unfavorable effect on the catalytic performance of titanosilicates (See section 1.2.2.1) [192].

According to previous reports, hydrophobic catalysts performed better than hydrophilic ones. For instance, the hydrophobic TS-1 exhibited superior catalytic properties for the epoxidation of olefins compared to other hydrophilic titanosilicates such as Ti-Beta [90]. Therefore, several researchers focused on the improvement of the hydrophobicity of titanosilicates. Nevertheless, recent studies showed that the increase of silanol density enhanced the epoxide yields of cyclohexene and 1-hexene [39,77,259–261]. Bregante et al. performed an extensive study about the catalytic epoxidation of alkenes with $H_2O_2$ as oxidant and Ti-Beta as catalyst. It was concluded that water clusters anchored to silanol nests $(SiOH)_4$ (which correspond to hydrogen-bonded Si-OH) on the catalyst surface play an important role stabilizing the epoxidation species and thus achieving high epoxidation rates. This conclusion was drawn by comparing the catalytic activity of Ti-Beta catalysts with different contents of silanol nests. In the first step of the synthesis, commercial Beta zeolites with initial Si/Al ratios ranging from 12.5 to 250 were dealuminated creating vacancy defects which in a second step were partially occupied by Ti atoms producing materials with different remaining contents of silanol nests $(SiOH)_4$ and thus, with different degrees of hydrophilicity. Additionally, a hydrophobic Ti-Beta was synthesized in fluoride medium to produce silanol-free surface. These catalysts were used in the epoxidation of 1-octene with $H_2O_2$. Thermodynamic and kinetic analysis evidenced that turnover rates for epoxidation of 1-octene increased with higher $(SiOH)_4$ surface density, concluding that the most hydrophilic catalyst was the most active one. In fact, materials containing ~5 $(SiOH)_4$ per unit cell displayed rates that were 100 times greater than defect-free Ti-

Beta. Spectroscopic, thermodynamic, and kinetic studies indicated that these differences in the epoxidation activity were not related either with the nature of Ti active intermediate species (Ti-OOH) or the epoxidation mechanism, but with the molecular interactions between Ti-OOH, $(SiOH)_4$ density and polar surface [39].

Another approach to modify the hydrophobicity of titanosilicates is the direct functionalization or one-pot synthesis. For instance, the hydrophobicity of Ti-MCM-41 was modified by adding some organo-alkoxysilanes precursors, such as methyl [40,195,203], phenyl [40], vinyl [40] and pentyl [40] organo-alkoxysilanes. These modified catalysts were used on the oxidation of cyclohexene using TBHP and $H_2O_2$ as oxidants. A significant improvement on the activity was observed with the methyl-functionalized Ti-MCM-41 [40,195,203]. The insertion of organic groups increased the hydrophobicity of the catalysts. TGA analysis of pristine and functionalized Ti-MCM-41, pretreated with saturated $NH_4Cl$ solution to reach the maximum water adsorption, confirmed the superior hydrophobicity of functionalized Ti-MCM-41 compared to the pristine analogous. Indeed, the number of water molecules adsorbed per $nm^2$ decreased as the incorporation of methyl groups on the surface increased. The silanol surface density was also evaluated by $^{29}Si$ MAS NMR spectroscopy by following the contributions of $Q^4$ $(Si(OSi)_4)$, $Q^3$ $(HOSi(OSi)_3)$, $Q^2$ $((HO)_2Si(OSi)_2)$, $T^3$ $(RSi(OSi)_3)$, and $T^2$ $(R(HO)Si(OSi)_2)$. Peak deconvolution allowed to quantify both the organic group bound to Si and the SiOH content expressed in mol%. It was possible to observe that the hydrolysis and condensation of organic precursors were affected by inductive, resonance and stearic effects. For example, in the case of the methyl group, a low functionalization degree ($Si\text{-}CH_3/Si$=8.9% and Si-OH/Si=65.8%) was reached, contrarily to the phenyl group which displayed a fast hydrolysis and a higher functionalization degree (Si-phenyl/Si=27.8% and Si-OH/Si=60.6%). Water adsorption measurements revealed that all functionalized Ti-MCM-41 adsorbed less water than the pristine material [40]. The DRUV-Vis characterization showed that octahedral Ti was present in the pristine samples, while tetrahedral Ti was principally detected in the methyl-functionalized samples [195].

Amorphous titanosilicates $Ti\text{-}SiO_2$ were modified by one-pot functionalization with phenyltrimethoxysilane (PHTMS) (nominal 30%). The BET surface areas of functionalized catalysts exhibited a reduction in the pore volume and average pore diameter compared with unmodified catalysts. The Ti dispersion was also affected by the insertion of phenyl groups. The organic functionalization was confirmed by the presence of $T^2$ and $T^3$ contributions in the $^{29}Si$ MAS NMR spectrum. The epoxidation of cyclohexene using both modified and unmodified $Ti\text{-}SiO_2$ was compared using three different solvents, toluene, acetone, and ethanol. The initial epoxide production rate and the epoxide yield (after 2 hours) were higher with all solvents using functionalized materials compared with the pristine samples. These values increased in polar solvents (acetone and ethanol) in comparison with toluene for the functionalized $Ti\text{-}SiO_2$. The selectivity to epoxide using functionalized materials was 95, 87 and 94% for toluene, acetone, and ethanol, respectively. This was attributed to the presence of non-polar organic groups on the modified surface catalyst which increased the hydrophobic character and improved the selectivity to epoxide. A positive effect of one-pot insertion of organic groups on the catalytic activity could be reached by properly choosing of the sol-gel parameters and the concentration of organic groups on the catalyst surface since the steric effects and polarity modification (polar Si-OH replaced by organic groups) affect the textural and chemical properties [46].

As seen, one-pot functionalization with organic groups increased the hydrophobic character of $Ti\text{-}SiO_2$ aerogels, but an excessive functionalization is detrimental for the catalytic performance. For example, $Ti\text{-}SiO_2$ was modified by one-pot functionalization with methyl groups using methyltrimethoxysilane, and effects on the Ti dispersion were evidenced. The formation of Ti in tetrahedral coordination diminished due the direct functionalization method. According to the FTIR spectrum, the pristine $Ti\text{-}SiO_2$ had a Si-O-Ti/Si-O-Si ratio of 0.75, whereas this ratio in methylated materials was in the range of 0.49-0.57. It was suggested that Ti dispersion into the silica matrix was reduced by the insertion of methyl groups. The deconvolution of $^{29}Si$ MAS NMR peaks showed that the effective functionalization degree ($Si\text{-}CH_3/Si$) was 25.6% (30% nominal). A negative effect was

observed in the epoxidation of 1-hexene and cyclohexene using the methylated Ti-$SiO_2$. This behavior was attributed to three main causes: the lower surface area, the lower Ti dispersion and the pore blockage due to excessive functionalization [47].

The catalytic activity improves as the insertion of organic groups increases until a limit is reached, after which, the catalytic performance is negatively affected. Indeed, one-pot methyl-functionalization was attempted to produce hydrophobic Ti-$SiO_2$ with 1, 5 and 14% degrees of methyl-functionalization. These catalysts were tested in cyclooctene epoxidation and $H_2O_2$ as oxidant. The trend of the initial epoxidation rate normalized by the fraction of Ti active sites showed that the methyl-functionalized Ti-$SiO_2$ reached higher epoxidation rates. This behavior was attributed to the improved affinity of the hydrophobic catalyst surface with the olefin and lower affinity with the epoxide. However, at the maximum degree of methyl-functionalization of 14% (determined from $^{29}$Si DE MAS NMR measurements by the formula $\%Me=(T^i/(\sum T^i\text{-}Q^i))*100$), the epoxidation rate decreased even compared to the epoxidation rate of the reference (non-functionalized) Ti-$SiO_2$. This led the authors to suggest that an excessive functionalization could affect the adsorption of the oxidant [45].

An interesting comparison between one-pot and post-grafting functionalization of Ti-$SiO_2$ synthesized by non-hydrolytic sol-gel (NHSG) method was published by Smeets and co-workers [48]. The catalytic activity and water resistance were evaluated for the methylated Ti-$SiO_2$ (NHSG_Ti-$SiO_2$_Me) in cyclohexene epoxidation with $H_2O_2$ as oxidant. To evaluate the catalytic activity of NHSG_Ti-$SiO_2$_Me, acetonitrile was used as solvent while an acetonitrile/water mixture (75:25 v/v) was used to determine the water resistance. Prior to the use of methylated catalysts, pristine NHSG_Ti-$SiO_2$ was compared to TS-1, and both catalysts displayed a comparable catalytic activity in acetonitrile, but NHSG_Ti-$SiO_2$ displayed a lower epoxide yield (2.1% in comparison with 18.3% obtained with acetonitrile) than TS-1 in acetonitrile/water mixture. However, the diol formation increased for both TS-1 and NHSG_Ti-$SiO_2$ due to oxirane ring opening caused by water. Hence, the NHSG_Ti-$SiO_2$ wasfunctionalized by the one-pot method (NHSG_Ti-$SiO_2$_Me) to prevent the oxirane ring opening in the presence of water. However, this strategy negatively affected the activity even more than pristine samples in acetonitrile/water mixture, this was attributed to capping of Ti active sites by methyl groups. On the other hand, post-grafting was also applied to obtain functionalized Ti-$SiO_2$ (NHSG_Ti-$SiO_2$@Me), and it displayed the same conversion (~13%) that NHSG_Ti-$SiO_2$, but an enhancement in the epoxide yield (5.1% vs. 2.1%) was reached. The authors concluded that the presence of water affected the mechanism of epoxidation not only by favoring the oxirane ring opening, but also by deactivating the Ti active species, preventing the direct epoxidation route. Activated intermediate species of Ti (formed by the coordination between Ti active sites and $H_2O_2$), that are responsible for oxidizing the olefin, can be deactivated by a second hydrolysis [262–264]. Consequently, these deactivated species cause poor activity and epoxide yield. The functionalization by post-grafting prevented the deactivation of titanium active sites while the textural properties of catalysts were affected and probably, the active one were capped by one-pot functionalization [48].

To overcome the limitation of Ti dispersion via one-pot synthesis, Ti-$SiO_2$ catalysts were synthesized by aerosol-assisted one-pot sol–gel. From DRUV-Vis, XPS and ICP characterization, higher content of framework Ti was detected in the modified catalysts which confirmed a high Ti dispersion. According to the $^{29}$Si direct-excitation (DE) MAS NMR results, the presence of $T^3$ ($Si(OSi)_3Me$) and $T^2$ ($Si(OSi)_2(OH)Me$) were observed, which are absent in pristine samples. FTIR-ATR spectra confirmed the presence of Si-C band at 1279 $cm^{-1}$. Mass losses at high temperature (around 803 K) also evidenced the presence of methyl groups in the functionalized catalysts. In addition, the hydrophobic character of methylated Ti-$SiO_2$ was proved by the TGA, $^{29}$Si DE MAS NMR and adsorption studies. Mass losses of physisorbed water normalized by the specific area and the water affinity were higher in the unfunctionalized samples and lower in the functionalized samples [11]. The catalyst characterization indicated that the functionalization by aerosol-assisted one-pot sol–gel was successful and when the catalysts were probed in the epoxidation of cyclooctene with TBHP, an improved catalytic performance was shown with functionalized Ti-$SiO_2$ [11].

Another functionalization method is post-grafting used to modify the hydrophobicity of titanosilicates. For example, the hydrophobic character of Ti-MCM-41 and Ti-MCM-48 titanosilicates was controlled by grafting organosilanes to silanol groups on the materials surface. Ti-MCM-41 and Ti-MCM-48 were modified by trimethylsilylation using trimethylchlorosilane (TMCS) as silylating reagent. The deconvolution of the $^{29}$Si MAS NMR spectrum into three contributions $Q^4$, $Q^3$ and the peak of trimethylsilylation TMS ($(CH_3)_3Si(OSi)$ at $\delta$ 14.3) showed that the amount of silanol groups was 0.263 mol Si-OH/mol Si and 0.208 mol Si-OH/mol Si before and after the silylation, respectively. The incomplete silylation was attributed to the size of trimethylsilyl group (*ca.* 0.6 nm). Despite the partial silylation (21% of Si-OH were silylated), TGA showed that the functionalized Ti-MCM-41 adsorbed much less water (0.29 mass%) than non-silylated ones (55 mass%). Prior to TGA analysis samples were exposed to moisture over saturated aqueous solution of $NH_4Cl$. The hydrophobic character of Ti-MCM-41 and Ti-MCM-48 improved the conversion and TON in the epoxidation of cyclohexene resulting in a ca. 20-fold increase compared to the catalytic activity of the non-silylated samples. Trimethylsilylation improved the olefin (no polar) adsorption on methylated Ti-MCM-41 and the interaction of the olefin with the active sites. In addition, the $H_2O_2$ efficiency improved by the trimethylsilylation [42].

Igarashi et al. in 2007 probed several organosilanes such as trimethylchlorosilane (TMCS), hexamethyldisiloxane (HMDSO) and hexamethyldisilizane (HMDS) as silylating reagents (alone or forming mixtures) in the post-grafting of Ti-MCM-41 and Ti-MCM-48. Samples were evacuated at 273 °C before silylation to prevent the decomposition of TMCS due to the reaction with water molecules adsorbed on the solid surface. According to the $^{29}$Si MAS NMR spectra of samples before and after the silylation, the highest trimethylsilylation degree (according to the TMS peak) was attained with HMDS (25% for Ti-MCM-41 and 26% for Ti-MCM-48). Even though the initial amount of silanol groups ($Q^3$) of Ti-MCM-41 was higher (49%) than Ti-MCM-48 (36%). In contrast, the lowest degree of silylation was obtained with TMCS despite the pre-evacuation. On the other hand, IR spectra of silylated Ti-MCM-41 with HMDS showed that in addition to the band at 3600 $cm^{-1}$ (corresponding to hydrogen-bonded silanol groups), a new band appeared at 3700 $cm^{-1}$ which was attributed to new isolated silanol groups because of the reaction between HMDS with hydrogen-bonded Si-OH. This fact can explain the higher silylation degree obtained with HMDS in contrast with the TMCS and HMDSO [41]. The catalytic performance of silylated materials was proved in the epoxidation of cyclohexene and cyclododecene without solvent and using acetonitrile and methanol as solvents. Silylated catalysts displayed higher conversions and TONs than non-silylated catalysts in all cases. For both silylated and non-silylated catalysts, the selectivity to epoxide was lower in the absence of solvents, while the epoxide was the major product using solvents. In contrast, in the cyclododecene oxidation with $H_2O_2$ and TBHP, cyclododecene epoxide was preferentially formed with both silylated Ti-MCM-41 and silylated Ti-MCM-48 with the difference that higher conversion and selectivity were reached with TBHP (70% aqueous solution) than with $H_2O_2$. The diol product was obtained only over the non-functionalized ones, in absence of solvent. Two possible explanations for epoxide production were proposed: i) acetonitrile acted as a Lewis base neutralizing the acidity of catalysts which prevented the epoxide ring opening, and ii) the polarity of acetonitrile that allows the desorption of epoxide from catalysts surface. The enhanced activity using TBHP could be ascribed to the amphiphilic nature of the organic oxidant which presents both hydrophobic and hydrophilic parts, allowing it to solvate both organic and aqueous phases. Finally, the $H_2O_2$ efficiency was improved with silylated Ti-MCM-41 and Ti-MCM-48, as seen in previous studies [41].

Another variable besides the silylating agent is the silylation time. In this line, Ti-MCM-41 was silylated with TMCS for 9 hours (Ti-MCM-41(S9)) and 5 hours (Ti-MCM-41(S5)). These samples were compared with the pristine Ti-MCM-41 in the catalytic epoxidation of 1-octene using $H_2O_2$ and TBHP as oxidants. Higher activities were reached with trimethylsilylated Ti-MCM-41(S9) (9.7% for $H_2O_2$ and 13.8% for TBHP) compared with pristine Ti-MCM-41 (5.3% for $H_2O_2$ and 4.8% for TBHP). New features appeared in the $^{29}$Si MAS NMR spectra of Ti-MCM-41(S9) and Ti-MCM-41 at 11 ppm and 5.1 ppm, which were assigned to $(CH_3)_3SiOSi(OSi)_3$ and $(CH_3)_3SiOTi(OSi)_3$ species, respectively. The peak

at 5.1 ppm increased with the silylation time and depended on the Ti content. On the other hand, the $Q^4/Q^3$ ratio of the pristine Ti-MCM-41 was 2.4, while the $Q^4/Q^3$ ratio of Ti-MCM-41(S9) was 4.7. This last value did not differ greatly from Ti-MCM-41(S5)) where $Q^4/Q^3$ ratio was of 4.4. It appeared that silylation occurred mostly between titanol [$(OH)Ti(OSi)_2OSi(OSi)_3$, $Q^3$] and TMCS, explaning why the $Q^4/Q^3$ ratio did not vary. Consequently, the enhanced activity of trimethylsilylated Ti-MCM-41 was related to both an increment of hydrophobicity of the catalyst surface and the formation of catalytically active Ti species ($((CH_3)_3SiOTi(OSi)_3$) [256].

Ti-SBA-15 was functionalized with three silyl amides of varying chain length, $Me_2NSiMe_2(R)$ (R: methyl, n-butyl, or n-octyl) producing the Me_Ti-SBA-15, Bu_Ti-SBA-15 and Oc_Ti-SBA-15 samples. Functionalized catalysts were used in the epoxidation of cyclohexene using $H_2O_2$ as oxidant and acetonitrile as solvent. In all cases, functionalized Ti-SBA-15 showed higher catalytic performance for the epoxidation of cyclohexene than the corresponding non-functionalized ones. The improved yield and selectivity were related not only to the surface hydrophobicity, but also to the modification of the Ti active site. First, the hydrophobic character of the functionalized Ti-SBA-15 was confirmed by TGA analysis of saturated samples (with saturated $H_2O$ atmosphere for 24 hours). The mass losses of physisorbed water measured at temperature below 150°C were 32% and ~3% for the non-functionalized and functionalized catalysts, respectively. A functionalization degree from 63% to 74% of the total available OH sites was reached, including Si-OH and Ti-OH. This was determined by combustion and TGA analysis and corroborated by $^1H$ solid-state NMR. To study the influence of the surface functionalization over the Ti sites, the authors synthesized SBA-15 with silylated Si-OH groups, and later, Ti was grafted to the surface to obtain a hydrophobic surface with only uncapped Ti-OH. The selectivity to epoxide with this catalyst was comparable with the pristine Ti-SBA-15 and lower than functionalized Ti-SBA-15, suggesting that Ti-OH sites favor the allylic route. Furthermore, the remaining TiOH sites were silylated to produce $(R)_3SiOTi(OSi)_3$ species which were believed to favor direct epoxidation. Indeed, the epoxide selectivity was higher than the catalyst with Ti-OH and sylilated Si-OH, proving that the presence of Ti-OH played an important role in the selectivity to epoxide. Epoxide selectivity decreased in the following order: Bu_Ti-SBA-15 66% (silylated Si-OH and Ti-OH)> Bu_Ti-SBA-15 45% (silylated Si-OH)> Ti-SBA-15 11.6% (non-silylated) [33]. These results confirmed the hypothesis that the selectivity to epoxide improved due to the higher hydrophobicity, but mainly due to the presence of $(R)_3SiOTi(OSi)_3$ species.

Amorphous $Ti/SiO_2$ titanosilicates (this notation corresponds to amorphous titanosilicates which Ti atoms were inserted into the silica by post-grafting) were post-modified to improve their stability in water during epoxidation reactions. Conventional $Ti/SiO_2$ catalysts were modified with polymethylhydrosiloxane (PMHS, MW=390 g/mol) for 1 hour and 16 hours (PMHS-1 and PMHS-16). An additional $Ti/SiO_2$ sample was modified with TMS. Pristine and functionalized $Ti/SiO_2$ were tested in the epoxidation of 1-octene using TBHP as oxidant. In batch catalytic tests, $Ti/SiO_2$ modified with PMHS displayed a decrease in catalytic activity compared with the pristine $Ti/SiO_2$. This was attributed to the reduced specific surface area and pore plugging. Moreover, the rate of catalyst deactivation was studied using a flow system. In this experiment, 132 umol/L of water were added in the feed to the flow reactor, and the measured initial rate of deactivation of TMS Ti/SiO2 was -0.32%/h, whereas for both PMHS-1 and PMHS-16, the deactivation rates were -0.03%/h and -0.09%/h, correspondingly. TBHP conversions measured after 50 hours in the flow reactor were 5.3%, 7.6%, 8.2%, 9.7% for $Ti/SiO_2$, TMS $Ti/SiO_2$, PMHS-16, and PMHS-1, respectively. Moreover, values of selectivity averaged during 50 hours in flow reactor for PMHS-1 (82%) and PMHS-16 (93%) were higher than pristine Ti-$SiO_2$ (79%) but lower than for TMS $Ti/SiO_2$ (100%). On the other hand, the TON (epoxide (mol)/ Ti (mol)) for the pristine sample was higher than for PMHS-1 and PMSH-16. After hot-water Soxhlet extraction (to simulate catalyst deactivation processes), $Ti/SiO_2$ exhibited 62% drop in TON and 45% drop in conversion, whereas PMHS-1 displayed no loss of TON and loss of 8% in conversion. This loss was attributed to Ti aggregation, and this was confirmed by DRUV-Vis analysis, which showed that a significant amount of tetrahedral Ti sites transformed into octahedral

Ti sites. Hence, PMHS post-grafting increased the hydrolytic stability of Ti-$SiO_2$ as a result of its hydrophobic character [49].

A summary of hydrophobization methodologies applied to titanosilicates which were discussed in this section, is presented in table 5.

**Table 5** Hydrophobization methodologies applied to titanosilicates.

| Material | Hydrophobization technique | | | |
|---|---|---|---|---|
| | **Improvement of crystallization** | **Synthesis in fluoride ($F^-$) medium** | **One-pot synthesis** | **Post-grafting** |
| **TS-1** | [34] | | | |
| **Ti-Beta** | | [37,38] | | |
| **Ti-MCM-41** | | | [40,195,203] | [41,42,256] |
| **Ti-MCM-48** | | | | [41,42,256] |
| **Ti-SBA-15** | | | | [33] |
| **Ti-$SiO_2$** | [11,45–48] | | | [49] |

**Section 3: Current needs in the research area**

*3.1 Discussion of current challenges in understanding the effect of the hydrophobization of titanosilicates on their catalytic activity.*

Various titanosilicates were hydrophobized in an attempt to enhance their catalytic performance on the basis that the olefin adsorption and epoxide desorption would be improved by a hydrophobic catalyst surface. With the advance in catalyst synthesis, characterization and hydrophobization methodologies, the nature of the active sites was identified as an important role-player in the selectivity to epoxide. Thus, the fabrication of titanosilicates with high hydrophobicity and well distribution of Ti active sites became crucial to promote the direct epoxidation over the allylic route. Several works have been published about this topic, but these results have not yet been compiled in a review. In this context, we discuss about the challenges in understanding the effect of hydrophobization of titanosilicates over the catalytic performance in the epoxidation of olefins according to the hydrophobization methodology.

The control of the surface silanol density was studied as an alternative to modify the hydrophobicity of titanosilicates. For example, the use of $(NH_4)_2CO_3$ (crystallization-mediating agent) improved the crystallization process of TS-1. This facilitated the insertion of Ti into the zeolite framework and lowered the number of defect sites (Si-OH), increasing the hydrophobicity of TS-1. The more hydrophobic TS-1 displayed a higher resistance to water attack and better catalytic activity. However, in this case, the positive catalytic effect cannot be totally attributed to hydrophobicity considering that the crystallization process increased the incorporation of FW-Ti which could be the main reason for the enhanced catalytic activity.

TS-1 is known for its hydrophobicity and good catalytic performance in epoxidation of small substrates. However, titanosilicates with better textural properties had to be synthesized for larger substrates. This is the case of Ti-Beta that was originally an aluminosilicate. The aluminum content increased the hydrophilicity and acidity of the Ti-Beta surface which is undesirable for the epoxidation reaction. For this reason, two strategies were developed to reduce the hydrophilicity (Si-OH, Si-OH-Al) and acidity of Ti-Beta: i) dealumination and post-insertion of titanium (Ti), and ii) direct synthesis in fluoride ($F^-$) medium. In the first strategy, the number of remaining vacancies (silanol nests) caused by dealumination decreased with Ti incorporation, while in the second strategy, the vacancies were totally eliminated by the action of fluoride ($F^-$) anions, rendering a more hydrophobic character to the catalyst. In general, the hydrophobic Ti-Beta were more selective to epoxide due to the improved epoxide desorption and reduced water adsorption, preventing the oxirane ring opening and deactivation of Ti sites. However, a lack of agreement about the effect of

hydrophobization over the catalytic activity arose from comparing the results of some studies. For example, some authors found that the catalytic activity of hydrophobic Ti-Beta synthesized in $F^-$ medium was comparable to the activity of hydrophilic Ti-Beta synthesized in $OH^-$ medium. In contrast, a recent study determined that Ti-Beta ($F^-$) was the least active compared to hydrophilic Ti-Beta which contained silanol nests (hydrogen-bonded silanols). The contrast in the measured catalytic activities in both studies could be attributed to the different synthesis procedure. In the case of the hydrophilic Ti-Beta (OH), the synthesis produces a material that has isolated and hydrogen-bonded silanols on the surface, but in the case of hydrophilic Ti-Beta obtained from dealumination and post-insertion of Ti, the material contains vacancies that improved the catalytic activity in the presence of hydrogen-bonding reactants. This indicates that the synthesis procedure has an important effect over the surface chemistry of the material, which consequently impacts its catalytic activity.

One-pot functionalization has also been tested as a methodology to synthesize more hydrophobic Ti-MCM-41 and Ti-$SiO_2$ using precursors such as organo-alkoxysilanes and organo-chlorosilanes. In general, it has been observed that the modified catalysts exhibited improved catalytic activity and selectivity in comparison with the pristine samples. The authors attributed the positive effect of hydrophobization to the improved affinity for the olefin, easy epoxide desorption and less water adsorption. The latter avoids the oxirane ring opening, which improves the selectivity to epoxide. The authors also observed that the excessive functionalization was detrimental to the catalytic performance since the textural properties and the Ti dispersion were affected. In fact, the specific surface area, pore diameter, and pore volume decreased due to pore blockage. Moreover, the formation of tetrahedral Ti was affected due to the addition of the organic precursor during synthesis. Thus, the success of one-pot functionalization for titanosilicates depends on factors such as steric effects (organic group size), polarity of the organic group, and organic precursor ratio that affect the hydrolysis and condensation reactions during the synthesis. To prepare materials with better catalytic properties, one-pot functionalization has been optimized by applying pre-hydrolysis of precursors and appropriate drying conditions. Recently, the aerosol-assisted sol-gel synthesis method helped to tackle the limitations of one-pot functionalization by producing hydrophobic Ti-$SiO_2$ with controlled textural properties and Ti dispersion.

Post-grafting with organosilanes, hexamethyldisiloxane (HMDSO), hexamethyldisilizane (HMDS), and silyl amides has been used to hydrophobize Ti-MCM-41, Ti-MCM-48, Ti-SBA-15 and Ti-$SiO_2$. All functionalized titanosilicates displayed better olefin conversion, selectivity to epoxide, and oxidant efficiency than the pristine analogous. This enhanced catalytic performance was mainly explained by the improved interaction between the olefin and the Ti active site on a hydrophobic surface where silanols were replaced by organic groups. Additionally, the higher selectivities were attributed to reduced deactivation of Ti sites and oxirane ring opening caused by the presence of water in the medium of reaction. Some authors realized that post-grafting could be used to functionalize both silanols and titanols on the surface of Ti-MCM-41 and Ti-SBA-15. Indeed, Brutchey et al demonstrated that a preferential functionalization of titanols modifies the nature of the Ti sites. The functionalized Ti is more electron-deficient, which increases the electrophilicity of the oxygen closer to the Ti center in the active intermediate species, favoring the direct epoxidation route.

Functionalized titanosilicates either by one-pot method or post-grafting consistently displayed higher conversions and selectivities in the epoxidation of olefins as a result of their hydrophobicity. However, isolating the effect of hydrophobization was not possible in many studies since the hydrophobization methodology had an impact over the Ti active sites and textural properties.

In most of the articles presented in this review, hydrophobization strategies improved the catalytic performance, but other factors such as the nature and number of the active sites, the titanosilicate surface chemistry, the type of oxidant, the polarity and basicity of the solvent, the polarity and size of the olefin, and the environment surrounding the active site could not be disregarded. In fact, the direct epoxidation route depends on the electrophilicity (strength of the Lewis acidity) of the Ti active species. Moreover, the choice of the oxidant also plays an important

role, since the reaction route depends on the electrophilicity of the active intermediate species. It is known that Ti-OOR (R=alkyl), formed from the activation of an organic hydroperoxide with the Ti active sites, displays lower electrophilicity than Ti-OOH, formed from the activation of hydrogen peroxide with the Ti active sites. The alkyl group is an electron-donor group that decreases the electrophilicity of the oxygen-donating species for epoxidation [23].

In addition, the hydrophobic character of the modified titanosilicates originates from different chemical properties. In some cases, the hydrophobicity is related to the silanol surface density and the type of silanol (isolated or hydrogen-bonded silanols), whereas in other cases, the hydrophobicity is related to the functionalization degree with organic moieties. Therefore, there is not a specific characterization technique to measure the hydrophobicity of a catalyst.

As explained in section 1.2.3, measuring the hydrophobicity/philicity of a catalyst surface remains a challenge considering all the analytical techniques available and their respective theoretical basis. Therefore, a combination of these techniques is required to reach a more precise surface characterization. In fact, the combination of two or more analytical techniques has been successful at ranking titanosilicates according to their hydrophobic character in each research work. However, comparison of the hydrophobicity among materials from different studies has not yet been achieved. We consider that the quantification of the hydrophobic character could improve if it is expressed as the number of hydrophilic sites or degree of organic functionalization per specific surface area.

Even if hydrophobicity is successfully measured, this property will not totally reflect the behavior of the catalyst under the reaction conditions since epoxidation in liquid phase involves different interactions between the catalyst surface and the liquid medium, which is composed of the olefin, oxidant, solvent, and active intermediate species; all of them with different polarities.

To conclude, a great development on the study of hydrophobicity and the effects on the catalytic activity of titanosilicates has been reached from the contributions cited in this review; nevertheless, more systematic studies that combine spectroscopic, thermodynamic, kinetic, and even computational analysis are required to gain more understanding about the interactions between the catalyst surface and the liquid-phase reaction medium.

This review focused on the catalytic performance of hydrophobized titanosilicates in olefin epoxidation, but this discussion could have implications for other reaction systems such as those for biomass valorization, where the interaction between the hydrophobic/hydrophilic catalyst surface with water is decisive.

**Supporting Research Project:** This work is supported by the internal non-funded research project PII-DEMEX-2020-03 developed in the Department of Extractive Metallurgy of Escuela Politécnica Nacional.

**Acknowledgments:** A.B.L.M acknowledges all the support from Department of Extractive Metallurgy of Escuela Politécnica Nacional and Santiago Molina.

## References

1. Vayssilov, G.N. Structural and Physicochemical Features of Titanium Silicalites. *Catal. Rev.* **1997**, *39*, 209–251. 10.1080/01614949709353777.
2. Přech, J. Catalytic performance of advanced titanosilicate selective oxidation catalysts – a review. *Catal. Rev. - Sci. Eng.* **2018**, *60*, 71–131. 10.1080/01614940.2017.1389111.
3. Hutter, R.; Dutoit, D.C.M.; Mallat, T.; Schneider, M.; Baiker, A. Novel mesoporous titania-silica aerogels highly active for the selective epoxidation of cyclic olefins. *J. Chem. Soc. Chem. Commun.* **1995**, 163–164. 10.1039/C39950000163.
4. Ward, D.A.; Ko, E.I. Preparing Catalytic Materials by the Sol-Gel Method. *Ind. Eng. Chem. Res.* **1995**, *34*, 421–433. 10.1021/ie00041a001.
5. Keshavaraja, A.; Ramaswamy, V.; Soni, H.S.; Ramaswamy, A. V; Ratnasamy, P. Synthesis, Characterization, and Catalytic Properties of Micro-Mesoporous, Amorphous Titanosilicate Catalysts. *J.*

*Catal.* **1995**, *157*, 501–511. https://doi.org/10.1006/jcat.1995.1314.

6. Fan, W.; Wu, P.; Tatsumi, T. Unique solvent effect of microporous crystalline titanosilicates in the oxidation of 1-hexene and cyclohexene. *J. Catal.* **2008**, *256*, 62–73. https://doi.org/10.1016/j.jcat.2008.03.001.
7. Liu, Z.F.; Tabora, J.; Davis, R.J. Relationships between Microstructure and Surface Acidity of Ti-Si Mixed Oxide Catalysts. *J. Catal.* **1994**, *149*, 117–126. https://doi.org/10.1006/jcat.1994.1277.
8. Liu, Z.; Crumbaugh, G.M.; Davis, R.J. Effect of structure and composition on epoxidation of hexene catalyzed by microporous and mesoporous Ti-Si mixed oxides. *J. Catal.* **1996**, *159*, 83–89. 10.1006/jcat.1996.0066.
9. Kochkar, H.; Figueras, F. Synthesis of Hydrophobic TiO2–SiO2Mixed Oxides for the Epoxidation of Cyclohexene. *J. Catal.* **1997**, *171*, 420–430. https://doi.org/10.1006/jcat.1997.1820.
10. Smeets, V.; Boissière, C.; Sanchez, C.; Gaigneaux, E.M.; Peeters, E.; Sels, B.F.; Dusselier, M.; Debecker, D.P. Aerosol Route to TiO2–SiO2 Catalysts with Tailored Pore Architecture and High Epoxidation Activity. *Chem. Mater.* **2019**, *31*, 1610–1619. 10.1021/acs.chemmater.8b04843.
11. Manangon-Perugachi, L.E.; Smeets, V.; Vivian, A.; Kainthla, I.; Eloy, P.; Aprile, C.; Debecker, D.P.; Gaigneaux, E.M. Mesoporous Methyl-Functionalized Titanosilicate Produced by Aerosol Process for the Catalytic Epoxidation of Olefins. *Catal.* 2021, *11*. 10.3390/catal11020196.
12. Xu, H.; Wu, P. Recent Progresses in Titanosilicates. *Chinese J. Chem.* **2017**, *35*, 836–844. 10.1002/cjoc.201600739.
13. Kong, Z.; Yue, B.; Deng, W.; Zhu, K.; Yan, M.; Peng, Y.; He, H. Direct synthesis of hierarchically porous TS-1 through a solvent-evaporation route and its application as an oxidation catalyst. *Appl. Organomet. Chem.* **2014**, *28*, 239–243. https://doi.org/10.1002/aoc.3115.
14. Drago, R.S.; Dias, S.C.; McGilvray, J.M.; Mateus, A.L.M.L. Acidity and Hydrophobicity of TS-1. *J. Phys. Chem. B* **1998**, *102*, 1508–1514. 10.1021/jp973249k.
15. Alba-Rubio, A.C.; Fierro, J.L.G.; León-Reina, L.; Mariscal, R.; Dumesic, J.A.; López Granados, M. Oxidation of furfural in aqueous H2O2 catalysed by titanium silicalite: Deactivation processes and role of extraframework Ti oxides. *Appl. Catal. B Environ.* **2017**, *202*, 269–280. https://doi.org/10.1016/j.apcatb.2016.09.025.
16. Bellussi, G.; Carati, A.; Clerici, M.G.; Maddinelli, G.; Millini, R. Reactions of titanium silicalite with protic molecules and hydrogen peroxide. *J. Catal.* **1992**, *133*, 220–230. https://doi.org/10.1016/0021-9517(92)90199-R.
17. Xia, Q.-H.; Chen, X.; Tatsumi, T. Epoxidation of cyclic alkenes with hydrogen peroxide and tert-butyl hydroperoxide on Na-containing Tiβ zeolites. *J. Mol. Catal. A Chem.* **2001**, *176*, 179–193. 10.1016/S1381-1169(01)00256-4.
18. Ouyang, X.; Hwang, S.-J.; Xie, D.; Rea, T.; Zones, S.I.; Katz, A. Heteroatom-Substituted Delaminated Zeolites as Solid Lewis Acid Catalysts. *ACS Catal.* **2015**, *5*, 3108–3119. 10.1021/cs5020546.
19. Boronat, M.; Corma, A.; Renz, M.; Viruela, P.M. Predicting the Activity of Single Isolated Lewis Acid Sites in Solid Catalysts. *Chem. – A Eur. J.* **2006**, *12*, 7067–7077. https://doi.org/10.1002/chem.200600478.
20. Boronat, M.; Concepción, P.; Corma, A.; Renz, M.; Valencia, S. Determination of the catalytically active oxidation Lewis acid sites in Sn-beta zeolites, and their optimisation by the combination of theoretical and experimental studies. *J. Catal.* **2005**, *234*, 111–118. https://doi.org/10.1016/j.jcat.2005.05.023.
21. Boronat, M.; Concepción, P.; Corma, A.; Navarro, M.T.; Renz, M.; Valencia, S. Reactivity in the confined

spaces of zeolites: the interplay between spectroscopy and theory to develop structure–activity relationships for catalysis. *Phys. Chem. Chem. Phys.* **2009**, *11*, 2876–2884. 10.1039/B821297J.

22. Jenzer, G.; Mallat, T.; Maciejewski, M.; Eigenmann, F.; Baiker, A. Continuous epoxidation of propylene with oxygen and hydrogen on a Pd–Pt/TS-1 catalyst. *Appl. Catal. A Gen.* **2001**, *208*, 125–133. https://doi.org/10.1016/S0926-860X(00)00689-X.

23. Ratnasamy, P.; Srinivas, D.; Knözinger, H. Active Sites and Reactive Intermediates in Titanium Silicate Molecular Sieves. *Adv. Catal.* 2004, *48*, 1–169. 10.1016/S0360-0564(04)48001-8.

24. Burtch, N.C.; Jasuja, H.; Walton, K.S. Water stability and adsorption in metal-organic frameworks. *Chem. Rev.* **2014**, *114*, 10575–10612. 10.1021/cr5002589.

25. Chen, X.; Qian, P.; Zhang, T.; Xu, Z.; Fang, C.; Xu, X.; Chen, W.; Wu, P.; Shen, Y.; Li, S.; et al. Catalyst surfaces with tunable hydrophilicity and hydrophobicity: metal–organic frameworks toward controllable catalytic selectivity. *Chem. Commun.* **2018**, *54*, 3936–3939. 10.1039/C8CC00318A.

26. Jayaramulu, K.; Geyer, F.; Schneemann, A.; Kment, Š.; Otyepka, M.; Zboril, R.; Vollmer, D.; Fischer, R.A. Hydrophobic Metal–Organic Frameworks. *Adv. Mater.* **2019**, *31*. 10.1002/adma.201900820.

27. Wang, C.; Guo, H.; Leng, S.; Yu, J.; Feng, K.; Cao, L.; Huang, J. Regulation of hydrophilicity/hydrophobicity of aluminosilicate zeolites: a review. *Crit. Rev. Solid State Mater. Sci.* **2020**, 1–19. 10.1080/10408436.2020.1819198.

28. Ruddy, D.A.; Brutchey, R.L.; Tilley, T.D. The Influence of Surface Modification on the Epoxidation Selectivity and Mechanism of TiSBA15 and TaSBA15 Catalysts with Aqueous Hydrogen Peroxide. *Top. Catal.* **2008**, *48*, 99–106. 10.1007/s11244-008-9040-0.

29. Figueras, F.; Kochkar, H.; Caldarelli, S. Crystallization of hydrophobic mesoporous titano-silicates useful as epoxidation catalysts. *Microporous Mesoporous Mater.* **2000**, *39*, 249–256. https://doi.org/10.1016/S1387-1811(00)00200-6.

30. Sheldon, R.A.; Dakka, J. Heterogeneous catalytic oxidations in the manufacture of fine chemicals. *Catal. Today* **1994**, *19*, 215–245. https://doi.org/10.1016/0920-5861(94)80186-X.

31. Bregante, D.T.; Flaherty, D.W. Periodic Trends in Olefin Epoxidation over Group IV and V Framework-Substituted Zeolite Catalysts: A Kinetic and Spectroscopic Study. *J. Am. Chem. Soc.* **2017**, *139*, 6888–6898. 10.1021/jacs.7b01422.

32. Gläser, R.; Weitkamp, J. Surface Hydrophobicity or Hydrophilicity of Porous Solids. *Handb. Porous Solids* 2002, 395–431. https://doi.org/10.1002/9783527618286.ch12.

33. Brutchey, R.L.; Ruddy, D.A.; Andersen, L.K.; Tilley, T.D. Influence of Surface Modification of Ti−SBA15 Catalysts on the Epoxidation Mechanism for Cyclohexene with Aqueous Hydrogen Peroxide. *Langmuir* **2005**, *21*, 9576–9583. 10.1021/la051182j.

34. Fan, W.; Duan, R.-G.; Yokoi, T.; Wu, P.; Kubota, Y.; Tatsumi, T. Synthesis, Crystallization Mechanism, and Catalytic Properties of Titanium-Rich TS-1 Free of Extraframework Titanium Species. *J. Am. Chem. Soc.* **2008**, *130*, 10150–10164. 10.1021/ja7100399.

35. B. D'Amore, M.; Schwarz, S. Trimethylsilylation of ordered and disordered titanosilicates: improvements in epoxidation with aqueous H2O2 from micro- to meso-pores and beyond†. *Chem. Commun.* **1999**, 121–122. 10.1039/A809396B.

36. Corma, A.; Esteve, P.; Martinez, A.; Valencia, S. Oxidation of Olefins with Hydrogen Peroxide and tert-Butyl Hydroperoxide on Ti-Beta Catalyst. *J. Catal.* **1995**, *152*, 18–24. https://doi.org/10.1006/jcat.1995.1055.

37. Blasco, T.; Camblor, M.A.; Corma, A.; Esteve, P.; Martínez, A.; Prieto, C.; Valencia, S. Unseeded synthesis

of Al-free Ti-β zeolite in fluoride medium: a hydrophobic selective oxidation catalyst. *Chem. Commun.* **1996**, 2367–2368. 10.1039/CC9960002367.

38. Blasco, T.; Camblor, M.A.; Corma, A.; Esteve, P.; Guil, J.M.; Martínez, A.; Perdigón-Melón, J.A.; Valencia, S. Direct Synthesis and Characterization of Hydrophobic Aluminum-Free Ti−Beta Zeolite. *J. Phys. Chem. B* **1998**, *102*, 75–88. 10.1021/jp973288w.

39. Bregante, D.T.; Johnson, A.M.; Patel, A.Y.; Ayla, E.Z.; Cordon, M.J.; Bukowski, B.C.; Greeley, J.; Gounder, R.; Flaherty, D.W. Cooperative effects between hydrophilic pores and solvents: Catalytic consequences of hydrogen bonding on alkene epoxidation in zeolites. *J. Am. Chem. Soc.* **2019**, *141*, 7302–7319. 10.1021/jacs.8b12861.

40. Igarashi, N.; Kidani, S.; Ahemaito, R.; Hashimoto, K.; Tatsumi, T. Direct organic functionalization of Ti–MCM-41: Synthesis condition, organic content, and catalytic activity. *Microporous Mesoporous Mater.* **2005**, *81*, 97–105. https://doi.org/10.1016/j.micromeso.2005.01.022.

41. Igarashi, N.; Hashimoto, K.; Tatsumi, T. Catalytical studies on trimethylsilylated Ti-MCM-41 and Ti-MCM-48 materials. *Microporous Mesoporous Mater.* **2007**, *104*, 269–280. 10.1016/j.micromeso.2007.02.041.

42. Tatsumi, T.; A. Koyano, K.; Igarashi, N. Remarkable activity enhancement by trimethylsilylation in oxidation of alkenes and alkanes with H2O2 catalyzed by titanium-containing mesoporous molecular sieves. *Chem. Commun.* **1998**, 325–326. 10.1039/A706175G.

43. Bu, J.; Rhee, H.-K. Improvement in hydrophobicity of Ti-MCM-41 using a new silylation agent MSTFA. *Catal. Letters* **2000**, *65*, 141–145. 10.1023/a:1019096617082.

44. Bu, J.; Rhee, H.-K. Silylation of Ti-MCM-41 by trimethylsilyl-imidazole and its effect on the olefin epoxidation with aqueous H2O2. *Catal. Letters* **2000**, *66*, 245–249. 10.1023/A:1019072228411.

45. Manangon-Perugachi, L.E.; Vivian, A.; Eloy, P.; Debecker, D.P.; Aprile, C.; Gaigneaux, E.M. Hydrophobic titania-silica mixed oxides for the catalytic epoxidation of cyclooctene. *Catal. Today* **2019**. 10.1016/j.cattod.2019.05.020.

46. Müller, C.A.; Deck, R.; Mallat, T.; Baiker, A. Hydrophobic titania-silica aerogels: Epoxidation of cyclic compounds. *Top. Catal.* **2000**, *11–12*, 369–378.

47. Müller, C.A.; Maciejewski, M.; Mallat, T.; Baiker, A. Organically modified titania-silica aerogels for the epoxidation of olefins and allylic alcohols. *J. Catal.* **1999**, *184*, 280–293. 10.1006/jcat.1999.2424.

48. Smeets, V.; Ben Mustapha, L.; Schnee, J.; Gaigneaux, E.M.; Debecker, D.P. Mesoporous SiO2-TiO2 epoxidation catalysts: Tuning surface polarity to improve performance in the presence of water. *Mol. Catal.* **2018**, *452*, 123–128. 10.1016/j.mcat.2018.04.011.

49. Guo, Y.; Hwang, S.-J.; Katz, A. Hydrothermally robust Ti/SiO2 epoxidation catalysts via surface modification with oligomeric PMHS. *Mol. Catal.* **2019**, *477*, 110509. https://doi.org/10.1016/j.mcat.2019.110509.

50. Notari, B. Microporous Crystalline Titanium Silicates. In; Eley, D.D., Haag, W.O., Gates, B.B.T.-A. in C., Eds.; Academic Press, 1996; Vol. 41, pp. 253–334 ISBN 0360-0564. https://doi.org/10.1016/S0360-0564(08)60042-5.

51. Taramasso, M.; Perego, G.; Notari, B. No Title 1983.

52. Corma, A.; Nemeth, L.T.; Renz, M.; Valencia, S. Sn-zeolite beta as a heterogeneous chemoselective catalyst for Baeyer-Villiger oxidations. *Nature* **2001**, *412*, 423–425. 10.1038/35086546.

53. van Grieken, R.; Martos, C.; Sánchez-Sánchez, M.; Serrano, D.P.; Melero, J.A.; Iglesias, J.; Cubero, A.G. Synthesis of Sn-silicalite from hydrothermal conversion of SiO2-SnO2 xerogels. *Microporous Mesoporous*

*Mater.* **2009**, *119*, 176–185. 10.1016/j.micromeso.2008.10.020.

54. Ione, K.G.; Vostrikova, L.A.; Mastikhin, V.M. Synthesis of crystalline metal silicates having zeolite structure and study of their catalytic properties. *J. Mol. Catal.* **1985**, *31*, 355–370. https://doi.org/10.1016/0304-5102(85)85118-X.

55. Millini, R.; Previde Massara, E.; Perego, G.; Bellussi, G. Framework composition of titanium silicalite-1. *J. Catal.* **1992**, *137*, 497–503. https://doi.org/10.1016/0021-9517(92)90176-I.

56. Notari, B. Synthesis and Catalytic Properties of Titanium Containing Zeolites. In *Innovation in Zeolite Materials Science*; Grobet, P.J., Mortier, W.J., Vansant, E.F., Schulz-Ekloff, G.B.T.-S. in S.S. and C., Eds.; Elsevier, 1988; Vol. 37, pp. 413–425 ISBN 0167-2991. https://doi.org/10.1016/S0167-2991(09)60618-2.

57. Davis, M.E.; Lobo, R.F. Zeolite and molecular sieve synthesis. *Chem. Mater.* **1992**, *4*, 756–768. 10.1021/cm00022a005.

58. Li, Y.; Li, L.; Yu, J. Applications of Zeolites in Sustainable Chemistry. *Chem* **2017**, *3*, 928–949. https://doi.org/10.1016/j.chempr.2017.10.009.

59. Ackley, M.W.; Rege, S.U.; Saxena, H. Application of natural zeolites in the purification and separation of gases. *Microporous Mesoporous Mater.* **2003**, *61*, 25–42. https://doi.org/10.1016/S1387-1811(03)00353-6.

60. Munakata, H.; Koyama, T.; Yashima, T.; Asakawa, N.; O-Nuki, T.; Motokura, K.; Miyaji, A.; Baba, T. Temperature Effect on 1H Chemical Shift of Hydroxyl Groups in Zeolites and Their Catalytic Activities as Solid Acids. *J. Phys. Chem. C* **2012**, *116*, 14551–14560. 10.1021/jp3043945.

61. Weingarten, R.; Tompsett, G.A.; Conner, W.C.; Huber, G.W. Design of solid acid catalysts for aqueous-phase dehydration of carbohydrates: The role of Lewis and Brønsted acid sites. *J. Catal.* **2011**, *279*, 174–182. https://doi.org/10.1016/j.jcat.2011.01.013.

62. Bonelli, B.; Forni, L.; Aloise, A.; Nagy, J.B.; Fornasari, G.; Garrone, E.; Gedeon, A.; Giordano, G.; Trifirò, F. Beckmann rearrangement reaction: About the role of defect groups in high silica zeolite catalysts. *Microporous Mesoporous Mater.* **2007**, *101*, 153–160. https://doi.org/10.1016/j.micromeso.2006.11.006.

63. Young, G.J. Interaction of water vapor with silica surfaces. *J. Colloid Sci.* **1958**, *13*, 67–85. https://doi.org/10.1016/0095-8522(58)90010-2.

64. Chen, N.Y. Hydrophobic properties of zeolites. *J. Phys. Chem.* **1976**, *80*, 60–64. 10.1021/j100542a013.

65. Gounder, R. Hydrophobic microporous and mesoporous oxides as Brønsted and Lewis acid catalysts for biomass conversion in liquid water. *Catal. Sci. Technol.* **2014**, *4*, 2877–2886. 10.1039/c4cy00712c.

66. Cundy, C.S.; Cox, P.A. The Hydrothermal Synthesis of Zeolites: History and Development from the Earliest Days to the Present Time. *Chem. Rev.* **2003**, *103*, 663–702. 10.1021/cr020060i.

67. Bonino, F.; Damin, A.; Bordiga, S.; Lamberti, C.; Zecchina, A. Interaction of CD3CN and Pyridine with the Ti(IV) Centers of TS-1 Catalysts: a Spectroscopic and Computational Study. *Langmuir* **2003**, *19*, 2155–2161. 10.1021/la0262194.

68. Manoilova, O. V; Dakka, J.; Sheldon, R.A.; Tsyganenko, A.A. Infrared study of Ti-containing zeolites using CO as a probe molecule. In *Catalysis by Microporous Materials*; Beyer, H.K., Karge, H.G., Kiricsi, I., Nagy, J.B.B.T.-S. in S.S. and C., Eds.; Elsevier, 1995; Vol. 94, pp. 163–170 ISBN 0167-2991. https://doi.org/10.1016/S0167-2991(06)81218-8.

69. Ertl, G.; Knözinger, H.; Weitkamp, J. *Preparation of Solid Catalysts*; Wiley, 2008; ISBN 9783527620685.

70. Arca, V.; Boscolo Boscoletto, A.; Fracasso, N.; Meda, L.; Ranghino, G. Epoxidation of propylene on Zn-treated TS-1 catalyst. *J. Mol. Catal. A Chem.* **2006**, *243*, 264–277. https://doi.org/10.1016/j.molcata.2005.08.040.

71. Ramakrishna Prasad, M.; Hamdy, M.S.; Mul, G.; Bouwman, E.; Drent, E. Efficient catalytic epoxidation of olefins with silylated Ti-TUD-1 catalysts. *J. Catal.* **2008**, *260*, 288–294. https://doi.org/10.1016/j.jcat.2008.09.021.

72. Lin, W.; Frei, H. Photochemical and FT-IR Probing of the Active Site of Hydrogen Peroxide in Ti Silicalite Sieve. *J. Am. Chem. Soc.* **2002**, *124*, 9292–9298. 10.1021/ja012477w.

73. Busca, G.; Saussey, H.; Saur, O.; Lavalley, J.C.; Lorenzelli, V. FT-IR characterization of the surface acidity of different titanium dioxide anatase preparations. *Appl. Catal.* **1985**, *14*, 245–260. https://doi.org/10.1016/S0166-9834(00)84358-4.

74. Moliner, M.; Corma, A. Advances in the synthesis of titanosilicates: From the medium pore TS-1 zeolite to highly-accessible ordered materials. *Microporous Mesoporous Mater.* **2014**, *189*, 31–40. 10.1016/j.micromeso.2013.08.003.

75. Bai, R.; Song, Y.; Bai, R.; Yu, J. Creation of Hierarchical Titanosilicate TS-1 Zeolites. *Adv. Mater. Interfaces* **2020**. 10.1002/admi.202001095.

76. Sasaki, M.; Sato, Y.; Tsuboi, Y.; Inagaki, S.; Kubota, Y. Ti-YNU-2: A Microporous Titanosilicate with Enhanced Catalytic Performance for Phenol Oxidation. *ACS Catal.* **2014**, *4*, 2653–2657. 10.1021/cs5007926.

77. Ge, T.; Hua, Z.; Lv, J.; Zhou, J.; Guo, H.; Zhou, J.; Shi, J. Hydrophilicity/hydrophobicity modulated synthesis of nano-crystalline and hierarchically structured TS-1 zeolites. *CrystEngComm* **2017**, *19*, 1370–1376. 10.1039/c6ce02435a.

78. Wang, B.; Lu, L.; Ge, B.; Chen, S.; Zhu, J.; Wei, D. Hydrophobic and hierarchical modification of TS-1 and application for propylene epoxidation. *J. Porous Mater.* **2019**, *26*, 227–237. 10.1007/s10934-018-0647-7.

79. Blasco, T.; Corma, A.; Navarro, M.T.; Pariente, J.P. Synthesis, Characterization, and Catalytic Activity of Ti-MCM-41 Structures. *J. Catal.* **1995**, *156*, 65–74. https://doi.org/10.1006/jcat.1995.1232.

80. Koyano, K.A.; Tatsumi, T. Synthesis of titanium-containing mesoporous molecular sieves with a cubic structure. *Chem. Commun.* **1996**, 145–146. 10.1039/CC9960000145.

81. Camblor, M.A.; Corma, A.; Pérez-Pariente, J. Synthesis of titanoaluminosilicates isomorphous to zeolite Beta, active as oxidation catalysts. *Zeolites* **1993**, *13*, 82–87. https://doi.org/10.1016/0144-2449(93)90064-A.

82. Wu, P.; Komatsu, T.; Yashima, T. Characterization of Titanium Species Incorporated into Dealuminated Mordenites by Means of IR Spectroscopy and 18O-Exchange Technique. *J. Phys. Chem.* **1996**, *100*, 10316–10322. 10.1021/jp960307d.

83. Přech, J.; Čejka, J. UTL titanosilicate: An extra-large pore epoxidation catalyst with tunable textural properties. *Catal. Today* **2016**, *277*, 2–8. 10.1016/j.cattod.2015.09.036.

84. Na, K.; Jo, C.; Kim, J.; Ahn, W.-S.; Ryoo, R. MFI Titanosilicate Nanosheets with Single-Unit-Cell Thickness as an Oxidation Catalyst Using Peroxides. *ACS Catal.* **2011**, *1*, 901–907. 10.1021/cs2002143.

85. Wu, P.; Nuntasri, D.; Ruan, J.; Liu, Y.; He, M.; Fan, W.; Terasaki, O.; Tatsumi, T. Delamination of Ti-MWW and High Efficiency in Epoxidation of Alkenes with Various Molecular Sizes. *J. Phys. Chem. B* **2004**, *108*, 19126–19131. 10.1021/jp037459a.

86. Chen, H.L.; Li, S.W.; Wang, Y.M. Synthesis and catalytic properties of multilayered MEL-type titanosilicate nanosheets. *J. Mater. Chem. A* **2015**, *3*, 5889–5900. 10.1039/C4TA06473A.

87. Corma, A.; Diaz, U.; Domine, M.E.; Fornés, V. New Aluminosilicate and Titanosilicate Delaminated Materials Active for Acid Catalysis, and Oxidation Reactions Using H2O2. *J. Am. Chem. Soc.* **2000**, *122*, 2804–2809. 10.1021/ja9938130.

88. Wang, J.; Zhao, Y.; Yokoi, T.; Kondo, J.N.; Tatsumi, T. High-Performance Titanosilicate Catalyst Obtained through Combination of Liquid-Phase and Solid-Phase Transformation Mechanisms. *ChemCatChem* **2014**, *6*, 2719–2726. https://doi.org/10.1002/cctc.201402239.

89. Chen, L.Y.; Chuah, G.K.; Jaenicke, S. Propylene epoxidation with hydrogen peroxide catalyzed by molecular sieves containing framework titanium. *J. Mol. Catal. A Chem.* **1998**, *132*, 281–292. https://doi.org/10.1016/S1381-1169(97)00276-8.

90. Corma, A.; Esteve, P.; Martínez, A. Solvent Effects during the Oxidation of Olefins and Alcohols with Hydrogen Peroxide on Ti-Beta Catalyst: The Influence of the Hydrophilicity–Hydrophobicity of the Zeolite. *J. Catal.* **1996**, *161*, 11–19. https://doi.org/10.1006/jcat.1996.0157.

91. Clerici, M.G.; Ingallina, P. Epoxidation of Lower Olefins with Hydrogen Peroxide and Titanium Silicalite. *J. Catal.* **1993**, *140*, 71–83. https://doi.org/10.1006/jcat.1993.1069.

92. Wang, J.; Yokoi, T.; Kondo, J.N.; Tatsumi, T.; Zhao, Y. Titanium(IV) in the Organic-Structure-Directing-Agent-Free Synthesis of Hydrophobic and Large-Pore Molecular Sieves as Redox Catalysts. *ChemSusChem* **2015**, *8*, 2476–2480. 10.1002/cssc.201500443.

93. Fan, W.; Wu, P.; Namba, S.; Tatsumi, T. Synthesis and catalytic properties of a new titanosilicate molecular sieve with the structure analogous to MWW-type lamellar precursor. *J. Catal.* **2006**, *243*, 183–191. 10.1016/j.jcat.2006.07.003.

94. Zuo, Y.; Song, W.; Dai, C.; He, Y.; Wang, M.; Wang, X.; Guo, X. Modification of small-crystal titanium silicalite-1 with organic bases: Recrystallization and catalytic properties in the hydroxylation of phenol. *Appl. Catal. A Gen.* **2013**, *453*, 272–279. https://doi.org/10.1016/j.apcata.2012.12.027.

95. Shan, Z.; Lu, Z.; Wang, L.; Zhou, C.; Ren, L.; Zhang, L.; Meng, X.; Ma, S.; Xiao, F.-S. Stable Bulky Particles Formed by TS-1 Zeolite Nanocrystals in the Presence of H2O2. *ChemCatChem* **2010**, *2*, 407–412. https://doi.org/10.1002/cctc.200900312.

96. Xin, H.; Zhao, J.; Xu, S.; Li, J.; Zhang, W.; Guo, X.; Hensen, E.J.M.; Yang, Q.; Li, C. Enhanced Catalytic Oxidation by Hierarchically Structured TS-1 Zeolite. *J. Phys. Chem. C* **2010**, *114*, 6553–6559. 10.1021/jp912112h.

97. Serrano, D.; Sanz, R.; Pizarro, P.; Moreno, I. Turning TS-1 zeolite into a highly active catalyst for olefin epoxidation with organic hydroperoxides. *Chem. Commun.* **2009**, 1407–1409. 10.1039/B821545F.

98. Kwon, S.; Schweitzer, N.M.; Park, S.; Stair, P.C.; Snurr, R.Q. A kinetic study of vapor-phase cyclohexene epoxidation by H2O2 over mesoporous TS-1. *J. Catal.* **2015**, *326*, 107–115. https://doi.org/10.10 16/j.jcat.2015.04.005.

99. Wilkenhöner, U.; Langhendries, G.; van Laar, F.; Baron, G. V; Gammon, D.W.; Jacobs, P.A.; van Steen, E. Influence of Pore and Crystal Size of Crystalline Titanosilicates on Phenol Hydroxylation in Different Solvents. *J. Catal.* **2001**, *203*, 201–212. https://doi.org/10.1006/jcat.2001.3308.

100. Notari, B. Titanium silicalites. *Catal. Today* **1993**, *18*, 163–172. https://doi.org/10.1016/0920-5861(93)85029-Y.

101. Perego, C.; Carati, A.; Ingallina, P.; Mantegazza, M.A.; Bellussi, G. Production of titanium containing molecular sieves and their application in catalysis. *Appl. Catal. A Gen.* **2001**, *221*, 63–72. https://doi.org/10.1016/S0926-860X(01)00797-9.

102. Hwang, Y.K.; Chang, J.-S.; Park, S.-E.; Kim, D.S.; Kwon, Y.-U.; Jhung, S.H.; Hwang, J.-S.; Park, M.S. Microwave Fabrication of MFI Zeolite Crystals with a Fibrous Morphology and Their Applications. *Angew. Chemie Int. Ed.* **2005**, *44*, 556–560. https://doi.org/10.1002/anie.200461403.

103. Camblor, M.A.; Corma, A.; Martínez, A.; Pérez-Pariente, J. Synthesis of a titaniumsilicoaluminate isomorphous to zeolite beta and its application as a catalyst for the selective oxidation of large organic molecules. *J. Chem. Soc. Chem. Commun.* **1992**, 589–590. 10.1039/C39920000589.

104. Camblor, M.A.; Costantini, M.; Corma, A.; Gilbert, L.; Esteve, P.; Martínez, A.; Valencia, S. Synthesis and catalytic activity of aluminium-free zeolite Ti-β oxidation catalysts. *Chem. Commun.* **1996**, 1339–1340. 10.1039/CC9960001339.

105. Camblor, M.A.; Corma, A.; Mifsud, A.; Pérez-Pariente, J.; Valencia, S. Synthesis of nanocrystalline zeolite beta in the absence of alkali metal cations. In *Progress in Zeolite and Microporous Materials*; Chon, H., Ihm, S.-K., Uh, Y.S.B.T.-S. in S.S. and C., Eds.; Elsevier, 1997; Vol. 105, pp. 341–348 ISBN 0167-2991. https://doi.org/10.1016/S0167-2991(97)80574-5.

106. Lami, E.B.; Fajula, F.; Anglerot, D.; Des Courieres, T. Single step dealumination of zeolite beta precursors for the preparation of hydrophobic adsorbents. *Microporous Mater.* **1993**, *1*, 237–245. https://doi.org/10.1016/0927-6513(93)80067-5.

107. Corma, A.; Camblor, M.A.; Esteve, P.; Martinez, A.; Perezpariente, J. Activity of Ti-Beta Catalyst for the Selective Oxidation of Alkenes and Alkanes. *J. Catal.* **1994**, *145*, 151–158. https://doi.org/10.1006/jcat.1994.1017.

108. Ren, W.; Hua, Z.; Ge, T.; Zhou, X.; Chen, L.; Zhu, Y.; Shi, J. Post-synthesis of hierarchically structured Ti-β zeolites and their epoxidation catalytic performance. *Chinese J. Catal.* **2015**, *36*, 906–912. https://doi.org/10.1016/S1872-2067(14)60267-9.

109. Nogier, J.-P.; Millot, Y.; Man, P.P.; Shishido, T.; Che, M.; Dzwigaj, S. Probing the Incorporation of Ti(IV) into the BEA Zeolite Framework by XRD, FTIR, NMR, and DR UV−jp810722bis. *J. Phys. Chem. C* **2009**, *113*, 4885–4889. 10.1021/jp8099829.

110. Tang, B.; Dai, W.; Sun, X.; Guan, N.; Li, L.; Hunger, M. A procedure for the preparation of Ti-Beta zeolites for catalytic epoxidation with hydrogen peroxide. *Green Chem.* **2014**, *16*, 2281–2291. 10.1039/c3gc42534g.

111. Hoeven, N.; Mali, G.; Mertens, M.; Cool, P. Design of Ti-Beta zeolites with high Ti loading and tuning of their hydrophobic/hydrophilic character. *Microporous Mesoporous Mater.* **2019**, *288*, 109588. 10.1016/j.micromeso.2019.109588.

112. Tatsumi, T.; Jappar, N. Properties of Ti-Beta Zeolites Synthesized by Dry-Gel Conversion and Hydrothermal Methods. *J. Phys. Chem. B* **1998**, *102*, 7126–7131. 10.1021/jp9816216.

113. Camblor, M.A.; Constantini, M.; Corma, A.; Esteve, P.; Gilbert, L.; Martinez, A.; Valencia, S. A new highly efficient method for the synthesis of Ti-Beta zeolite oxidation catalyst. *Appl. Catal. A Gen.* **1995**, *133*, L185–L189. https://doi.org/10.1016/0926-860X(95)00252-9.

114. Galacho, C.; Ribeiro Carrott, M.M.L.; Carrott, P.J.M. Evaluation of the thermal and mechanical stability of Si-MCM-41 and Ti-MCM-41 synthesised at room temperature. *Microporous Mesoporous Mater.* **2008**, *108*, 283–293. 10.1016/j.micromeso.2007.04.010.

115. Atienzar, P.; Navarro, M.; Corma, A.; Garcia, H. Photovoltaic activity of Ti/MCM-41. *ChemPhysChem* **2009**, *10*, 252–256. 10.1002/cphc.200800548.

116. Corma, A.; Navarro, M.T.; Pariente, J.P. Synthesis of an ultralarge pore titanium silicate isomorphous to MCM-41 and its application as a catalyst for selective oxidation of hydrocarbons. *J. Chem. Soc. Chem. Commun.* **1994**, 147–148. 10.1039/C39940000147.

117. Park, S.S.; Park, D.H. Temperature dependence of pore size distribution of highly crystalline titanosilicate MCM-41. *Solid State Phenom.* 2007, *119*, 131–134. 10.4028/www.scientific.net/SSP.119.131.

118. Beck, J.S.; Vartuli, J.C.; Roth, W.J.; Leonowicz, M.E.; Kresge, C.T.; Schmitt, K.D.; Chu, C.T.W.; Olson, D.H.; Sheppard, E.W.; McCullen, S.B.; et al. A new family of mesoporous molecular sieves prepared with liquid crystal templates. *J. Am. Chem. Soc.* **1992**, *114*, 10834–10843. 10.1021/ja00053a020.

119. Zhang, W.; Fröba, M.; Wang, J.; Tanev, P.T.; Wong, J.; Pinnavaia, T.J. Mesoporous titanosilicate molecular sieves prepared at ambient temperature by electrostatic (S+I-, S+X-I+) and neutral (S°I°) assembly pathways: A comparison of physical properties and catalytic activity for peroxide oxidations. *J. Am. Chem. Soc.* **1996**, *118*, 9164–9171. 10.1021/ja960594z.

120. Silva, T.N.; Lopes, J.M.; Ribeiro, F.R.; Carrott, M.R.; Galacho, P.C.; Sousa, M.J.; Carrott, P. Catalytic and adsorption properties of Al-and Ti-MCM-41 synthesized at room temperature. *React. Kinet. Catal. Lett.* **2002**, *77*, 83–90. 10.1023/A:1020343920133.

121. Chatterjee, M.; Hayashi, H.; Saito, N. Role and effect of supercritical fluid extracion of template on the Ti(IV) active sites Ti-MCM-41. *Microporous Mesoporous Mater.* **2003**, *57*, 143–155. 10.1016/S1387-1811(02)00561-9.

122. Campelo, J.M.; Hidalgo, J.M.; Luna, D.; Marinas, J.M.; Romero, A.A. Effect of post-synthesis salt solution treatment on Ti-MCM-41 acid-basic properties. Influence on their activity and selectivity in catalytic liquid-phase epoxidation of cyclohexene. *Stud. Surf. Sci. Catal.* 2005, *158 B*, 1429–1436. 10.1016/s0167-2991(05)80494-x.

123. Wu, P.; Tatsumi, T. A new generation of titanosilicate catalyst: Preparation and application to liquid-phase epoxidation of alkenes. *Catal. Surv. from Asia* **2004**, *8*, 137–148. 10.1023/B:CATS.0000027015.37277.fb.

124. Meng, X.; Li, D.; Yang, X.; Yu, Y.; Wu, S.; Han, Y.; Yang, Q.; Jiang, D.; Xiao, F.-S. Synthesis, characterization, and catalytic activity of mesostructured titanosilicates assembled from polymer surfactants with preformed titanosilicate precursors in strongly acidic media. *J. Phys. Chem. B* **2003**, *107*, 8972–8980. 10.1021/jp027405l.

125. Qi, C.; Akita, T.; Okumura, M.; Kuraoka, K.; Haruta, M. Effect of surface chemical properties and texture of mesoporous titanosilicates on direct vapor-phase epoxidation of propylene over Au catalysts at high reaction temperature. *Appl. Catal. A Gen.* **2003**, *253*, 75–89. 10.1016/S0926-860X(03)00526-X.

126. Chen, X.-Y.; Chen, S.-L.; Jia, A.-P.; Lu, J.-Q.; Huang, W.-X. Gas phase propylene epoxidation over Au supported on titanosilicates with different Ti chemical environments. *Appl. Surf. Sci.* **2017**, *393*, 11–22. 10.1016/j.apsusc.2016.09.159.

127. Wang, Z.; Balkus Jr, K.J. Liquid phase propylene oxidation with tert-butyl hydroperoxide over titanium containing wrinkled mesoporous silica. *Catal. Commun.* **2017**, *96*, 15–18. 10.1016/j.catcom.2017.03.014.

128. Wang, Z.; Balkus Jr., K.J. Synthesis and modification of titanium containing wrinkled mesoporous silica for cyclohexene epoxidation. *Microporous Mesoporous Mater.* **2017**, *243*, 76–84. 10.1016/j.micromeso.2017.01.035.

129. Zhu, Z.; Hartmann, M.; Maes, E.M.; Czernuszewicz, R.S.; Kevan, L. Physicochemical Characterization of Chromium Oxides Immobilized in Mesoporous MeMCM-41 (Me = Al, Ti, and Zr) Molecular Sieves. *J. Phys. Chem. B* **2000**, *104*, 4690–4698. 10.1021/jp994335i.

130. Díaz, I.; Mohino, F.; Pérez-Pariente, J.; Sastre, E. Synthesis, characterization and catalytic activity of MCM-41-type mesoporous silicas functionalized with sulfonic acid. *Appl. Catal. A Gen.* **2001**, *205*, 19–30. https://doi.org/10.1016/S0926-860X(00)00808-5.

131. Kresge, C.T.; Leonowicz, M.E.; Roth, W.J.; Vartuli, J.C.; Beck, J.S. Ordered mesoporous molecular sieves synthesized by a liquid-crystal template mechanism. *Nature* **1992**, *359*, 710–712. 10.1038/359710a0.

132. Tatsumi, T.; Koyano, K.A.; Tanaka, Y.; Nakata, S. Stabilization of M41S materials by trimethylsilylation. *Stud. Surf. Sci. Catal.* 1998, *117*, 143–150. 10.1016/s0167-2991(98)80988-9.

133. Pinnavaia, T.J.; Tanev, P.T.; Wang, J.; Zhang, W. Ti-substituted mesoporous molecular sieves for catalytic oxidation of large aromatic compounds prepared by neutral templating route. In Proceedings of the Materials Research Society Symposium - Proceedings; 1995; Vol. 371, pp. 53–62.

134. Wróblewska, A.; Ławro, E.; Milchert, E. Epoxidation of 2-buten-1-ol over Ti-MCM-41 and Ti-MCM-48 titanium silicalite catalysts. *Polish J. Chem. Technol.* **2007**, *9*, 1–4. 10.2478/v10026-007-0041-8.

135. Wroblewska, A.; Wajzberg, J.; Milchert, E. Epoxidation of methallyl chloride with hydrogen peroxide over Ti-MCM-48 catalyst. *Oxid. Commun.* **2008**, *31*, 826–840.

136. Wróblewska, A.; Milchert, E. Liquid phase epoxidation of allylic compounds with hydrogen peroxide at autogenic and atmospheric pressure over mesoporous Ti-MCM-48 Catalyst. *J. Adv. Oxid. Technol.* **2009**, *12*, 170–177. 10.1515/jaots-2009-0204.

137. Wroblewska, A.; Butwin, A.; Lawro, E. Epoxidation of crotyl alcohol at autogenic and atmospheric pressure over Ti-MCM-48 catalyst. *Oxid. Commun.* **2009**, *32*, 796–810.

138. Rasalingam, S.; Peng, R.; Koodali, R.T. An insight into the adsorption and photocatalytic degradation of rhodamine B in periodic mesoporous materials. *Appl. Catal. B Environ.* **2015**, *174–175*, 49–59. 10.1016/j.apcatb.2015.02.040.

139. Chen, J.; Fang, K.; Wu, L.; Qian, Z.; Chen, J. Removal of Cd(II) from aqueous by adsorption onto mesoporous Ti-MCM-48. In Proceedings of the Procedia Environmental Sciences; 2011; Vol. 10, pp. 2491–2497. 10.1016/j.proenv.2011.09.388.

140. Peng, R.; Wu, C.M.; Baltrusaitis, J.; Dimitrijevic, N.M.; Rajh, T.; Koodali, R.T. Ultra-stable CdS incorporated Ti-MCM-48 mesoporous materials for efficient photocatalytic decomposition of water under visible light illumination. *Chem. Commun.* **2013**, *49*, 3221–3223. 10.1039/c3cc41362d.

141. Peng, R.; Wu, C.-M.; Baltrusaitis, J.; Dimitrijevic, N.M.; Rajh, T.; Koodali, R.T. Solar hydrogen generation over CdS incorporated in Ti-MCM-48 mesoporous materials under visible light illumination. *Int. J. Hydrogen Energy* **2016**, *41*, 4106–4119. 10.1016/j.ijhydene.2016.01.040.

142. Maneesuwan, H.; Chaisuwan, T.; Wongkasemjit, S. Synthesis of Fe-Ti-MCM-48 from silatrane precursor via sol-gel process and its hydrothermal stability. *Mater. Chem. Phys.* **2014**, *146*, 374–379. 10.1016/j.matchemphys.2014.03.041.

143. Peng, R.; Baltrusaitis, J.; Wu, C.-M.; Koodali, R.T. Pd-Ti-MCM-48 cubic mesoporous materials for solar simulated hydrogen evolution. *Int. J. Hydrogen Energy* **2015**, *40*, 905–918. 10.1016/j.ijhydene.2014.11.089.

144. Duan, Y.; Zhai, D.; Zhang, X.; Zheng, J.; Li, C. Synthesis of CuO/Ti-MCM-48 Photocatalyst for the Degradation of Organic Pollutions Under Solar-Simulated Irradiation. *Catal. Letters* **2018**, *148*, 51–61. 10.1007/s10562-017-2258-3.

145. Nadeem, S.; Mumtaz, A.; Mumtaz, M.; Abdul Mutalib, M.I.; Shaharun, M.S.; Abdullah, B. Visible light driven CO2 reduction to methanol by Cu-porphyrin impregnated mesoporous Ti-MCM-48. *J. Mol. Liq.* **2018**, *272*, 656–667. 10.1016/j.molliq.2018.09.077.

146. Morey, M.S.; O'Brien, S.; Schwarz, S.; Stucky, G.D. Hydrothermal and postsynthesis surface modification of cubic, MCM-48, and ultralarge pore SBA-15 mesoporous silica with titanium. *Chem. Mater.* **2000**, *12*, 898–911. 10.1021/cm9901663.

147. Newalkar, B.L.; Olanrewaju, J.; Komarneni, S. Direct Synthesis of Titanium-Substituted Mesoporous SBA-15 Molecular Sieve under Microwave−Hydrothermal Conditions. *Chem. Mater.* **2001**, *13*, 552–557. 10.1021/cm000748g.

148. Wu, P.; Tatsumi, T.; Komatsu, T.; Yashima, T. Postsynthesis, characterization, and catalytic properties in alkene epoxidation of hydrothermally stable mesoporous Ti-SBA-15. *Chem. Mater.* **2002**, *14*, 1657–1664. 10.1021/cm010910v.

149. Zhang, W.-H.; Lu, J.; Han, B.; Li, M.; Xiu, J.; Ying, P.; Li, C. Direct Synthesis and Characterization of Titanium-Substituted Mesoporous Molecular Sieve SBA-15. *Chem. Mater.* **2002**, *14*, 3413–3421. 10.1021/cm011686c.

150. Radu, D.C.; Ion, A.; Pârvulescu, V.I.; Câmpeanu, V.; Bartha, E.; Trong On, D.; Kaliaguine, S. Oxidation of methyl-propyl-thioether with hydrogen peroxide using Ti-SBA-15 as catalyst. *Stud. Surf. Sci. Catal.* 2003, *146*, 609–612. 10.1016/S0167-2991(03)80457-3.

151. Ganiyu, S.A.; Ali, S.A.; Alhooshani, K. Synthesis of a Ti-SBA-15-nimo hydrodesulfurization catalyst: The effect of the hydrothermal synthesis temperature of nimo and molybdenum loading on the catalytic activity. *Ind. Eng. Chem. Res.* **2017**, *56*, 5201–5209. 10.1021/acs.iecr.7b00719.

152. Vallés, V.A.; Ledesma, B.C.; Pecchi, G.A.; Anunziata, O.A.; Beltramone, A.R. Hydrogenation of tetralin in presence of nitrogen using a noble-bimetallic couple over a Ti-modified SBA-15. *Catal. Today* **2017**, *282*, 111–122. 10.1016/j.cattod.2016.07.004.

153. Mendoza-Nieto, J.A.; Vizueth-Montes de Oca, A.; Calzada, L.A.; Klimova, T.E. Trimetallic NiMoW and CoMoW catalysts supported on SBA-15 modified with titania or zirconia for deep hydrodesulfurization. *Catal. Today* **2021**, *360*, 78–89. 10.1016/j.cattod.2019.06.023.

154. Nguyen, T.T.; Qian, E.W. Synthesis of mesoporous Ti-inserted SBA-15 and CoMo/Ti-SBA-15 catalyst for hydrodesulfurization and hydrodearomatization. *Microporous Mesoporous Mater.* **2018**, *265*, 1–7. 10.1016/j.micromeso.2018.01.026.

155. Zhao, Q.; Yang, C.; Fang, M.; Jiang, T. Performance of Brönsted-Lewis acidic ionic liquids supported Ti-SBA-15 for the esterification of acetic acid to benzyl alcohol. *Appl. Catal. A Gen.* **2020**, *594*. 10.1016/j.apcata.2020.117470.

156. Liu, Z.; Crumbaugh, G.M.; Davis, R.J. Effect of Structure and Composition on Epoxidation of HexeneCatalyzed by Microporous and Mesoporous Ti–Si Mixed Oxides. *J. Catal.* **1996**, *159*, 83–89. https://doi.org/10.1006/jcat.1996.0066.

157. U.K Patent 1 249 079 1971.

158. Hutter, R.; Mallat, T.; Baiker, A. Titania-silica mixed oxides: III. Epoxidation of α-isophorone with hydroperoxides. *J. Catal.* **1995**, *157*, 665–675. 10.1006/jcat.1995.1332.

159. Calvino, J.J.; Cauqui, M.A.; Gatica, J.M.; Perez, J.A.; Rodriguez-Izquierdo, J.M. Development of acidity on sol-gel prepared TiO2-SiO2 catalysts. In Proceedings of the Materials Research Society Symposium - Proceedings; 1994; Vol. 346, pp. 685–690. 10.1557/proc-346-685.

160. Neumann, R.; Chava, M.; Levin, M. Hydrogen peroxide oxidations catalysed by metallosilicalite xerogels. *J. Chem. Soc. Chem. Commun.* **1993**, 1685–1687. 10.1039/C39930001685.

161. Hutter, R.; Mallat, T.; Baiker, A. Titania silica mixed oxides: II. Catalytic behavior in olefin epoxidation. *J. Catal.* **1995**, *153*, 177–189. 10.1006/jcat.1995.1119.

162. Dutoit, D.C.M.; Schneider, M.; Hutter, R.; Baiker, A. Titania-silica mixed oxides: IV. Influence of Ti content and aging on structural and catalytic properties of aerogels. *J. Catal.* **1996**, *161*, 651–658.

10.1006/jcat.1996.0227.

163. Itoh, M.; Hattori, H.; Tanabe, K. The acidic properties of TiO2-SiO2 and its catalytic activities for the amination of phenol, the hydration of ethylene and the isomerization of butene. *J. Catal.* **1974**, *35*, 225–231. https://doi.org/10.1016/0021-9517(74)90201-2.

164. Ko, E.I.; Chen, J.-P.; Weissman, J.G. A study of acidic titania/silica mixed oxides and their use as supports for nickel catalysts. *J. Catal.* **1987**, *105*, 511–520. https://doi.org/10.1016/0021-9517(87)90078-9.

165. Nakabayashi, H. Properties of Acid Sites on TiO2–SiO2 and TiO2–Al2O3 Mixed Oxides Measured by Infrared Spectroscopy. *Bull. Chem. Soc. Jpn.* **1992**, *65*, 914–916. 10.1246/bcsj.65.914.

166. Sohn, J.R.; Jang Taegu (Korea)], H.J. [Kyungpook N.U. Correlation between the infrared band frequency of the silanol bending vibration in TiO sub 2 -SiO sub 2 catalysts and activity for acid catalysis. **1991**. 10.1016/0021-9517(91)90172-Z.

167. Gao, X.; Wachs, I.E. Titania-silica as catalysts: Molecular structural characteristics and physico-chemical properties. *Catal. Today* **1999**, *51*, 233–254. 10.1016/S0920-5861(99)00048-6.

168. Clerici, M.G.; Kholdeeva, O.A. *Liquid Phase Oxidation via Heterogeneous Catalysis: Organic Synthesis and Industrial Applications*; Wiley, 2013; ISBN 9781118356753.

169. Dusi, M.; Mallat, T.; Baiker, A. Titania-silica mixed oxides: Influence of reaction additives on the epoxidation of (E)-2-hexen-1-ol. *J. Catal.* **1998**, *173*, 423–432. 10.1006/jcat.1997.1918.

170. Gisler, A.; Müller, C.A.; Schneider, M.; Mallat, T.; Baiker, A. Synthesis of organically modified titania-silica aerogels: Application for epoxidation of cyclohexenol. *Stud. Surf. Sci. Catal.* 2000, *130 B*, 1637–1642. 10.1016/s0167-2991(00)80435-8.

171. Murata, C.; Yoshida, H.; Hattori, T. Titania-silica catalysts prepared by sol-gel method for photoepoxidation of propene with molecular oxygen. *Stud. Surf. Sci. Catal.* 2000, *143*, 845–853. 10.1016/s0167-2991(00)80728-4.

172. Müller, C.A.; Schneider, M.; Gisler, A.; Mallat, T.; Baiker, A. Titania-silica epoxidation catalysts modified by acetoxypropyl groups. *Catal. Letters* **2000**, *64*, 9–14. 10.1023/A:1019074617565.

173. Müller, C.A.; Schneider, M.; Mallat, T.; Baiker, A. Titania-Silica Epoxidation Catalysts Modified by Polar Organic Functional Groups. *J. Catal.* **2000**, *189*, 221–232. 10.1006/jcat.1999.2697.

174. Berlini, C.; Ferraris, G.; Guidotti, M.; Moretti, G.; Psaro, R.; Ravasio, N. A comparison between [Ti]-MCM-41 and amorphous mesoporous s ilica silica-titanica as catalysts for the epoxidation of bulky unsaturated alcohols. *Microporous Mesoporous Mater.* **2001**, *44–45*, 595–602. 10.1016/S1387-1811(01)00239-6.

175. Radu, D.C.; Pârvulescu, V.I.; Câmpeanu, V.; Bartha, E.; Jonas, A.; Grange, P. Chemoselective oxidation of 2-thiomethyl-4,6-dimethyl-pyrimidine and 2-thiobenzyl-4,6-dimethyl-pyrimidine over titania-silica catalysts. *Appl. Catal. A Gen.* **2003**, *242*, 77–84. 10.1016/S0926-860X(02)00508-2.

176. Gisler, A.; Bürgi, T.; Baiker, A. Epoxidation on titania-silica aerogel catalysts studied by attenuated total reflection Fourier transform infrared and modulation spectroscopy. *Phys. Chem. Chem. Phys.* **2003**, *5*, 3539–3548. 10.1039/b304971j.

177. Beck, C.; Mallat, T.; Baiker, A. Epoxidation of allylic alcohols with TiO2-SiO2: Hydroxy-assisted mechanism and dynamic structural changes during reaction. *Catal. Letters* **2003**, *88*, 203–209. 10.1023/A:1024074108874.

178. Lorret, O.; Lafond, V.; Mutin, P.H.; Vioux, A. One-Step Synthesis of Mesoporous Hybrid Titania−Silica Xerogels for the Epoxidation of Alkenes. *Chem. Mater.* **2006**, *18*, 4707–4709. 10.1021/cm061478q.

179. Davis, R.J.; Liu, Z. Titania-Silica: A Model Binary Oxide Catalyst System. *Chem. Mater.* **1997**, *9*, 2311–2324. 10.1021/cm970314u.

180. Mariscal, R.; López-Granados, M.; Fierro, J.L.G.; Sotelo, J.L.; Martos, C.; Van Grieken, R. Morphology and surface properties of titania-silica hydrophobic xerogels. *Langmuir* **2000**, *16*, 9460–9467. 10.1021/la000876j.

181. Beck, C.; Mallat, T.; Bürgi, T.; Baiker, A. Nature of active sites in sol-gel TiO2-SiO2 epoxidation catalysts. *J. Catal.* **2001**, *204*, 428–439. 10.1006/jcat.2001.3407.

182. Beck, C.; Mallat, T.; Baiker, A. On the limited selectivity of silica-based epoxidation catalysts. *Catal. Letters* **2001**, *75*, 131–136. 10.1023/A:1016700323552.

183. Mohamed, M.M.; Salama, T.M.; Yamaguchi, T. Synthesis, characterization and catalytic properties of titania-silica catalysts. *Colloids Surfaces A Physicochem. Eng. Asp.* **2002**, *207*, 25–32. 10.1016/S0927-7757(02)00002-X.

184. Pabón, E.; Retuert, J.; Quijada, R.; Zarate, A. TiO2-SiO2 mixed oxides prepared by a combined sol-gel and polymer inclusion method. *Microporous Mesoporous Mater.* **2004**, *67*, 195–203. 10.1016/j.micromeso.2003.10.017.

185. Cao, S.; Yao, N.; Yeung, K.L. Synthesis of freestanding silica and titania-silica aerogels with ordered and disordered mesopores. *J. Sol-Gel Sci. Technol.* **2008**, *46*, 323–333. 10.1007/s10971-008-1701-8.

186. Gisler, A.; Müller, C.A.; Schneider, M.; Mallat, T.; Baiker, A. Titania-silica epoxidation catalysts modified by mono- and bidentate organic functional groups. *Top. Catal.* **2001**, *15*, 247–255. 10.1023/a:1016610117769.

187. Hu, S.; Willey, R.J.; Notari, B. An investigation on the catalytic properties of titania-silica materials. *J. Catal.* **2003**, *220*, 240–248. 10.1016/S0021-9517(03)00294-X.

188. Blokzijl, W.; Engberts, J.B.F.N. Hydrophobic Effects. Opinions and Facts. *Angew. Chemie Int. Ed. English* **1993**, *32*, 1545–1579. https://doi.org/10.1002/anie.199315451.

189. Kinloch, A.J. The science of adhesion. *J. Mater. Sci.* **1980**, *15*, 2141–2166. 10.1007/BF00552302.

190. Wang, L.; Xiao, F.-S. The Importance of Catalyst Wettability. *ChemCatChem* **2014**, *6*, 3048–3052. https://doi.org/10.1002/cctc.201402437.

191. Li, S.; Zhou, H.; Xiao, L.; Fan, J.; Zheng, X. Fabrication of Super-Hydrophobic Titanosilicate Sub-micro Sphere with Enhanced Epoxidation Catalytic Activity. *Catal. Letters* **2019**, *149*, 1396–1402. 10.1007/s10562-019-02720-y.

192. Bregante, D.T.; Potts, D.S.; Kwon, O.; Ayla, E.Z.; Tan, J.Z.; Flaherty, D.W. Effects of Hydrofluoric Acid Concentration on the Density of Silanol Groups and Water Adsorption in Hydrothermally Synthesized Transition-Metal-Substituted Silicalite-1. *Chem. Mater.* **2020**, *32*, 7425–7437. 10.1021/acs.chemmater.0c02405.

193. Xie, L.-H.; Xu, M.-M.; Liu, X.-M.; Zhao, M.-J.; Li, J.-R. Hydrophobic Metal–Organic Frameworks: Assessment, Construction, and Diverse Applications. *Adv. Sci.* **2020**, *7*. 10.1002/advs.201901758.

194. Iglesias, J.; Melero, J.A.; Sainz-Pardo, J. Direct synthesis of organically modified Ti-SBA-15 materials. *J. Mol. Catal. A Chem.* **2008**, *291*, 75–84. 10.1016/j.molcata.2008.06.004.

195. Lin, K.; Pescarmona, P.P.; Houthoofd, K.; Liang, D.; Van Tendeloo, G.; Jacobs, P.A. Direct room-temperature synthesis of methyl-functionalized Ti-MCM-41 nanoparticles and their catalytic performance in epoxidation. *J. Catal.* **2009**, *263*, 75–82. https://doi.org/10.1016/j.jcat.2009.01.013.

196. Csicsery, S.M. Catalysis by shape selective zeolites-science and technology. *Pure Appl. Chem.* **1986**, *58*,

841–856.

197. Takeuchi, M.; Kimura, T.; Hidaka, M.; Rakhmawaty, D.; Anpo, M. Photocatalytic oxidation of acetaldehyde with oxygen on TiO2/ZSM-5 photocatalysts: Effect of hydrophobicity of zeolites. *J. Catal.* **2007**, *246*, 235–240. https://doi.org/10.1016/j.jcat.2006.12.010.

198. Sano, T.; Yamashita, N.; Iwami, Y.; Takeda, K.; Kawakami, Y. Estimation of dealumination rate of ZSM-5 zeolite by adsorption of water vapor. *Zeolites* **1996**, *16*, 258–264. https://doi.org/10.1016/0144-2449(95)00161-1.

199. Zhang, K.; Lively, R.P.; Noel, J.D.; Dose, M.E.; McCool, B.A.; Chance, R.R.; Koros, W.J. Adsorption of Water and Ethanol in MFI-Type Zeolites. *Langmuir* **2012**, *28*, 8664–8673. 10.1021/la301122h.

200. Zhao, X.S.; Lu, G.Q.; Whittaker, A.K.; Millar, G.J.; Zhu, H.Y. Comprehensive Study of Surface Chemistry of MCM-41 Using 29Si CP/MAS NMR, FTIR, Pyridine-TPD, and TGA. *J. Phys. Chem. B* **1997**, *101*, 6525–6531. 10.1021/jp971366+.

201. Camblor, M.A.; Corma, A.; Valencia, S. Spontaneous nucleation and growth of pure silica zeolite-β free of connectivity defects. *Chem. Commun.* **1996**, 2365–2366. 10.1039/CC9960002365.

202. Gounder, R.; Davis, M.E. Beyond shape selective catalysis with zeolites: Hydrophobic void spaces in zeolites enable catalysis in liquid water. *AIChE J.* **2013**, *59*, 3349–3358. https://doi.org/10.1002/aic.14016.

203. Roy, S.K.; Dutta, D.; Talukdar, A.K. Highly effective methylated Ti MCM-41 catalyst for cyclohexene oxidation. *Mater. Res. Bull.* **2018**, *103*, 38–46. https://doi.org/10.1016/j.materresbull.2018.03.017.

204. Fraile, J.M.; García, J.I.; Mayoral, J.A.; Vispe, E. Effect of the Reaction Conditions on the Epoxidation of Alkenes with Hydrogen Peroxide Catalyzed by Silica-Supported Titanium Derivatives. *J. Catal.* **2001**, *204*, 146–156. https://doi.org/10.1006/jcat.2001.3355.

205. Debecker, D.P. Innovative Sol-Gel Routes for the Bottom-Up Preparation of Heterogeneous Catalysts. *Chem. Rec.* **2018**, *18*, 662–675. https://doi.org/10.1002/tcr.201700068.

206. Marmur, A.; Della Volpe, C.; Siboni, S.; Amirfazli, A.; Drelich, J.W. Contact angles and wettability: towards common and accurate terminology. *Surf. Innov.* **2017**, *5*, 3–8. 10.1680/jsuin.17.00002.

207. Young, T. III. An essay on the cohesion of fluids. *Philos. Trans. R. Soc. London* **1805**, *95*, 65–87. 10.1098/rstl.1805.0005.

208. Subedi, D. Contact angle measurement for the surface characterization of solids. *Himal. Phys.* **2011**, *2*, 1–4.

209. Amirfazli, A.; Neumann, A.W. Status of the three-phase line tension: a review. *Adv. Colloid Interface Sci.* **2004**, *110*, 121–141. https://doi.org/10.1016/j.cis.2004.05.001.

210. Drelich, J. The significance and magnitude of the line tension in three-phase (solid-liquid-fluid) systems. *Colloids Surfaces A Physicochem. Eng. Asp.* **1996**, *116*, 43–54. https://doi.org/10.1016/0927-7757(96)03651-5.

211. Schimmele, L.; Napiórkowski, M.; Dietrich, S. Conceptual aspects of line tensions. *J. Chem. Phys.* **2007**, *127*, 164715. 10.1063/1.2799990.

212. Dingle, N.M.; Harris, M.T. A robust algorithm for the simultaneous parameter estimation of interfacial tension and contact angle from sessile drop profiles. *J. Colloid Interface Sci.* **2005**, *286*, 670–680. https://doi.org/10.1016/j.jcis.2005.01.087.

213. Espinoza, D.N.; Santamarina, J.C. Water-CO2-mineral systems: Interfacial tension, contact angle, and diffusion—Implications to CO2 geological storage. *Water Resour. Res.* **2010**, *46*. https://doi.org/10.1029/2009WR008634.

214. Promraksa, A.; Chen, L.-J. Modeling contact angle hysteresis of a liquid droplet sitting on a cosine wave-

like pattern surface. *J. Colloid Interface Sci.* **2012**, *384*, 172–181. https://doi.org/10.1016/j.jcis.2012.06.064.

215. Iglauer, S.; Pentland, C.H.; Busch, A. CO2 wettability of seal and reservoir rocks and the implications for carbon geo-sequestration. *Water Resour. Res.* **2015**, *51*, 729–774. https://doi.org/10.1002/2014WR015553.

216. Schmitt, M.; Groß, K.; Grub, J.; Heib, F. Detailed statistical contact angle analyses; "slow moving" drops on inclining silicon-oxide surfaces. *J. Colloid Interface Sci.* **2015**, *447*, 229–239. https://doi.org/10.1016/j.jcis.2014.10.047.

217. Arif, M.; Al-Yaseri, A.Z.; Barifcani, A.; Lebedev, M.; Iglauer, S. Impact of pressure and temperature on CO2–brine–mica contact angles and CO2–brine interfacial tension: Implications for carbon geo-sequestration. *J. Colloid Interface Sci.* **2016**, *462*, 208–215. https://doi.org/10.1016/j.jcis.2015.09.076.

218. AlRatrout, A.; Raeini, A.Q.; Bijeljic, B.; Blunt, M.J. Automatic measurement of contact angle in pore-space images. *Adv. Water Resour.* **2017**, *109*, 158–169. https://doi.org/10.1016/j.advwatres.2017.07.018.

219. Scanziani, A.; Singh, K.; Blunt, M.J.; Guadagnini, A. Automatic method for estimation of in situ effective contact angle from X-ray micro tomography images of two-phase flow in porous media. *J. Colloid Interface Sci.* **2017**, *496*, 51–59. https://doi.org/10.1016/j.jcis.2017.02.005.

220. Andrew, M.; Menke, H.; Blunt, M.J.; Bijeljic, B. The Imaging of Dynamic Multiphase Fluid Flow Using Synchrotron-Based X-ray Microtomography at Reservoir Conditions. *Transp. Porous Media* **2015**, *110*, 1–24. 10.1007/s11242-015-0553-2.

221. Khishvand, M.; Alizadeh, A.H.; Oraki Kohshour, I.; Piri, M.; Prasad, R.S. In situ characterization of wettability alteration and displacement mechanisms governing recovery enhancement due to low-salinity waterflooding. *Water Resour. Res.* **2017**, *53*, 4427–4443. https://doi.org/10.1002/2016WR020191.

222. Sun, C.; McClure, J.E.; Mostaghimi, P.; Herring, A.L.; Berg, S.; Armstrong, R.T. Probing Effective Wetting in Subsurface Systems. *Geophys. Res. Lett.* **2020**, *47*, e2019GL086151. https://doi.org/10.1029/2019GL086151.

223. Santini, M.; Guilizzoni, M.; Fest-Santini, S. X-ray computed microtomography for drop shape analysis and contact angle measurement. *J. Colloid Interface Sci.* **2013**, *409*, 204–210. https://doi.org/10.1016/j.jcis.2013.06.036.

224. Mascini, A.; Cnudde, V.; Bultreys, T. Event-based contact angle measurements inside porous media using time-resolved micro-computed tomography. *J. Colloid Interface Sci.* **2020**, *572*, 354–363. https://doi.org/10.1016/j.jcis.2020.03.099.

225. Blunt, M.J.; Lin, Q.; Akai, T.; Bijeljic, B. A thermodynamically consistent characterization of wettability in porous media using high-resolution imaging. *J. Colloid Interface Sci.* **2019**, *552*, 59–65. https://doi.org/10.1016/j.jcis.2019.05.026.

226. Akai, T.; Alhammadi, A.M.; Blunt, M.J.; Bijeljic, B. Modeling Oil Recovery in Mixed-Wet Rocks: Pore-Scale Comparison Between Experiment and Simulation. *Transp. Porous Media* **2019**, *127*, 393–414. 10.1007/s11242-018-1198-8.

227. Gabbott, P. *Principles and Applications of Thermal Analysis*; Wiley, 2008; ISBN 9780470698129.

228. Ng, E.-P.; Mintova, S. Nanoporous materials with enhanced hydrophilicity and high water sorption capacity. *Microporous Mesoporous Mater.* **2008**, *114*, 1–26. https://doi.org/10.1016/j.micromeso.2007.12.022.

229. Cavuoto, D.; Zaccheria, F.; Ravasio, N. Some Critical Insights into the Synthesis and Applications of Hydrophobic Solid Catalysts. *Catalysts* **2020**, *10*, 1337. 10.3390/catal10111337.

230. Anderson, M.W.; Klinowski, J. Zeolites treated with silicon tetrachloride vapour. Part 1.—Preparation and characterisation. *J. Chem. Soc. Faraday Trans. 1 Phys. Chem. Condens. Phases* **1986**, *82*, 1449–1469.

10.1039/F19868201449.

231. Giaya, A.; Thompson, R.W.; Denkewicz Jr, R. Liquid and vapor phase adsorption of chlorinated volatile organic compounds on hydrophobic molecular sieves. *Microporous Mesoporous Mater.* **2000**, *40*, 205–218. https://doi.org/10.1016/S1387-1811(00)00261-4.

232. Mueller, R.; Kammler, H.K.; Wegner, K.; Pratsinis, S.E. OH Surface Density of SiO2 and TiO2 by Thermogravimetric Analysis. *Langmuir* **2003**, *19*, 160–165. 10.1021/la025785w.

233. Vansant, E.F.; Van Der Voort, P.; Vrancken, K.C. *Characterization and Chemical Modification of the Silica Surface*; ISSN; Elsevier Science, 1995; ISBN 9780080528953.

234. Bhagiyalakshmi, M.; Vishnu Priya, S.; Herbert Mabel, J.; Palanichamy, M.; Murugesan, V. Effect of hydrophobic and hydrophilic properties of solid acid catalysts on the esterification of maleic anhydride with ethanol. *Catal. Commun.* **2008**, *9*, 2007–2012. https://doi.org/10.1016/j.catcom.2008.03.038.

235. Fripiat, J.J.; Uytterhoeven, J. HYDROXYL CONTENT IN SILICA GEL "AEROSIL." *J. Phys. Chem.* **1962**, *66*, 800–805. 10.1021/j100811a007.

236. Peri, J.B. Infrared Study of OH and NH2 Groups on the Surface of a Dry Silica Aerogel. *J. Phys. Chem.* **1966**, *70*, 2937–2945. 10.1021/j100881a037.

237. Hambleton, F.H.; Hockey, J.A.; Taylor, J.A.G. Investigation by infra-red spectroscopic methods of deuterium exchange properties of aerosil silicas. *Trans. Faraday Soc.* **1966**, *62*, 801–807. 10.1039/TF9666200801.

238. Hockey, J.A.; Pethica, B.A. Surface hydration of silicas. *Trans. Faraday Soc.* **1961**, *57*, 2247–2262. 10.1039/TF9615702247.

239. Conrad, S.; Wolf, P.; Müller, P.; Orsted, H.; Hermans, I. Influence of Hydrophilicity on the Snβ-Catalyzed Baeyer–Villiger Oxidation of Cyclohexanone with Aqueous Hydrogen Peroxide. *ChemCatChem* **2017**, *9*, 175–182. https://doi.org/10.1002/cctc.201600893.

240. Lamberti, C.; Bordiga, S.; Zecchina, A.; Artioli, G.; Marra, G.; Spanò, G. Ti Location in the MFI Framework of Ti−Silicalite-1: A Neutron Powder Diffraction Study. *J. Am. Chem. Soc.* **2001**, *123*, 2204–2212. 10.1021/ja003657t.

241. Heitmann, G.P.; Dahlhoff, G.; Hölderich, W.F. Catalytically Active Sites for the Beckmann Rearrangement of Cyclohexanone Oxime to ε-Caprolactam. *J. Catal.* **1999**, *186*, 12–19. https://doi.org/10.1006/jcat.1999.2552.

242. Bui, T. V; Umbarila, S.J.; Wang, B.; Sooknoi, T.; Li, G.; Chen, B.; Resasco, D.E. High-Temperature Grafting Silylation for Minimizing Leaching of Acid Functionality from Hydrophobic Mesoporous Silicas Used as Catalysts in the Liquid Phase. *Langmuir* **2019**, *35*, 6838–6852. 10.1021/acs.langmuir.9b00487.

243. Wei, Y.; Li, G.; Liu, J.; Yi, Y.; Guo, H. Organic groups-regulated high-efficiency catalysis of hybrid Ti-Containing mesoporous silicates for Bi-Phase interfacial epoxidation. *Microporous Mesoporous Mater.* **2021**, *310*, 110668. https://doi.org/10.1016/j.micromeso.2020.110668.

244. Li, X.; Shi, B.; Li, M.; Mao, L. Synthesis of highly ordered alkyl-functionalized mesoporous silica by co-condensation method and applications in surface coating with superhydrophilic/antifogging properties. *J. Porous Mater.* **2015**, *22*, 201–210. 10.1007/s10934-014-9886-4.

245. Barczak, M.; Dąbrowski, A.; Iwan, M.; Rzączyńska, Z. Mesoporous organosilicas functionalized by alkyl groups: Synthesis, structure and adsorption properties. *J. Phys. Conf. Ser.* **2009**, *146*, 12002. 10.1088/1742-6596/146/1/012002.

246. Pires, J.; Pinto, M.; Estella, J.; Echeverría, J.C. Characterization of the hydrophobicity of mesoporous

silicas and clays with silica pillars by water adsorption and DRIFT. *J. Colloid Interface Sci.* **2008**, *317*, 206–213. https://doi.org/10.1016/j.jcis.2007.09.035.

247. Olson, D.H.; Haag, W.O.; Borghard, W.S. Use of water as a probe of zeolitic properties: interaction of water with HZSM-5. *Microporous Mesoporous Mater.* **2000**, *35–36*, 435–446. https://doi.org/10.1016/S1387-1811(99)00240-1.

248. WEITKAMP, J.; KLEINSCHMIT, P.; KISS, A.; BERKE, C.H. THE HYDROPHOBICITY INDEX – A VALUABLE TEST FOR PROBING THE SURFACE PROPERTIES OF ZEOLITIC ADSORBENTS OR CATALYSTS. In; von Ballmoos, R., Higgins, J.B., Treacy, M.M.J.B.T.-P. from the N.I.Z.C., Eds.; Butterworth-Heinemann, 1993; pp. 79–87 ISBN 978-1-4832-8383-8. https://doi.org/10.1016/B978-1-4832-8383-8.50094-5.

249. Rübner, K.; Balköse, D.; Robens, E. Methods of humidity determination Part I: Hygrometry. *J. Therm. Anal. Calorim.* **2008**, *94*, 669. 10.1007/s10973-008-9349-8.

250. Silvestre-Alberó, J.; Domine, M.E.; Jordá, J.L.; Navarro, M.T.; Rey, F.; Rodríguez-Reinoso, F.; Corma, A. Spectroscopic, calorimetric, and catalytic evidences of hydrophobicity on Ti-MCM-41 silylated materials for olefin epoxidations. *Appl. Catal. A Gen.* **2015**, *507*, 14–25. https://doi.org/10.1016/j.apcata.2015.09.029.

251. Silvestre-Albero, J.; Gómez de Salazar, C.; Sepúlveda-Escribano, A.; Rodríguez-Reinoso, F. Characterization of microporous solids by immersion calorimetry. *Colloids Surfaces A Physicochem. Eng. Asp.* **2001**, *187–188*, 151–165. https://doi.org/10.1016/S0927-7757(01)00620-3.

252. Piraján, J.C.M. *Calorimetry: Design, Theory and Applications in Porous Solids*; IntechOpen, 2018; ISBN 9781789234381.

253. Rule, G.S.; Hitchens, T.K. *Fundamentals of Protein NMR Spectroscopy*; Focus on Structural Biology; Springer Netherlands, 2006; ISBN 9781402035005.

254. Koutcher, J.A.; Burt, C.T. Principles of nuclear magnetic resonance. *J. Nucl. Med.* **1984**, *25*, 101–111. 10.1142/9789812831521_0010.

255. Vivian, A.; Fusaro, L.; Debecker, D.P.; Aprile, C. Mesoporous Methyl-Functionalized Sn-Silicates Generated by the Aerosol Process for the Sustainable Production of Ethyl Lactate. *ACS Sustain. Chem. Eng.* **2018**, *6*, 14095–14103. 10.1021/acssuschemeng.8b02623.

256. Lin, K.; Wang, L.; Meng, F.; Sun, Z.; Yang, Q.; Cui, Y.; Jiang, D.; Xiao, F.-S. Formation of better catalytically active titanium species in Ti-MCM-41 by vapor-phase silylation. *J. Catal.* **2005**, *235*, 423–427. https://doi.org/10.1016/j.jcat.2005.08.003.

257. Laha, S.C.; Kumar, R. Selective Epoxidation of Styrene to Styrene Oxide over TS-1 Using Urea–Hydrogen Peroxide as Oxidizing Agent. *J. Catal.* **2001**, *204*, 64–70. https://doi.org/10.1006/jcat.2001.3352.

258. Jorda, E.; Tuel, A.; Teissier, R.; Kervennal, J. Synthesis, Characterization, and Activity in the Epoxidation of Cyclohexene with Aqueous H2O2of Catalysts Prepared by Reaction of TiF4with Silica. *J. Catal.* **1998**, *175*, 93–107. https://doi.org/10.1006/jcat.1998.1982.

259. Grosso-Giordano, N.A.; Schroeder, C.; Okrut, A.; Solovyov, A.; Schöttle, C.; Chassé, W.; Marinković, N.; Koller, H.; Zones, S.I.; Katz, A. Outer-Sphere Control of Catalysis on Surfaces: A Comparative Study of Ti(IV) Single-Sites Grafted on Amorphous versus Crystalline Silicates for Alkene Epoxidation. *J. Am. Chem. Soc.* **2018**, *140*, 4956–4960. 10.1021/jacs.7b11467.

260. Wang, L.; Sun, J.; Meng, X.; Zhang, W.; Zhang, J.; Pan, S.; Shen, Z.; Xiao, F.-S. A significant enhancement of catalytic activities in oxidation with H2O2 over the TS-1 zeolite by adjusting the catalyst wettability. *Chem. Commun.* **2014**, *50*, 2012–2014. 10.1039/C3CC48220K.

261. Wu, L.; Tang, Z.; Yu, Y.; Yao, X.; Liu, W.; Li, L.; Yan, B.; Liu, Y.; He, M. Facile synthesis of a high-performance titanosilicate catalyst with controllable defective Ti(OSi)3OH sites. *Chem. Commun.* **2018**, *54*, 6384–6387. 10.1039/C8CC02794C.

262. Munakata, H.; Oumi, Y.; Miyamoto, A. A DFT Study on Peroxo-Complex in Titanosilicate Catalyst: Hydrogen Peroxide Activation on Titanosilicalite-1 Catalyst and Reaction Mechanisms for Catalytic Olefin Epoxidation and for Hydroxylamine Formation from Ammonia. *J. Phys. Chem. B* **2001**, *105*, 3493–3501. 10.1021/jp0022196.

263. Panyaburapa, W.; Nanok, T.; Limtrakul, J. Epoxidation Reaction of Unsaturated Hydrocarbons with H2O2 over Defect TS-1 Investigated by ONIOM Method: Formation of Active Sites and Reaction Mechanisms. *J. Phys. Chem. C* **2007**, *111*, 3433–3441. 10.1021/jp065544n.

264. Stare, J.; Henson, N.J.; Eckert, J. Mechanistic Aspects of Propene Epoxidation by Hydrogen Peroxide. Catalytic Role of Water Molecules, External Electric Field, and Zeolite Framework of TS-1. *J. Chem. Inf. Model.* **2009**, *49*, 833–846. 10.1021/ci800227n.

# ANNEX

# ANNEX INDEX

# ANNEX I

# OTHER TYPES OF TITANOSILICATES

Several types of titanosilicates have been modified hydrophobically and these were described in the section 1.1.1. Other titanosilicates such as Ti-MWW and Ti-MOR with important applications are described in this part.

## AI.1 Ti-MWW

Ti-MWW is a medium pore Ti-zeolite with 2-dimensional sinusoidal system of 10-MR, structural diversity of supercages (7.1 x 18.1 Å) and side pockets that enhance the catalytic activity because they act as reactions spaces where bulky substrates are accommodated (Figure A1) [1,2].

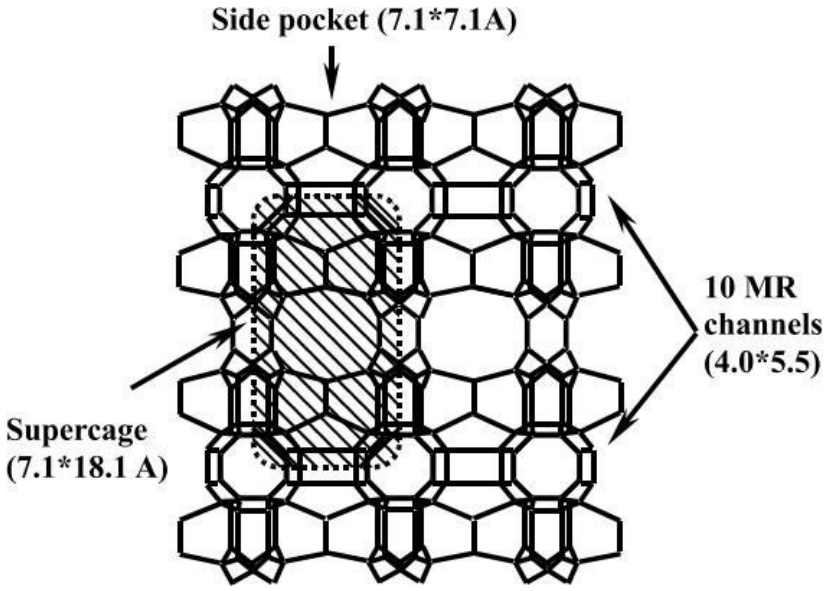


**Figure A1** Topology of MWW zeolite framework [1].

The Ti(IV) substitution into the MWW zeolite framework was achieved by hydrothermal synthesis in boric acid media and using the SDAs, piperidine [3] or hexamethylene imine (HM) [4]. The MWW borosilicate crystalline structure (known as MCM-22) can be obtained from lamellar precursor by a dihydroxylation between layered sheets during the calcination process [5]. The titanosilicate Ti-MWW can be prepared by the same process and post-synthesis methods can be applied to form Ti-MWW with better accessibility to active sites, such as the preparation of

hierarchical Ti-MWW by the appropriate interlayer silylation with dimeric silane [6] and the reversible structural conversion of MWW for preparation of interlayer-expanded Ti-MWW [7]. Both materials were highly active in the epoxidation of cyclohexene using $H_2O_2$ as oxidant. Ti-MWW has been used as a successful catalyst in ammoxidation of cyclohexanone [8], liquid-phase oxidation of cyclohexane [9], epoxidation of alkenes [10] and selective oxidation of pyridine [11].

### AI.2 Ti-MOR

Zeolites with MOR framework are a type of aluminosilicates synthesized by hydrothermally method without the use of SDAs. They are an important group of catalysts used in petrochemical processes [12,13]. Incorporation of titanium atoms into dealuminated MOR zeolite to prepare Ti-MOR was studied with the use of post-synthesis method using $TiCl_4$ vapor, this method was called as “atom-planting” method [14]. A scheme of the preparation of Ti-MOR by dealumination and a solid-gas reaction between dealuminated MOR and $TiCl_4$ is shown in Figure A2 [15].

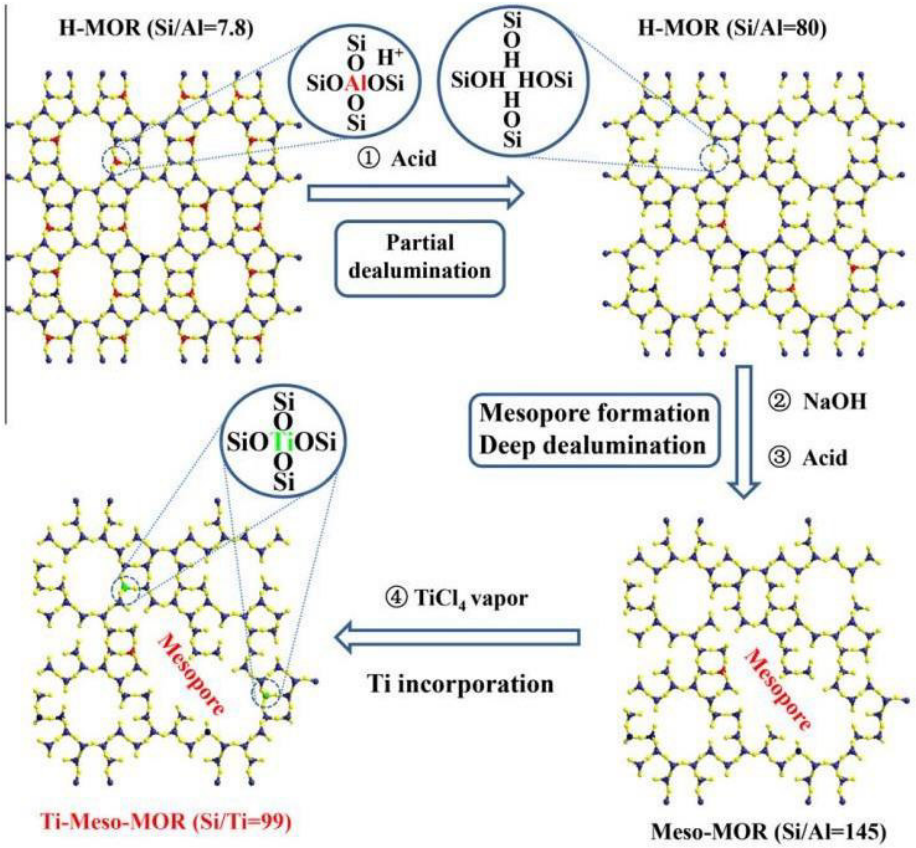


**Figure A2** Preparation of Ti-MOR by dealumination a solid-gas reaction between dealuminated MOR and $TiCl_4$ [15].

Directly hydrothermal synthesis cannot be used due to the specific structure features that makes the crystallization of MOR framework impossible in silicious conditions and in absence of alkali source [15]. In the preparation of Ti-MOR, the molecules of TiCl4 should diffuse into the 12-MR channels to be effectively incorporated into the structure. This allows a better contact with the reactant molecules when Ti-MOR is used as catalyst in liquid-phase oxidation reactions [16]. Ti-MOR is a large pore Ti-zeolite with parallel 12-membered ring (MR) (6.5 x 7.0 Å) and 8-MR (2.6 x 5.7 Å) channels [16,17]. Ti-MOR has been demonstrated to be an efficient catalyst with higher activity than TS-1 in the hydroxylation of aromatics [18,19] and ammoximation of ketones [20] such as ammoximation of cyclohexanone in a continuous reactor [15,21] and ammoximation of dimethyl ketones [17].

# ANNEX II

# INTERMOLECULAR INTERACTIONS

For understanding the basics of hydrophobicity, it is convenient to review the intermolecular interactions.

## AII.1 Van der Waals interactions

The term "van der Waals forces" collectively encompasses the forces of attraction between molecules. They are weak attractive forces that are established between electrically neutral molecules (both polar and nonpolar), but they are very numerous and play a fundamental role in many chemical and biological processes [22].

### AII.1.1 Dipole-dipole interactions (Orientational or Keesom)

A molecule is dipolar when there is an asymmetric distribution of electrons because the molecule is formed by atoms with different electronegativities. As a consequence, the electrons are preferably in the vicinity of the most electronegative atom. Thus, two regions (or poles) are created in the molecule, one with a partial negative charge and the other with a partial positive charge. When two polar molecules (dipolar molecules) come together, there is an attraction between the positive pole of one of them and the negative pole of the other. This attractive force between two dipoles is more intense the greater the polarization of said polar molecules or, in other words, the greater the difference in electronegativity between the bonded atoms. The dipole moment (μ) is a vector oriented towards the negative charge whose magnitude depends on the intensity of the charge and the distance between the atoms. The dipole moment allows to quantify the asymmetry of charges in the molecule. The shape of the molecule also affects the dipole moment [23].

Dipole-dipole interactions are substantial only in systems with very polar molecules or in the case of small molecules with very large dipole moments such as ammonia (N-H), hydrogen fluoride (F-H) and water (O-H). These interactions are more complex and are called “hydrogen bonding” interactions [24]. The hydrogen bonds are shorth-range directional interactions, between very polar molecules, and the hydrogen atom is the center of positive charges that will be attracted to the unshared pairs of electrons from the electronegative atoms of other molecules. It is a weak

bond. However, as they are very abundant, their contribution to the cohesion between biomolecules is great [23].

### AII.1.2 Dipole-induced interactions (Induced or Debye)

These interactions take place between a polar molecule and an apolar molecule. In this case, the charge of a polar molecule causes a distortion in the electron cloud of the apolar molecule and transiently converts it into a dipole (induced dipole). In this way, an attractive force is established between the molecules [24].

### AII.1.3 Instantaneous dipole-induced interactions (Dispersion or London)

Dispersion forces are weak forces that are established mainly between nonpolar substances, although they are also present in polar substances. They occur due to the irregularities that exist in the electronic cloud of the atoms of the molecules as a result of mutual proximity. The presence of an instantaneous dipole in a molecule causes the formation of an induced dipole in a neighboring molecule so that a weak attractive force is created between the two molecules [22].

The side or end where the nucleus is partially exposed is slightly more positive (δ+), and the end towards which the electron density has shifted has a partial negative charge (δ-). This separation of charges is known as an instantaneous dipole. The partially exposed nucleus of an atom attracts electron density from a neighboring atom, and it is this induced dipole between molecules that represents the scattering force between atoms and molecules. However, an instant later the electron density has already shifted, and the partial charges causing the attraction have changed. The intensity of the dispersion force depends on a number of factors. However, taking a qualitative and predictive approach must consider that the dispersion forces are related to the number of electrons found in the atom or in the molecule. Thus, it is the number of electrons that will determine the ease with which the density of the electron can be polarized and a greater polarization, the dispersion forces are more intense [24,25].

Dispersion forces are long-range interactions (10 nm or more), they may be repulsive or attractive and they are nonadditive due to the presence of other near atoms and molecules affect the interactions between two specific atoms and molecules [24].

## REFERENCES


1. Wu, P.; Tatsumi, T. A new generation of titanosilicate catalyst: Preparation and application to liquid-phase epoxidation of alkenes. *Catal. Surv. from Asia* **2004**, *8*, 137–148. 10.1023/B:CATS.0000027015.37277.fb.

2. Xu, H.; Yan, J.; Lu, X.; Yin, J.; Wu, P. Comparison of titanosilicates with different topologies as liquid-phase oxidation catalysts. *Catal. Today* **2020**, *347*, 48–55. 10.1016/j.cattod.2018.04.026.

3. Wu, P.; Tatsumi, T. Preparation of B-free Ti-MWW through reversible structural conversion. *Chem. Commun.* **2002**, 1026–1027. 10.1039/B201170K.

4. Wu, P.; Tatsumi, T.; Komatsu, T.; Yashima, T. A Novel Titanosilicate with MWW Structure. I. Hydrothermal Synthesis, Elimination of Extraframework Titanium, and Characterizations. *J. Phys. Chem. B* **2001**, *105*, 2897–2905. 10.1021/jp002816s.

5. Wu, P.; Tatsumi, T.; Komatsu, T.; Yashima, T. Hydrothermal Synthesis of a Novel Titanosilicate with MWW Topology. *Chem. Lett.* **2000**, *29*, 774–775. 10.1246/cl.2000.774.

6. Xu, H.; Fu, L.; Jiang, J.-G.; He, M.; Wu, P. Preparation of hierarchical MWW-type titanosilicate by interlayer silylation with dimeric silane. *Microporous Mesoporous Mater.* **2014**, *189*, 41–48. https://doi.org/10.1016/j.micromeso.2013.09.041.

7. Yoshioka, M.; Yokoi, T.; Tatsumi, T. Effectiveness of the reversible structural conversion of MWW zeolite for preparation of interlayer-expanded Ti-MWW with high catalytic performance in olefin epoxidation. *Microporous Mesoporous Mater.* **2014**, *200*, 11–18. https://doi.org/10.1016/j.micromeso.2014.08.007.

8. Song, F.; Liu, Y.; Wu, H.; He, M.; Wu, P.; Tatsumi, T. A novel titanosilicate with MWW structure: Highly effective liquid-phase ammoximation of cyclohexanone. *J. Catal.* **2006**, *237*, 359–367. 10.1016/j.jcat.2005.11.018.

9. Zhou, W.-J.; Wischert, R.; Xue, K.; Zheng, Y.-T.; Albela, B.; Bonneviot, L.; Clacens, J.-M.; De Campo, F.; Pera-Titus, M.; Wu, P. Highly selective liquid-phase oxidation of cyclohexane to KA oil over Ti-MWW catalyst: Evidence of formation of oxyl radicals. *ACS Catal.* **2014**, *4*, 53–62. 10.1021/cs400757j.

10. Wu, P.; Tatsumi, T. Extremely high trans selectivity of Ti-MWW in epoxidation of alkenes with hydrogen peroxide. *Chem. Commun.* **2001**, 897–898. 10.1039/b101426i.

11. Xie, W.; Zheng, Y.; Zhao, S.; Yang, J.; Liu, Y.; Wu, P. Selective oxidation of pyridine to pyridine-N-oxide with hydrogen peroxide over Ti-MWW catalyst. *Catal. Today* **2010**, *157*, 114–118. 10.1016/j.cattod.2010.02.045.

12. Flanigen, E.M.; Jansen, J.C.; van Bekkum, H. *Introduction to Zeolite Science and Practice*; ISSN; Elsevier Science, 1991; ISBN 9780080887111.

13. Yang, Y.; Ding, J.; Wang, B.; Wu, J.; Zhao, C.; Gao, G.; Wu, P. Influences of fluorine implantation on catalytic performance and porosity of MOR-type titanosilicate. *J. Catal.* **2014**, *320*, 160–169. 10.1016/j.jcat.2014.10.008.

14. Wu, P.; Komatsu, T.; Yashima, T. Characterization of Titanium Species Incorporated into Dealuminated Mordenites by Means of IR Spectroscopy and 18O-Exchange Technique. *J. Phys. Chem.* **1996**, *100*, 10316–10322. 10.1021/jp960307d.

15. Xu, H.; Zhang, Y.; Wu, H.; Liu, Y.; Li, X.; Jiang, J.; He, M.; Wu, P. Postsynthesis of mesoporous MOR-type titanosilicate and its unique catalytic properties in liquid-phase oxidations. *J. Catal.* **2011**, *281*, 263–272. 10.1016/j.jcat.2011.05.009.

16. Yang, Y.; Ding, J.; Xu, C.; Zhu, W.; Wu, P. An insight into crystal morphology-dependent catalytic properties of MOR-type titanosilicate in liquid-phase selective oxidation. *J. Catal.* **2015**, *325*, 101–110. 10.1016/j.jcat.2015.03.001.

17. Ding, J.; Wu, P. Selective synthesis of dimethyl ketone oxime through ammoximation over Ti-MOR catalyst. *Appl. Catal. A Gen.* **2014**, *488*, 86–95. 10.1016/j.apcata.2014.09.038.

18. Wu, P.; Komatsu, T.; Yashima, T. Preparation of titanosilicate with mordenite structure by atomplanting method and its catalytic properties for hydroxylation of aromatics. In *Progress in Zeolite and Microporous Materials*; Chon, H., Ihm, S.-K., Uh, Y.S.B.T.-S. in S.S. and C., Eds.; Elsevier, 1997; Vol. 105, pp. 663–670 ISBN 0167-2991. https://doi.org/10.1016/S0167-2991(97)80614-3.

19. Wu, P.; Komatsu, T.; Yashima, T. Hydroxylation of Aromatics with Hydrogen Peroxide over Titanosilicates with MOR and MFI Structures: Effect of Ti Peroxo Species on the Diffusion and Hydroxylation Activity. *J. Phys. Chem. B* **1998**, *102*, 9297–9303. 10.1021/jp982951t.

20. Wu, P.; Komatsu, T.; Yashima, T. Ammoximation of Ketones over Titanium Mordenite. *J. Catal.* **1997**, *168*, 400–411. https://doi.org/10.1006/jcat.1997.1679.

21. Xu, L.; Ding, J.; Yang, Y.; Wu, P. Distinctions of hydroxylamine formation and decomposition in cyclohexanone ammoximation over microporous titanosilicates. *J. Catal.* **2014**, *309*, 1–10. https://doi.org/10.1016/j.jcat.2013.08.021.

22. Winterton, R.H.S. Van der Waals forces. *Contemp. Phys.* **1970**, *11*, 559–574. 10.1080/00107517008202194.

23. Wade, R.C. Calculation and Application of Molecular Interaction Fields. In *Molecular Interaction Fields: Applications in Drug Discovery and ADME Prediction*; 2006; Vol. 27, pp. 27–42. 10.1002/3527607676.ch2.

24. Myers, D. *Surfaces, interfaces, and colloids*; 1999; Vol. 4; ISBN 0471330604.

25. Margenau, H. Van der waals forces. *Rev. Mod. Phys.* **1939**, *11*, 1–35. 10.1103/RevModPhys.11.1.